References

1. D. R. Hardesty ed., "Assessment of Optical Daignostics for In Situ Measurements in High Temperature Coal Combustion and Conversion Flows," Sandia Tech. Report No. SAND84-8724, Sandia National Laboratories, Livermore, CA (1984).
2. D. J. Holve, D. A. Tichenor, J. C. F. Wang, and D. R. Hardesty, Optical Engineering 20, 4 (1981).
3. W. L. Flower and J. A. Miller, "An Analysis of Particle-Temperature Modulation Induced by Pulsed-Laser Sources," Sandia Tech. Report No. SAND79-8607, Sandia National Laboratories, Livermore, CA (1979).
4. A. J. Mulac, W. L. Flower, R. A. Hill, and D. P. Aeschliman, Appl. Opt. 17, 2695 (1978).
5. W. L. Flower, "Raman Scattering Gas Temperature Measurements in Particle Laden Flows," Sandia Tech. Report No. SAND81-8606, Sandia National Laboratories, Livermore, CA (1981).
6. E. J. Beiting, Appl. Opt. 24, 18 (1985).
7. R. P. Lucht, "CARS Measurements of Temperature and Species Concentration in Coal Combustion Flows," pp. 367-370, Proceedings, 1985 International Conference on Coal Science, Sydney, NSW, Australia (October 28-31, 1985).
8. D. K. Ottesen, "In Situ Studies of Pulverized Coal Combustion by Fourier Transform Infrared Spectroscopy," pp. 351-354 in Ref. 7.
9. P. R. Solomon, D. G. Hamblen, R. M. Carangelo, and J. L. Krause, 19th Symposium (International) on Combustion, pp. 1139-1149, The Combustion Institute, Pittsburgh, Pa (1982).
10. P. R. Solomon, R. M. Carangelo, P. E. Best, J.R. Markham, and D. G. Hamblen, Am. Chem. Soc. Preprints 31, 141 (1986).
11. P. R. Solomon, "FT-IR Spectroscopy Diagnostic Techniques," paper presented at the NATO Workshop on Fundamental Physical Chemistry of Pulverized Coal Combustion, Les Arcs, France (July 30, 1986).
12. J. D. Bradshaw, N. Omenetto, G. Zizak, J. N. Bower, and J. D. Winefordner, Appl. Opt. 19, 2709 (1980).

13. D. J. Taylor, "CARS Concentration and Temperature Measurements in Coal Gasifiers," Los Alamos National Laboratory Report No. LA-UR-83-1840, LANL, Los Alamos, NM (1983).
14. A. Ferrario, M. Garbi, and C. Maluicini, "Real-Time CARS Spectroscopy in a Semi-Industrial Furnace," paper presented at the Conference on Lasers and Electro-Optics, Baltimore, MD (1983).
15. D. J. Holve and S. A. Self, Appl. Opt. 18, 10 (1979).
16. E. O. Hirleman, "Optical Techniques for Particle Characterization in Combustion, Multiple Ratio Particle Counter," Ph.D. Thesis, Purdue University, Lafayette, IN (1977).
17. D. H. Holve, "An SPC System for Measuring Fine Particles at High Number Density in Research and Industrial Applications," Sandia Tech. Report No. SAND83-8246, Sandia National Laboratories, Livermore, CA (1983).
18. D. J. Holve, "Comparison of Combustion Studies of Coal-Water Slurries and Pulverized Coal," paper presented at the 7th International Symposium on Coal Slurry Fuels Preparation and Utilization, New Orleans, LA (May 1985).
19. D. A. Tichenor, R. E. Mitchell, K. R. Hencken, and S. Niksa, "Simultaneous In Situ Measurement of Particle Size, Temperature, and Velocity in a Combustion Environment," 20th Symposium (International) on Combustion, pp. 1213-1221, The Combustion Institute, Pittsburgh, PA (1984).
20. R. E. Mitchell (in press in Comb. Sci. and Tech. 1986).
21. J. Swithenbark, J. M. Beer, D. S. Taylor, D. Abbot, and G. C. McCreath, "A Laser Diagnostic Technique for Measurement of Droplet and Particle Size Distribution," AIAA 14th Aerospace Science Meeting, Paper No. 76-69, NY (1976).
22. A. L. Wertheimer and W. L. Wilcox, Appl. Opt. 15, 1616 (1976).
23. W. L. Flower, Phys. Rev. Lett. 51, 2287 (1983).
24. D. K. Ottesen (private communication, 1986).
25. R. W. Schmieder, "Techniques and Applications of Laser Spark Spectroscopy," Sandia Tech. Report No. SAND83-8618, Sandia National Laboratories, Livermore, CA (1983).
26. L. J. Radziemski, T. R. Loree, D. A. Cremers, and N. M. Hoffman, Anal. Chem. 55, 1246 (1983).

27. J. C. F. Wang and K. R. Hencken, "In Situ Particle Size Measurement Using a Two-Color Laser Scattering Technique," Sandia Tech. Report No. SAND-85-8869, Sandia National Laboratories, Livermore, CA (1985).

CHAPTER 12:
FUNDAMENTALS OF COAL CONVERSION AND RELATION TO COAL PROPERTIES*

12.1. Introduction

In order to develop reliable coal-conversion technology, it is important to understand the conversion behavior of coal and the relationship between conversion behavior and measurable sets of coal properties. For example, what is the effect on gasifier performance of normal variations in the organic and mineral properties of a coal from a single mine, of variations in coal particle size, or of switching coals? Unscheduled shutdowns of coal plants are often caused by unexpected and uncontrolled behavior of the coal. What will be the effect of instituting pollution-control strategies such as the injection of sorbents? Can slagging and fouling behavior be predicted from the mineral distribution in the coal and the process conditions? Can the concentration of tars and fines exiting the gasifier be predicted and controlled? Can optimum gasifier operating conditions be predicted for new coals?

The design of new processes or scaling-up of a process should be improved by the availability of a good predictive capability. To design a process for producing condensable products by mild gasification, knowledge of the initial product slate from devolatilization (condensables, char and gas species) and the secondary reactions of the condensables is needed.

---

* This chapter has been written by P.R. Solomon (Secs. 12.1-12.3 and 12.5) and J.M. Beér (Sec. 12.4); the brief Appendix is by J.P. Longwell (M.I.T.).

The objective of the work on fundamentals of coal-conversion behavior should be the development of accurate predictive capabilities. The steps toward achieving this goal are: (i) development of chemical and physical understanding of coal-conversion phenomena and their relationship to coal properties; (ii) reduction of data and mechanisms to engineering correlations and submodels; (iii) development of comprehensive computer-simulation codes for gasification processes incorporating the submodels; and (iv) testing of the models by comparison with well-instrumented laboratory and pilot-scale experiments.

Important steps in coal conversion are summarized in Table 12.1-1. Coal characterization is discussed in Sec. 12.2. Gasification steps are divided into processes relating to coal organic structure (discussed in Sec. 12.3) and those relating to inorganic mineral matter (Sec. 12.4). Each topic is briefly discussed and the status of research and development in each area is assessed with regard to qualitative or quantitative level of

Table 12.1-1. Requirements relating to better understanding of coal-gasification steps.

Parameters	Problem Area(s)
Coal characteristics	Organic structure and minerals.
Heat transfer	Heat capacity, emissivity, evolving volatiles, and heats of reaction.
Pyrolysis rates	Variations in literature values, particle temperature measurements.
Formation of gases, condensables and char	Relationship to coal structure, crosslinking, sulfur, nitrogen, mass transport, vaporization, viscosity, melting, agglomeration, swelling, pore formation, surface area, and mineral matter distributions.
Gasification of char	Reactivity, active sites, surface area, mineral matter, catalysis, fragmentation, fines production, reactivity vs extent of conversion.
Secondary reactions of condensables and gases	Cracking, coking, gasification, soot formation, gas phase reactions
Mineral matter transformation in gasification	Minerals-to-ash transformation, ash properties (optical, thermal, size), catalytic activity.
Behavior of minerals in conversion devices	Slagging

understanding and controversial or accepted model availability. The status and needs of computer modeling of gasifiers are discussed briefly in Sec. 12.5 Recommendations are made in Sec. 12.6 for research in important areas where quantitative understanding is lacking.

12.2. Coal Characterization

While there are a number of standard characterization procedures for coal,[1] these often do not provide information appropriate to advanced processes. For example, while the proximate analysis may predict the volatile yield for coke making, it may be as much as 80% too low for bituminous coals in pulverized-coal combustion or entrained gasification. This increase in volatile yield was discussed by Badzioch and Hawksley.[2] Similarly, the free-swelling index cannot be easily correlated with swelling behavior, which varies with heating rate and final temperature.[3,4] The ASME has recently noted the need for improvements in the ash-fusion temperature test as an indication of slagging and fouling.[5] On the other hand, Neavel et al[6] have succeeded in correlating many process variables with the ultimate analysis for a set of low mineral matter vitrinites.

Ideally, the measured characteristics of the coal should allow prediction of the properties important to gasification, as listed in Table 12.1-1. In this section, we consider some recently applied measurement techniques which have been considered to improve predictability. Three symposia provide a good collection of the recent literature.[7-9] Selected techniques which provide data related to processing behavior are also considered.

12.2-1. Organic Structure (Functional Groups)

The advantage of a coal functional description has been discussed by Gavalas[10] and Solomon and Hamblen.[4] By providing a description of the conversion behavior of the functional groups as components of the coal, it is possible to develop a general model for coal behavior.

New NMR techniques are starting to provide data on the chemical forms of carbon and hydrogen in coal. A description of the techniques and references may be found in a recent review by Davidson.[11] Among the most recent advances are the techniques of dipolar dephasing[12] and 2-D and zero-field methods.[13]

Quantitative FTIR methods for determining mineral matter and functional group compositions have been developed.[4,14-22] Typical KBr pellet spectra for two bituminous coals and a lignite are illustrated in Fig. 12.2-1. Peaks due to their functional groups and mineral components are identified in this figure. In general, all coals have these absorption bands and the major variation with rank is reflected in their relative magnitudes. The gaseous and condensable products produced in pyrolysis have been related to the functional group composition of the coal.[4,10,19,23-29]

12.2-2. Viscosity

Recent work[30,31] has provided data on viscosity at high temperatures and heating-rates appropriate to gasification conditions. The viscosity can be correlated with the depolymerization and crosslinking reactions in the coal, and kinetics for these processes are being determined. Knowledge of the viscosity is essential to understand and predict swelling and agglomeration. These properties, in turn, affect char reactivity.

12.2-3. Pyrolysis

A number of pyrolysis techniques have been used as a characterization procedure for coal properties and process behavior.[4,32-34] These are useful in providing information on product distributions in devolatilization.

12.2-4. Reactivity

Gasification of char is the slowest process in gasification and, therefore, determines the throughput or size of the reactor. Most work has been performed on oxidation reactivity, which has been shown to correlate with CO_2 and H_2O reactivities.[35] Reviews of the char-reactivity literature have been published by Smith,[36] Essenhigh,[37] Laurendeau,[38] and van Heek and Muhlen[39] Published studies[35,40-47] have shown that a wide variation in char reactivities is related to coal rank, char-formation conditions, extent of devolatilization and gasification, mineral matter, and reactor conditions.

It is necessary to define a standard laboratory method to characterize char-reactivity parameters for typical reaction conditions.

12.2-5. Mineral Matter

The objective in characterizing the mineral matter in coal is the prediction of its conversion to ash, the properties of the ash (size, composition, optical properties, fluidity), and the disposition of ash in the reactor or in down-stream components. Recent reviews of research on ash in coal have been published.[48,49]

In order to study the relation between properties of the ash and mineral constituents in coal, information is required on the spatial distribution of minerals in coal and how these evolve into ash particles and subsequently into wall deposits. Mineral composition and spatial distribution are obtained with a scanning electron microscope (SEM) equipped with an X-ray analyzer. Automated analytical procedures have been employed.[50-52]

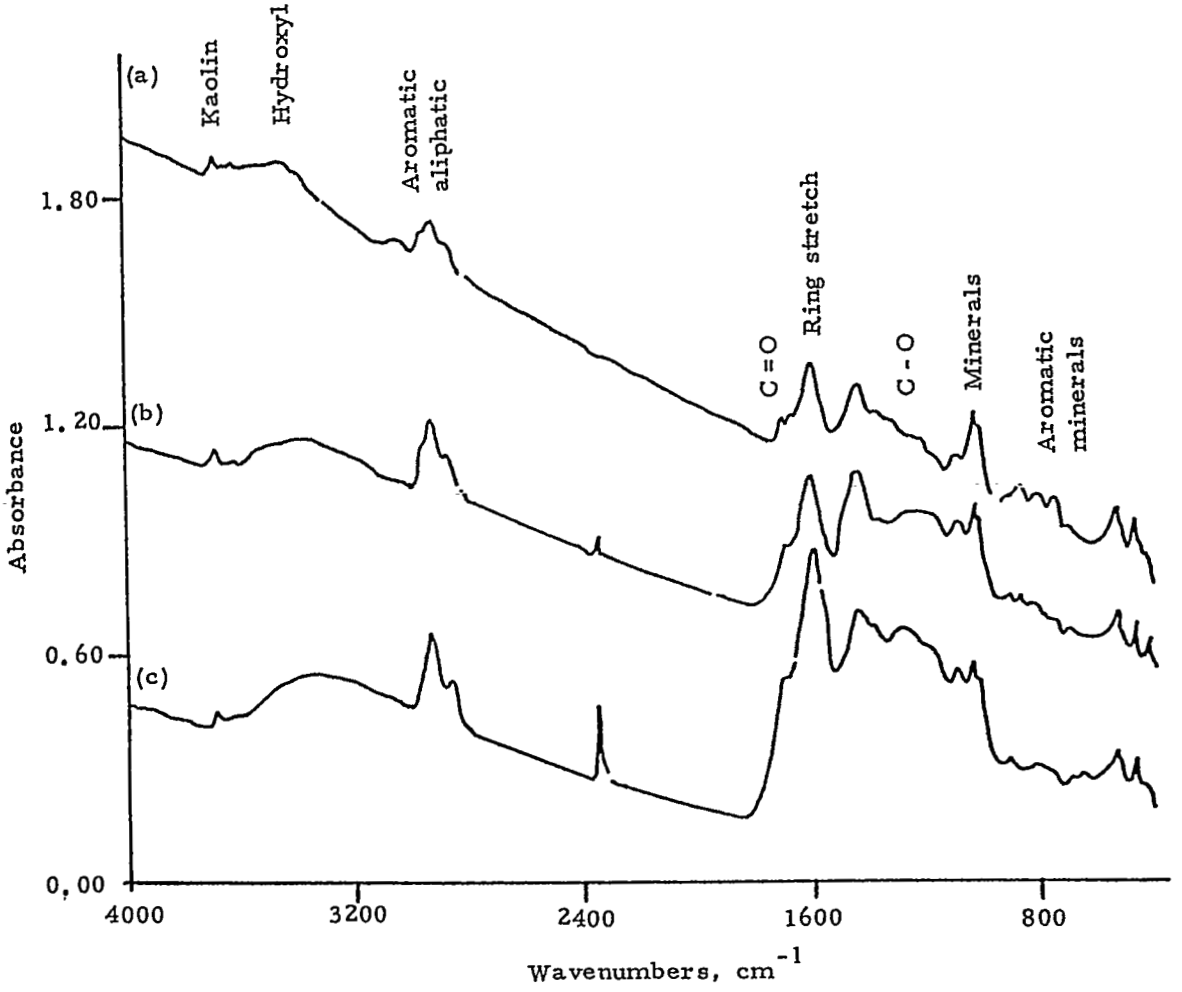

Fig. 12.2-1. FTIR spectra for (a) low-volatility bituminous coal, (b) high volatility bituminous coal, and (c) lignite.

An example of the sulfur and iron distribution in coal is presented in Fig 12.2-2. The concentration of each element is proportional to the density of dots. This figure shows clusters of iron and sulfur associated with pyrite and a more even distribution of organic sulfur.

12.3. Fundamental Processes in Gasification and Partial Gasification

Gasification steps are illustrated in Fig. 12.3-1 with SEM photographs of chars at different stages of gasification. Steps include particle heating and gas, condensables and char formation during primary devolatilization, as well as the subsequent char reaction with O_2, CO_2, or H_2O. Figure 12.3-1 illustrates important differences in char formation for thermosetting and swelling coals. This difference affects the size of the char particles, heat-transfer characteristics, aerodynamics, morphology, density, reactivity, and mineral-matter distribution. Coals show a continuum of behavior, depending on rank and gasification conditions.

Among the important properties which must be predicted are: rate of coal heating; rates and amounts of volatile evolution; secondary reactions of the condensables (cracking, coking, soot formation); properties of char during devolatilization (viscosity, agglomeration tendency, repolymerization); resulting physical properties of the char (size, porosity, etc.); intrinsic char reactivity; dependence of reactivity on reaction conditions and extent of reaction; and char fragmentation during reaction. These must be predicted from measurable coal characteristics.

12.3-1. Heat Transfer

To predict heat transfer to particles, a number of processes and properties need to be described, including particle heat capacity, emissivity and heats of reaction, as well as the effects of particle trajectories and volatile evolution on the convective heat transfer.

The room-temperature value of the heat capacity has typically been used. Data of Lee[53] and a model and data reported by Merrick[54] indicate, however, that the heat capacity is not constant. Predictions from Merrick's model[54] are illustrated in Fig. 12.3-2. The heat capacity increases by about a factor of 2.5 in going from temperature to 773K.

(a)

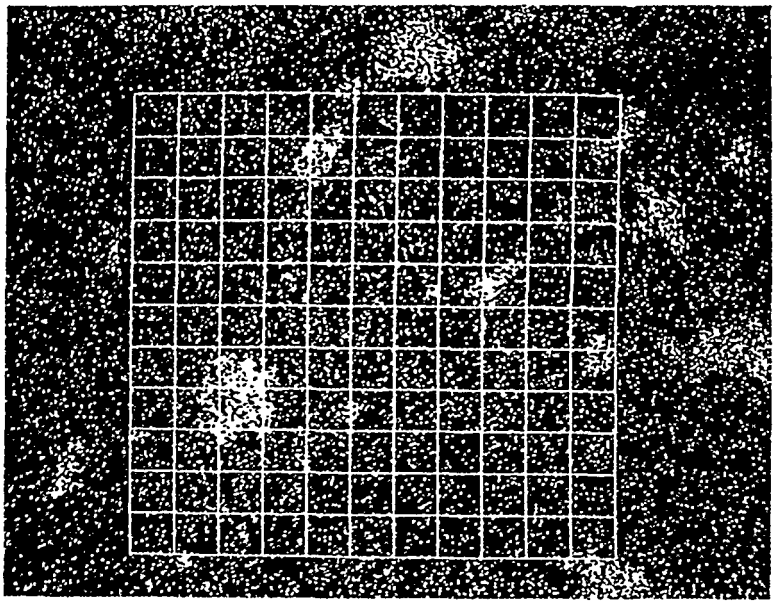

(b)

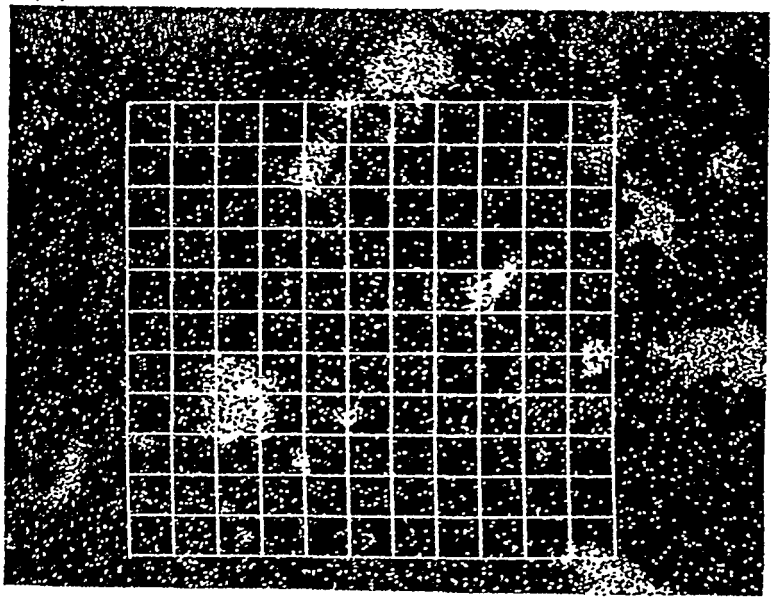

Fig. 12.2-2. X-ray maps for (a) sulfur and (b) iron on a sample of PSOC 330 coal. The grid outlines the subsamples used. Each subsample was 0.6 mm in dimension.

To calculate the absorption of radiation by coal particles, coal has typically been assumed to be a gray body with emissivity between 0.8 and 1.0. Recent measurements[55-57] have shown that, while these values apply to char particles, small coal particles typical of pulverized combustion are not gray and have spectral emittances which depend on particle size, coal rank and the extent of pyrolysis. Figure 12.3-3 shows a comparison between the emitted radiation from char and coal particles and that emitted by a black or gray body. The char is a gray body with an emissivity near 0.7. As may be seen in Fig. 12.3-3(b), coal particles emit (and absorb) much less radiation than a black body. The average emittance at a typical furnace temperature for the -200, +325 mesh fraction of lignite shown in Fig. 12.3-3b is about 0.4. It should be noted that these direct measurements of particle emissivity are in conflict with calculated emissivities based on previously measured optical constants.[58] This problem is discussed Ref. 56.

A sensitivity analysis was done to examine the importance of various assumptions in the prediction of particle temperatures.[59-61] Five cases were examined for two temperature levels (800 and 1600°C): (1) c_p = 0.3 cal/g-K, emissivity = 1.0, zero heat of pyrolysis, constant mass; (2) as in (1) but with the particle mass (kinetic) submodel included; (3) the heat-capacity submodel is added to (2); (4) the emissivity (ε) submodel is added to (3); and (5) a single particle is used in an infinite gas volume in (4). Results are presented for 200x325 mesh North Dakota lignite in Fig. 12.3-4 for experiments at 800 and 1600°C in an entrained-flow reactor.

At 800°C, the particle-temperature predictions are most sensitive to variations in the heat capacity with temperature and, to a lesser extent, to emissivity assumptions. These make a difference of 50-100°C in the maximum computed temperature. At 1600°C (Fig. 12.3-4), the predictions are very sensitive to the emissivity and the heat-capacity models. For this case, the predicted particle temperature during pyrolysis is 800°C lower for case (4) than for case (1).

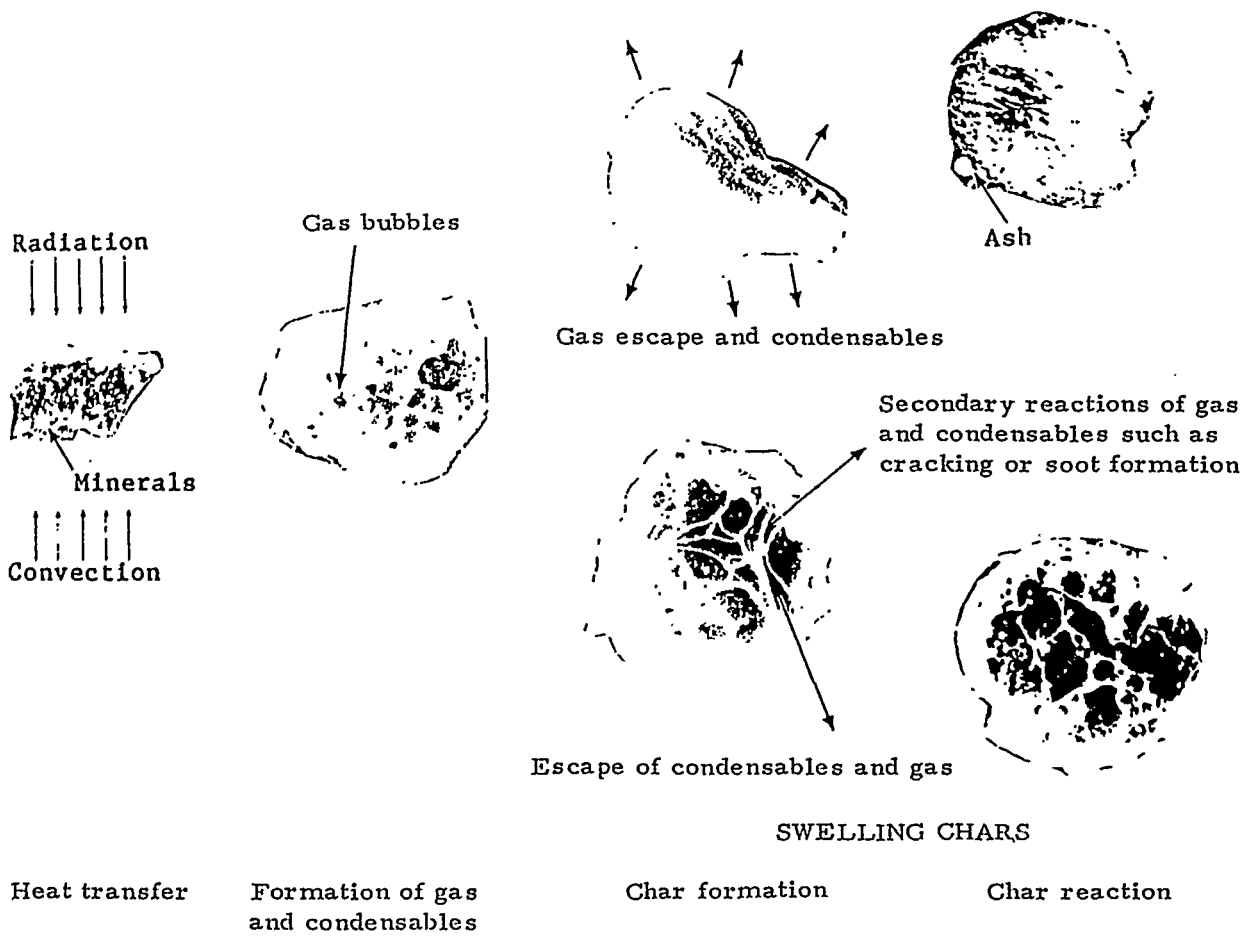

Fig. 12.3-1. Illustration of gasification steps for thermosetting and swelling chars.

The net pyrolysis heat of reaction was estimated to be between 60 and 80 cal/g (endothermic) for the experiments at 800 and 1600°C, respectively.[60,61] In both cases, the reaction heat had a negligible effect on the calculated particle temperature. This value is, however, controversial and needs to be determined accurately for a wide range of conditions and coals.

For both temperature levels, the heating rate for a single particle introduced without any cold gas (case 5) is significantly different from the more typical conditions applying to finite amounts of coal and applicable carrier-gas rates. This result illustrates the sensitivity of particle-temperature models to assumptions concerning mixing and particle loading. Volatiles evolution and its effect on convective heat transfer, particle trajectories and temperature gradients within the particle also need to be assessed.

12.3-2. Pyrolysis Rates

The development of accurate predictive models for coal gasification requires knowledge of the rates and amounts of volatiles released as a function of the particle temperature. The volatiles can account for up to 70% of the coal weight loss and control the ignition, temperature and stability of the flame, which, in turn, affect the subsequent reactivity of the char. Unfortunately, there is still controversy concerning the rate of coal pyrolysis. For example, at particle temperatures estimated to be 800°C, rates reported in the literature for rapid heating conditions (derived by using a single first-order process to define weight loss or tar evolution) vary from less[62-65] than 1 sec^{-1} to more[2,4,66-70] than 100 sec^{-1} with values in between.[24,71,72]

Useful gasification models cannot be developed with this wide range of values, as has been emphasized in recent discussions on coal pyrolysis and combustion modeling. These models yield particle temperatures and weight-loss for the assumed rates. Several authors[73-75] reported reasonably accurate modeling of results using very different pyrolysis kinetics; however, individual results were sensitive to which rates were assumed. For example, Lockwood et al[73] found the rates of Badzioch and Hawksley[2] and of Anthony et al[62] (distributed rate) acceptable, while the lower rates of Kobayashi et al[63] and of Anthony et al[62] (single rate) were not. Truelove[74] successfully used the high rates of Badzioch and Hawksley,[2] while Jost et al[75] employed the lower rates determined by Witte and Gat.[76] Also reported was a rate by Niksa et al,[64] which was close to that of Anthony (single-rate model),[62] and another by Maloney and Jenkins,[72] which was close to that of Badzioch and Hawsley.[2]

An important objective of research on fundamentals of coal conversion is to identify the source of variations in these reported rates and provide an accurate separation of the chemical-kinetic, heat-transfer, and mass-transfer rates which combine to produce the observed results.

An overview of measurements is given in Table 12.3-1 and a summary of pyrolysis rates for a number of high heating-rate experiments is presented in Fig. 12.3-5 and in Table 12.3-1. In Fig. 12.3-5, the rates (in sec^{-1}), which describe for various models the weight or tar loss, are plotted as a function of reciprocal particle temperature. The activation energies E_o and frequency factors k_o, which describe rates in Arrhenius

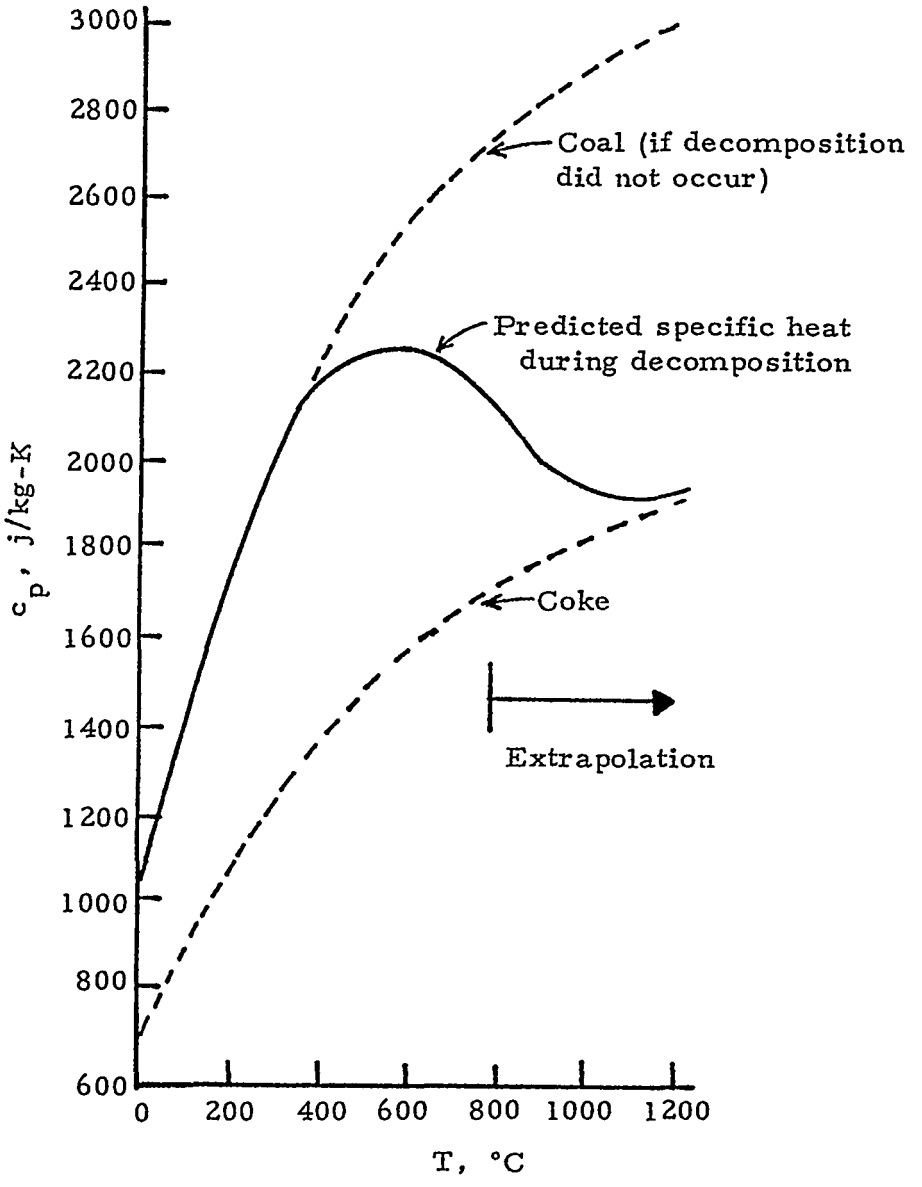

Fig. 12.3-2. Variation in specific heat with temperature for coal and coke according to the model of Merrick,[55] at a heating rate of 3 K/min, DAF Coal, 25 wt% volatile matter.

expressions, are summarized in Table 12.3-1. In some cases, a Gaussian distribution of activation energies[62] has been used to describe multiple parallel processes; this model requires the additional parameter σ for a description of the width of the distribution. In this case, the rate shown in Fig. 12.3-5 is the mean of the distribution. Data have been included from five different types of experiments: heated grid, entrained-flow reactor, laser-heating, heated-tube reactor, and a thermo-gravimetric and evolved-gas analysis.

Possible causes for these variations were reviewed in a recent publication,[59] which dealt with the following factors: (i) variations of rates with coal rank, (ii) variations in rates because of inaccuracies in determinations of weight-loss or residence time, (iii) mass-transfer limitations, (iv) influence of heat-transfer model assumptions, (v) inaccuracies in measuring particle temperature, and (vi) influence of model assumptions on the reported rates. The conclusion of this review is that differences in the determinations of particle temperatures appear to be a major source of the variations in rates reported from entrained-flow reactor experiments and direct particle-temperature measurements are essential to provide accurate rates. Also, model assumptions (i.e., single first order kinetics, a Gaussian distribution of activation energies, etc.) account for differences (especially activation energies) in the reported rates. These conclusions are, however, controversial.

12.3-3. Devolatilization: Formation of Gases, Condensables and Char

Coal devolatilization is important since it is the initial step in most coal-conversion processes and is the step which is most dependent on coal properties. In addition to the question of devolatilization rates, there are problems concerning the amount, composition and physical form of the devolatilization products. Devolatilization controls the initial yield of condensable products, their molecular weight distribution, and the competitive yields of gas species. Furthermore, the physical form and reactivity of the
non-volatile char are controlled by the pyrolysis reactions. In addition to the importance of pyrolysis in coal processing, analysis of pyrolysis products can supply important clues to the structure of the parent coal, especially since many of its structural elements are preserved in the condensable products (tar).

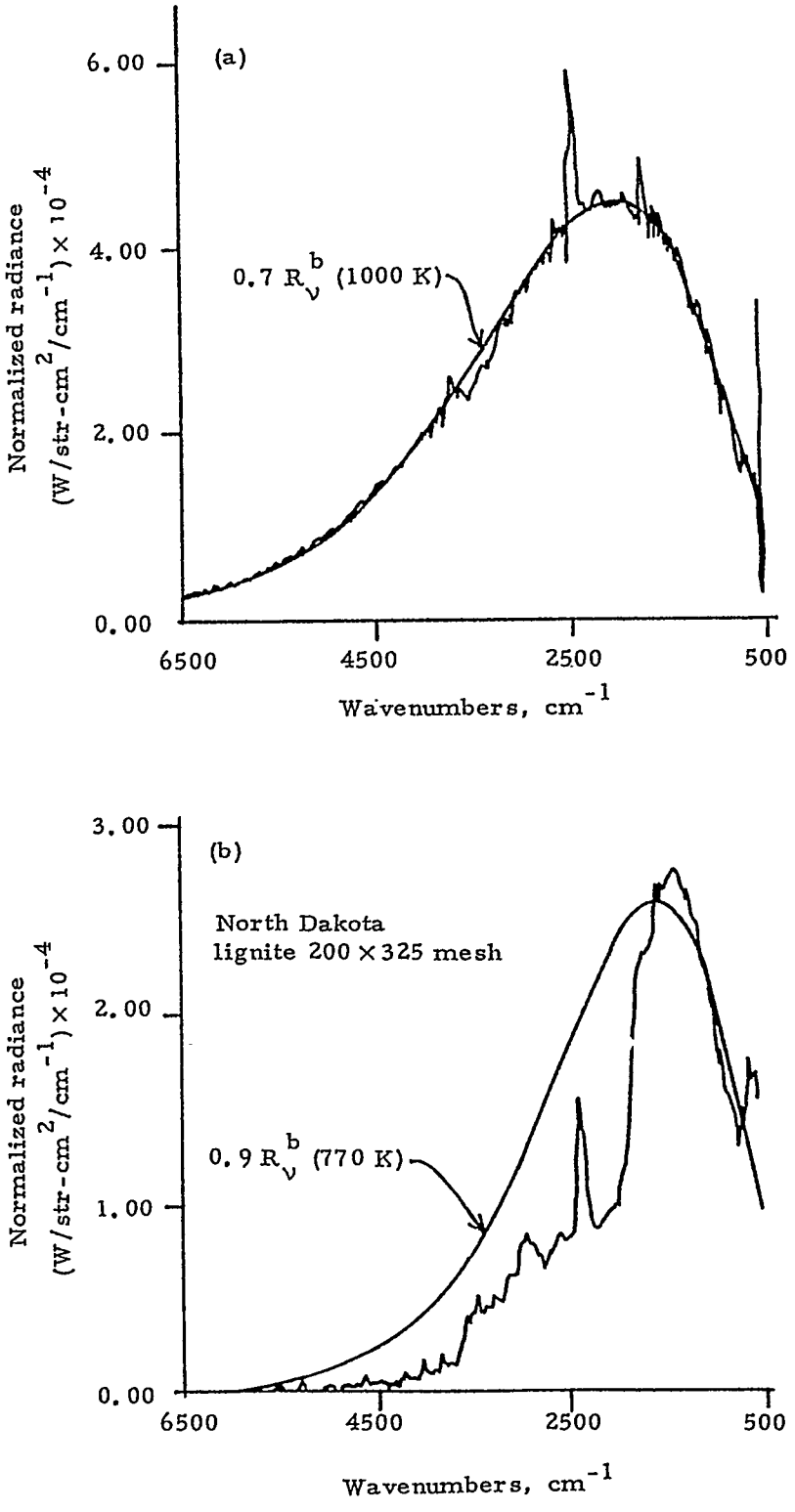

Fig. 12.3-3. Normalized emission spectra compared with theoretical gray-body curves for (a) North Dakota char formed at 1573 K and (b) North Dakota lignite; 200 × 325 mesh coal was used.

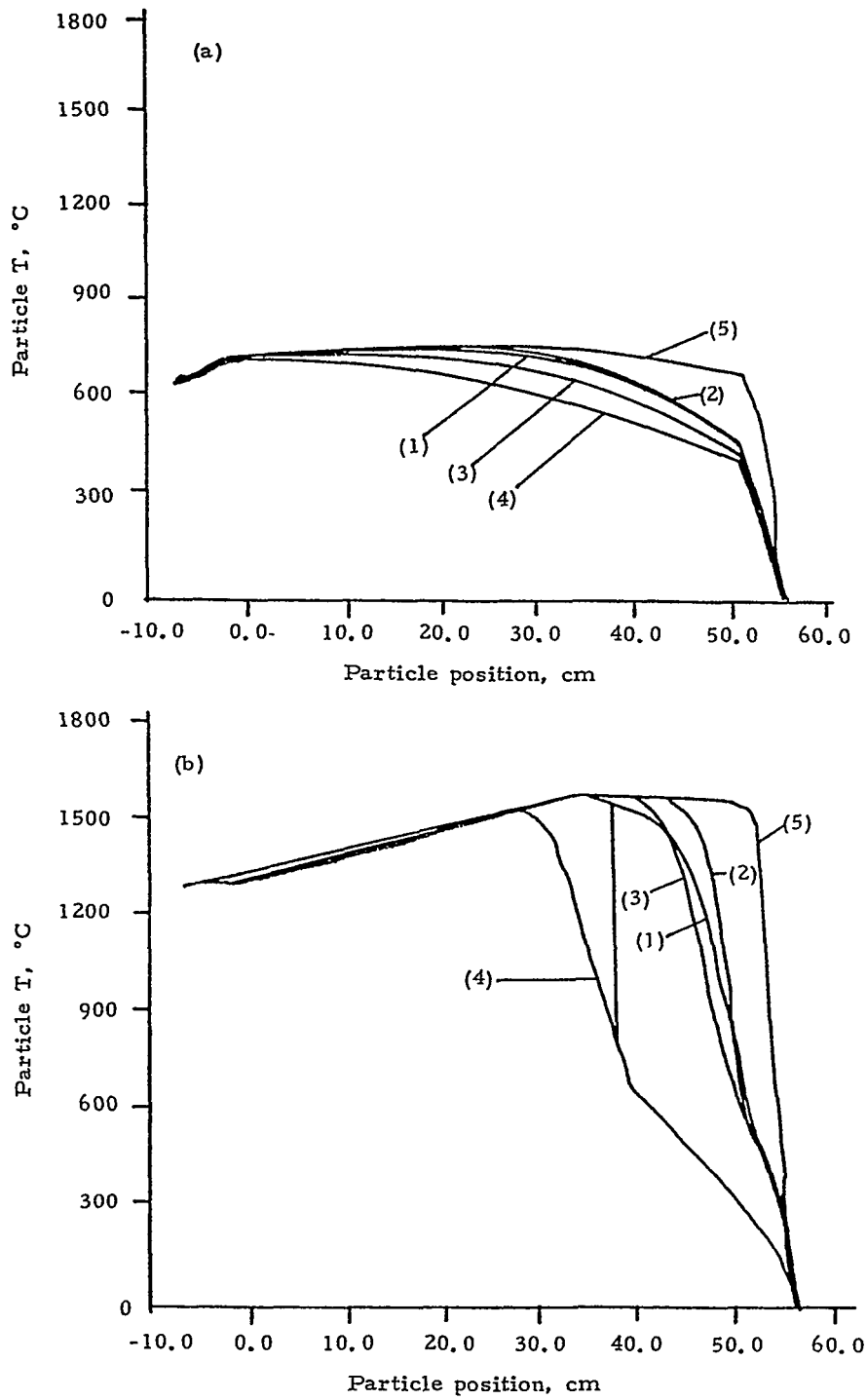

Fig. 12.3-4. Effect of various model assumptions on predicted temperatures in the entrained-flow reactor for North Dakota lignite (200 × 325 mesh), injected 56 cm above the optical port. Case (1): c_p = 0.3 cal/g-K; ϵ = 1.0; zero heat of pyrolysis, constant mass; case (2): the particle mass (kinetic) submodel is included in (1); case (3): the heat capacity submodel is included in (2); case (4): the emissivity submodel is included in (3); case (5): a single particle in an infinite gas volume is added to (4). Figure (a) refers to 800°C and (b) to 1600°C EFR experiments in nitrogen.

Table 12.3-1. A summary of rate expressions for coal pyrolysis.

Ref.	Model Rate (for)
62	weight loss from lignite at 10,000 K/sec (1 atm, excluding cooling)
62	weight loss from lignite at 10,000 K/sec (1 atm, including cooling)
62	weight loss from bituminous coal at 650 K/sec (1 atm)
62	weight loss from lignite (all pressures)
62	weight loss from bituminous coal (69 atm)
63	weight loss from lignite and bituminous coals
64	weight loss from bituminous coal
65	tar evolution
65	aliphatic gas evolution
2	weight loss for coal B
2	weight loss for coal F
66	tar evolution from bituminous coal
66	aliphatic gas evolution from bituminous coal
4	tar evolution from lignite, subbituminous, and bituminous coals
4	aliphatic gas from lignite, subbituminous, and bituminous coals
69	tar from lignite and subbituminous coals
69	aliphatic gases from lignite, subbituminous, and bituminous coals
69	weight loss from lignite, subbituminous, and bituminous coals
71	weight-loss rate for 50% reaction completion, subbituminous coal
24	tar from lignite, subbituminous, and bituminous coals
24	aliphatic gas from lignite, subbituminous, and bituminous coals
72	average for initial weight loss
76	weight loss for subbituminous coal
76	weight loss for bituminous coal
61	tar from lignite, subbituminous, and bituminous coals
61	aliphatic gases from lignite, subbituminous, and bituminous coals
61	weight loss from lignite, subbituminous, and bituminous coals
77,78	tar from ethylene-bridged anthracene polymer
77,78	tar from ethylene-bridged naphthalene polymer
77,78	tar from ethylene-bridged benzene polymer
79	bibenzyl decomposition in tetralin

Table 12.3-2. A summary of rate expressions for coal pyrolysis, continued. The following abbreviations apply: EFR, entrained-flow reactor; HTR, heated-tube reactor; Grid, heated grid reactor; Laser, laser-heating experiment; EGA, evolved gas analysis at 0.5 K/sec; S, single rate model; G, a model using a Gaussian distribution of activation energies; 2P, a model with two parallel rates.

Experiment and Reference	Frequency Factor k_o (sec^{-1})	Activation Energy, E_o (Kcal/mole)	Width of Activation Energy Distribution σ (Kcal/mole)	Model
Grid, 62	2.9×10^5	20.0	0.0	S
Grid, 62	283	11.1	0.0	S
Grid, 62	1800	13.3	0.0	S
Grid, 62	1.67×10^{13}	56.3	10.9	G
Grid, 62	1.67×10^{13}	50.7	7.0	G
EFR, 63	6.6×10^4	25.0	0.0	S
Grid, 64	70.5×10^2	17.2	0.0	S
Grid, 65	7.5×10^2	15.8	0.0	S
Grid, 65	4.2×10^3	17.7	0.0	S
EFR, 2	1.14×10^5	17.5	0.0	S
EFR, 2	3.12×10^5	17.5	0.0	S
Grid, 66	8.7×10^2	13.2	0.0	S
Grid, 66	2.3×10^{15}	68.9	11.4	G
Grid, EFR & EGA, 4	4.5×10^{13}	52.0	3.0	G
Grid, EFT & EGA, 4	1.7×10^{14}	59.1	3.0	G
HTR, 69	8.57×10^{14}	54.6	3.0	G
HTR, 69	8.35×10^{14}	59.1	3.0	G
HTR, 69	4.28×10^{14}	54.6	0.0	G
Drop tube, 71	1.0×10^3	7.6	0.0	S
Grid & EFR, 24	4.5×10^{12}	52.0	3.0	G
Grid & EFR, 24	1.7×10^{14}	59.1	3.0	G
EFR, 72	1.9×10^4	15.0	0.0	S
Laser, 76	2.25×10^4	28.0	0.0	2P
Laser, 76	2.85×10^5	33.4	0.0	2P
TGA/EGA, HTR & EFR, 61	8.6×10^{14}	54.6	3.0	G
TGA/EGA, HTR & EFR, 61	8.4×10^{14}	59.1	3.0	G
TGA/EGA, HTR & EFR, 61	4.3×10^{14}	54.6	0.0	S
TGA/EGA, 77,78	1.0×10^{15}	49.5	0.0	S
TGA/EGA, 77,78	1.0×10^{15}	56.2	0.0	S
TGA/EGA, 77,78	1.0×10^{15}	61.0	0.0	S
Tubing bomb, 79	7.9×10^{15}	65.0	0.0	S

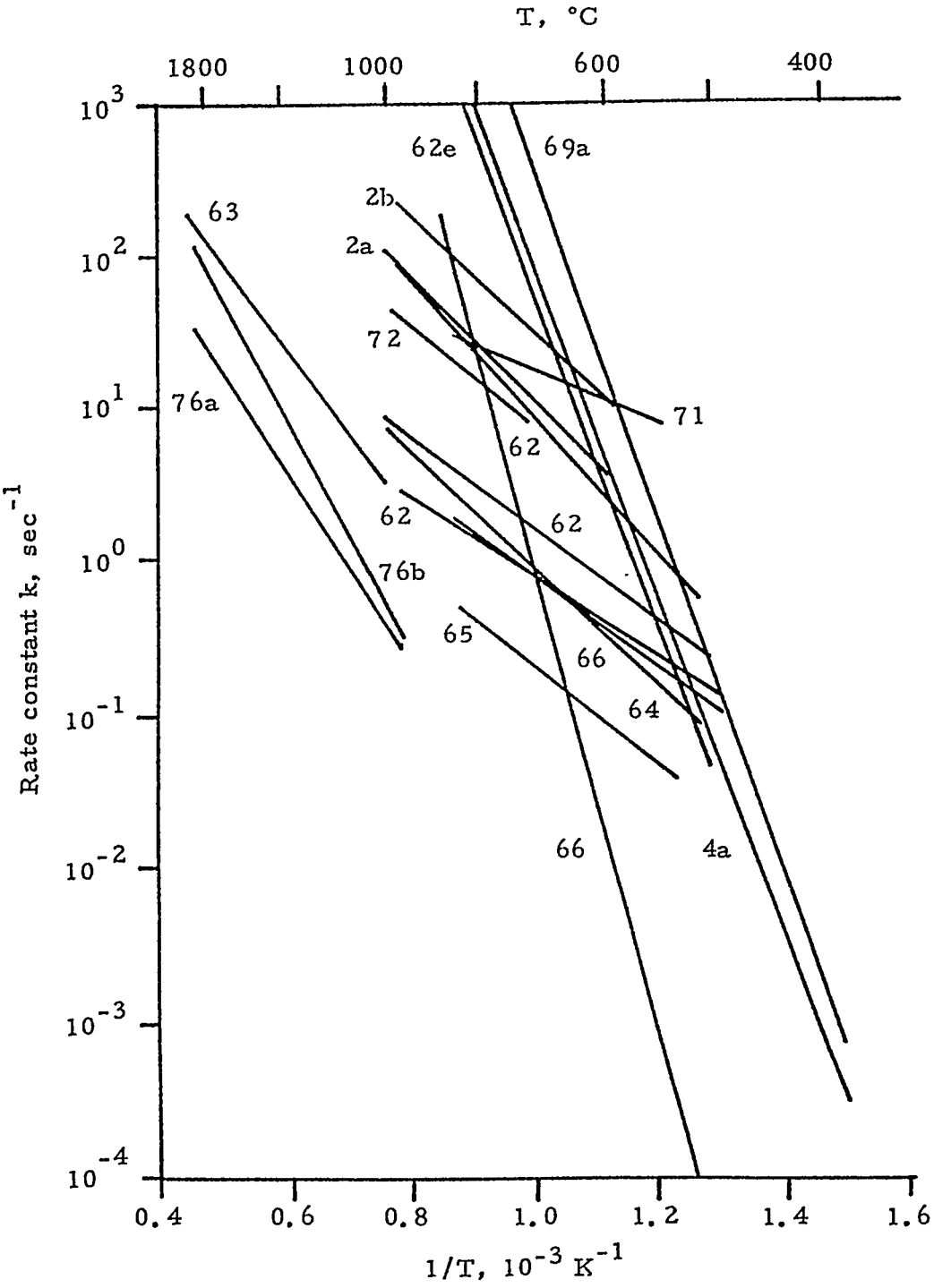

Fig. 12.3-5. Comparison of kinetic rates for weight loss (or tar loss) from many investigators. The numbers next to each line indicate the reference and case in Table 12.3-1.

Pyrolysis has been described by the following sequence:

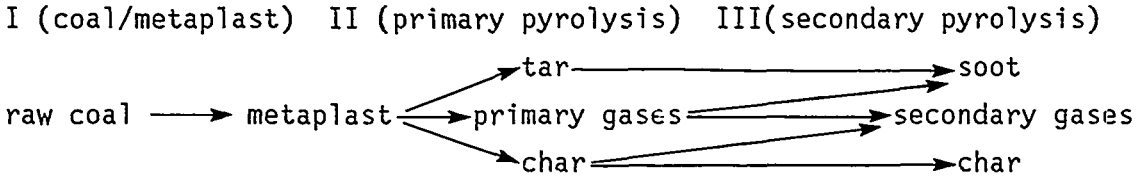

During stage I, the coal may undergo some bond-breaking reactions and reduction of hydrogen bonding, which may lead to melting. Some light species, which exist as guest molecules or are formed by the breaking of very weak bonds, are released. During stage II, further bond breaking occurs, leading to evolution of tar and gases and the formation of char. During stage III, the products may continue to react. The char may evolve secondary gases, mainly CO and H_2, while undergoing ring condensation. Ring condensation affects the active-site density. The tars can react to form soot, coke, and gases, and the gases may react to form lighter gases and soot.

A mechanistic description of these stages is shown in Fig. 12.3-6 by a hypothetical picture of the coal organic structure at successive stages of pyrolysis. Figure 12.3-6 represents: (a) the raw coal, (b) formation of tar and light HCs during primary pyrolysis, and (c) char condensation and cross-linking during secondary pyrolysis. The hypothetical structure in Fig. 12.3-6(a) represents the chemical and functional group compositions for a Pittsburgh seam bituminous coal.[80] which consists of aromatic and hydroaromatic clusters linked by aliphatic bridges. During pyrolysis, the weakest bridges [labeled 1 and 2 in Fig. 12.3-6(a)] may break, producing molecular fragments (depolymerizations). The fragments abstract hydrogen from the hydroaromatics or aliphatics, thus increasing the aromatic hydrogen concentration. These fragments will be released as tar if they reach a surface and vaporize. The two fragments labeled tar are small enough to vaporize under typical pyrolysis conditions, but the other two fragments are not. The other event during primary pyrolysis is the decomposition of functional groups to release CO_2, light aliphatic gases, and some CH_4 and H_2O. The release of CH_4, CO_2 and H_2O may produce repolymerization, CH_4 by a substitution reaction in which the attachment of a larger molecule releases

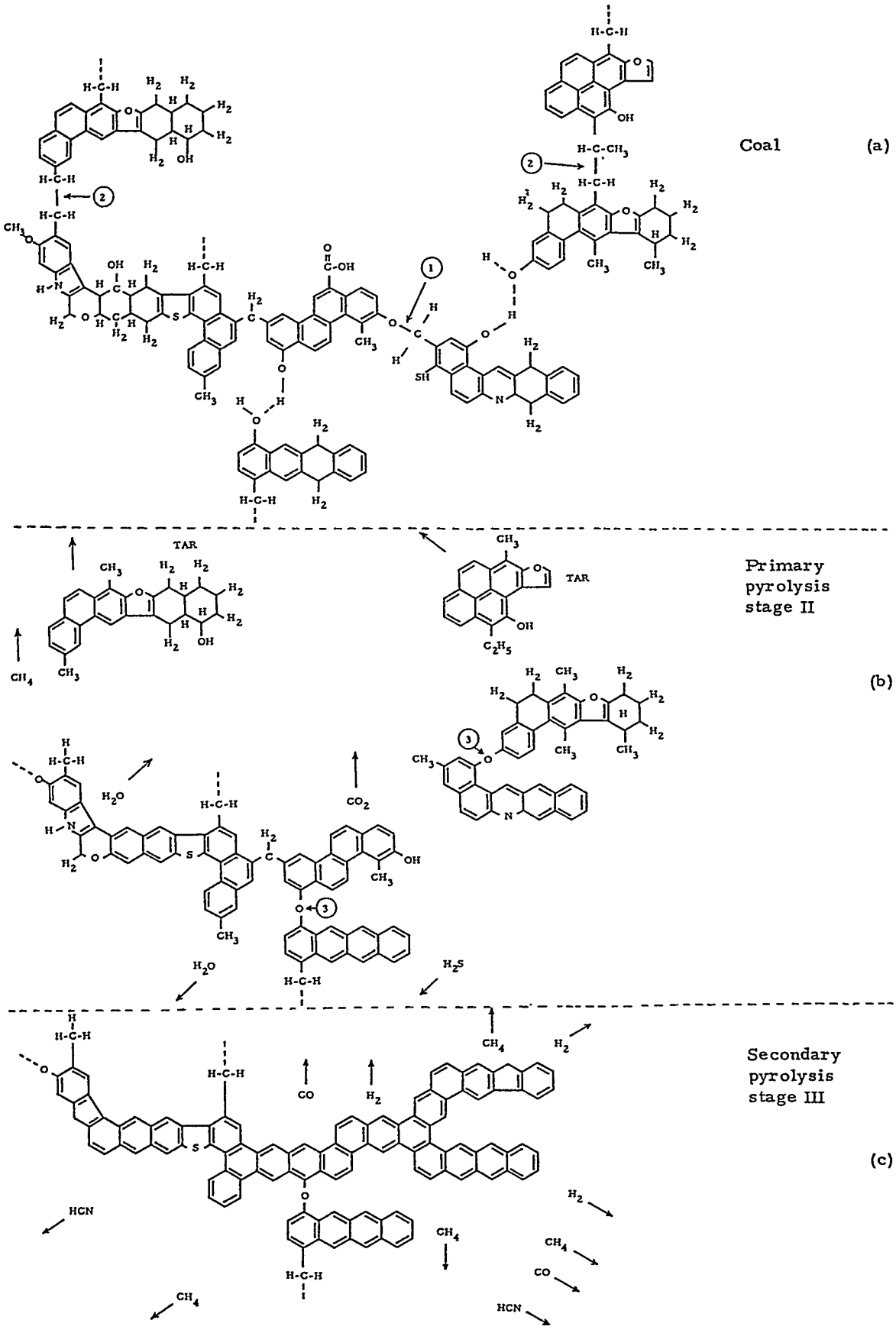

Fig. 12.3-6. A hypothetical coal molecule during three stages of pyrolysis.

the methyl group, CO_2 by radical stabilization after the CO_2 evolution creates a radical, and H_2O by the condensation of two OH-groups to produce an ether-link [labeled 3 in Fig. 12.3-6(b)]. The cross-linking is important to determine the tar release and the visco-elastic properties of the char. It may also be important in the rate of loss of active sites. The completion of primary pyrolysis occurs when the available hydrogen from hydroaromatics or aliphatics is depleted. The yield of tar can be correlated with the amount of aliphatic and hydroarmatic hydrogen in the coal.[24]

During secondary pyrolysis [Fig. 12.3-6(c)], there is additional evolution of CH_4 (from methyl groups), HCN from ring nitrogen compounds, CO from ether links, and H_2 from ring condensation. The ring condensation reduces the carbon available for oxygen attack and is therefore related to the intrinsic reactivity.

12.3-3A. Modeling

In view of the importance of coal pyrolysis in coal processing and in understanding coal structure, an accurate model of this phenomenon is highly desirable. There have been several recent reviews of the pyrolysis literature.[10,81-84] Coals have wide variability of volatile content, tar and soot production, swelling and sticking behavior, char reactivity, and pollutant formation. The behavior of coal depends not only on the chemical and physical properties of the coal but also on the conditions under which pyrolysis occurs. Most models of coal devolatilization have been developed to describe weight loss. While weight loss provides the split between char and volatiles, it does not involve questions about the chemical composition and heating value of the volatiles, release of polluting species, properties of the char (melting, swelling, agglomeration, reactivity), and dependence of these properties on bed geometry, pressure, and heating rate.

A number of more detailed models have recently been developed to address these issues. These range in complexity and include multiple reaction models, which describe the evolution of major species,[4,24-26,65,66,85] models incorporating the competition between depolymerization, mass transport and crosslinking to describe tar formation

(Refs. 62, 66, 27-29, 77, 78 and 86-93) and complete models with a detailed chemical description of coal decomposition.[27-29].

12.3-3B. Formation of Gas

Recent reviews of the pyrolysis literature have been presented by a number of authors.[81-84,10] A few models have been developed to describe the evolution of individual gas species. Individual product formations have been described by independent, first-order reactions, one for each product, have been employed.[85,82,25,66,93] Some of the products are formed by breaking two or more types of bonds, followed by a corresponding number of reactions. The number of reactions required for each product is judged from the shape of the experimental yield-temperature curves. An example comparing the model of Suuberg et al[93] with heated-grid data is presented in Fig. 12.3-7.

Solomon and coworkers[4,24-26,61,65,69] have described the parallel evolution of individual gas species in competition with tar formation. Tars can escape with some of the sources for the gas species. These sources have been related to the functional groups present in the coal by identifying corresponding changes in the functional group composition in the char as the gases evolve. A simplification introduced in this model is the assumption that the kinetics describing the evolution of individual species are insensitive to coal rank. This insensitivity to rank is reviewed in Ref. 94. An example from Ref. 60 of the application of this model to predict gas evolution from three different coals under different pyrolysis conditions is presented in Fig. 12.3-8. The same kinetic rates were used for other coals and temperature histories are varied.[60,61]

Most attention has been given to the major species (tar, CO, CO_2, H_2O, CH_4, etc.). There is some work on nitrogen evolution.[23,24,95] Data or models for sulfur release are scarce.[96]

12.3-3C. Formation of Condensables

The mechanisms of the formation of condensables (tar) have been considered by a number of investigators.[62,66,27-29,86-93] A review of current work was recently presented by Suuberg.[97] It is generally agreed

that the process includes the following steps: (i) formation of tar molecules, (ii) evaporation and transport, (iii) possible repolymerization to form char, and (iv) condensation to form soot. There is, however, little

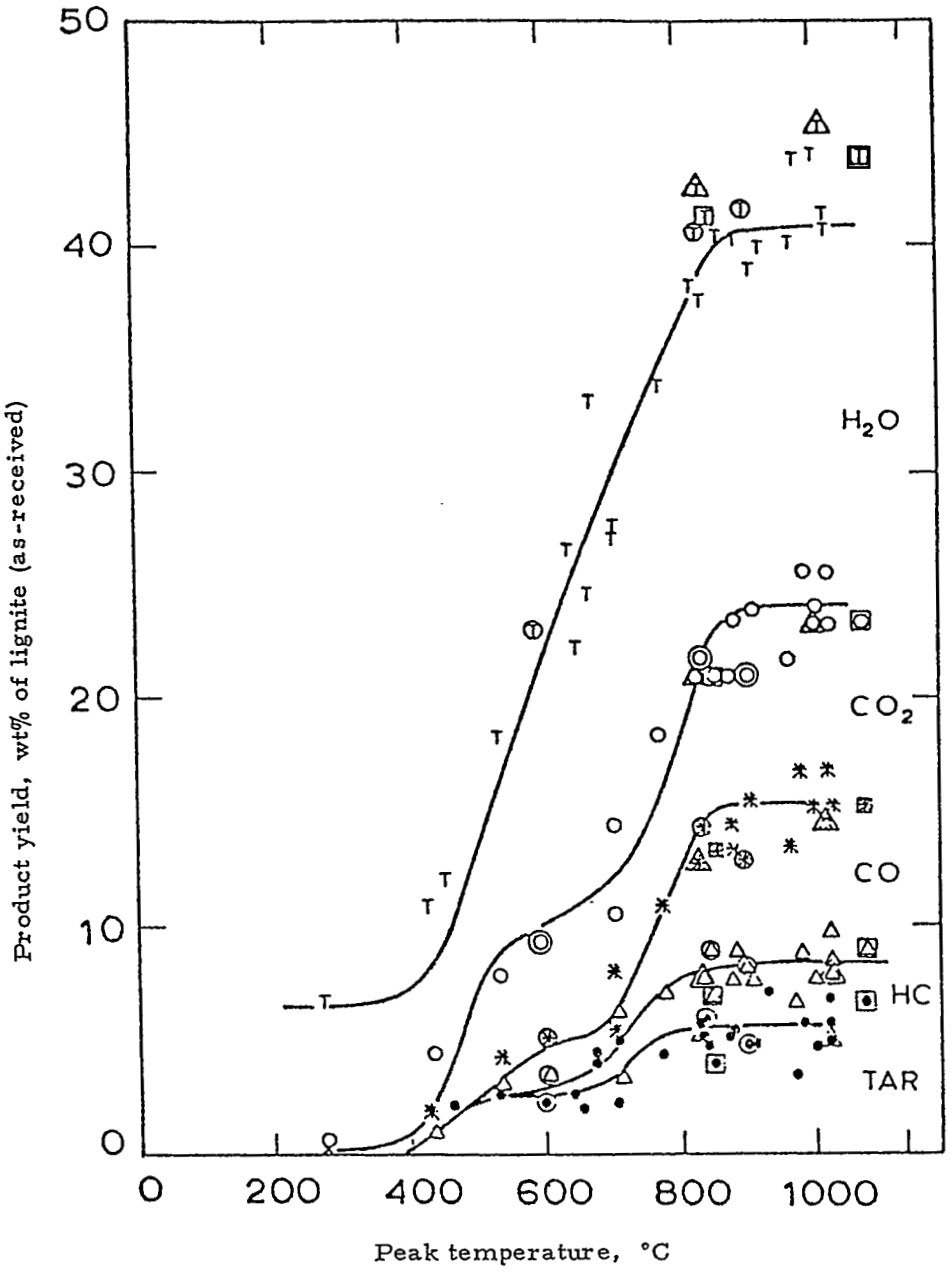

Fig. 12-3-7. Pyrolysis-product distributions from lignite heated to different peak temperatures [(●) tar; (△) tar and other hydrocarbons (HC); (✱) tar, HC, and CO; (O) tar, HC, CO, and CO_2; (T) total, i.e., tar, HC, CO, CO_2, and H_2O]. Pressure = 1 atm (He); heating rates: basic, 1000°C/s; points inside O, 7100 to 10,000°C/s; points inside △, 270 to 470°C/s; points inside □, 2-step heating. These curves are from Ref. 93 and are reprinted with permission.

agreement on the relative importance of these steps or how they are linked in a model which provides quantitative predictions. One problem is that the mechanisms are likely to change with coal rank.

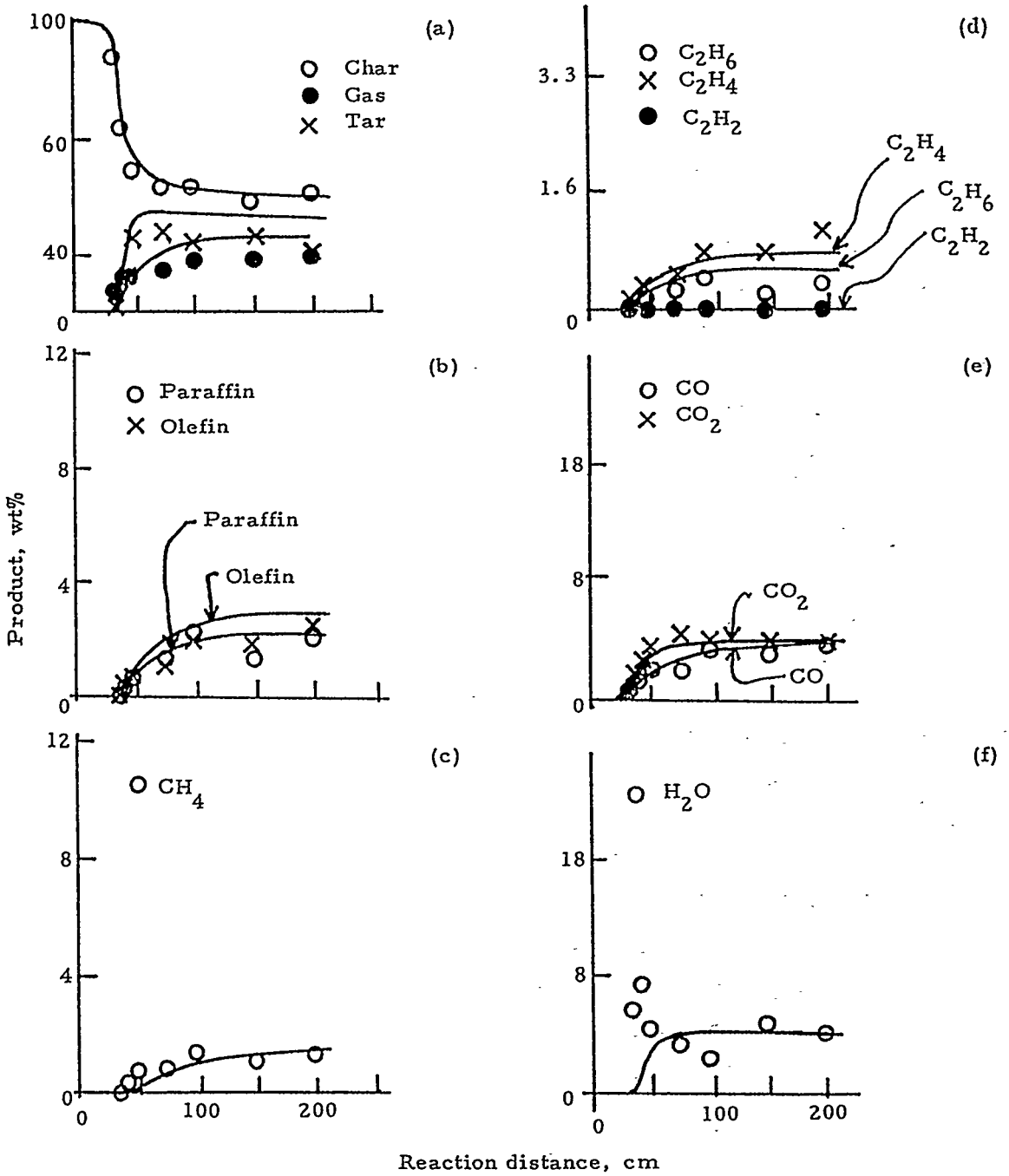

Fig. 12.3-8. Pyrolysis results for Illinois No. 6 coal, 200 × 325 mesh, in the heated tube reactor at an equilibrium tube temperature of 800°C. The solid lines are predictions from the functional group model. The gas and coal flows were 4.4 g/min (He) and 0.8 g/min, respectively.

Considering the available evidence reviewed in Ref. 88, tar formation in softening coals may be viewed as a combined depolymerization and evaporation process in which the pyrolytic depolymerization continually reduces the weight of the coal molecular fragments through bond breaking and stabilization of free radicals until the fragments are small enough to be evaporated. Crosslinking resolidifies the material.

Tar molecular weights for softening coals appear to be dominated by their vaporization characteristics. For non-softening coals, the average tar molecular weight, measured under slow heating conditions, is substantially less than predicted from vaporization.[88] It also appears to be much less than for tar measured under rapid heating conditions for the same coal.[89] The explanations, which must be tested, are repolymerization caused by crosslinking and/or transport limitations caused by the rigidity of the pore structure. Both effects will reduce the size of the oligomers that are released. Results of Suuberg et al[98] indicate that low-rank coals undergo substantial crosslinking prior to tar formation.

12.3-3D. Formation of Char

A methodology is needed to describe the physical and chemical development of char. This model is most difficult to obtain for a softening coal for which the physical structure changes from a pore system to a fluid medium with gas bubbles and cenospheres (for swelling coals). The required descriptions include an intra-particle transport model such as that of Simons,[99-102] which yields the pressure within the pores. The deformation of the pore walls is determined from this pressure and the viscosity of the melt. This model has been discussed by Melia and Bowman.[103] Descriptions of bubble transport have been given by Oh et al.[104] A description of bubble swelling and rupture has been presented by Solomon et al.[4] Bubble rupture may be the reason for the high-temperature disappearance of swelling at high heating rate.[3,4] Repolymerization and crosslinking effects are described by a number of authors[62,98,66,30,31,27-29,86-93] and will also be important.

A technique which has been employed to control the swelling properties of char is oxidation. It is important to develop an understanding and quantitative description of the effects of oxidation on swelling and the subsequent reactivity of the char.

12.3-3E. Gasification of Char

Understanding char reactivity is important since the consumption of char is the slowest and, therefore, the controlling process in gasification. Reviews of the char-oxidation literature have been published.[36,37] A comprehensive review of char gasification has been written by Laurendeau,[38] who discusses qualitative observations and quantitative models for reactions of char with CO_2, H_2O, O_2, and H_2. In a more recent review, van Heek and Muhlen[39] discuss the main factors influencing the reactivity of char in different gasifying agents. These reviews demonstrate that there is a wide variation in observed reactivities. Work described by Smoot[44] highlights the very large variations (1.5 orders of magnitude) in char reactivity depending on method of formation. Similarly, Ashu et al[105] found enhanced char reactivity caused by rapid heating of the precursor coal. More recently, Essenhigh and Farzar[106] measured very rapid burnout times for small coal particles in a vertical tunnel furnace. They ascribed their results to the firing condition, which gave heating rates in the 10^6 K/sec regime, compared with the more usual value of 10^4 K/sec in slower burning flames.

Both the formation conditions and reactivity vary with coal rank. Variations with coal type and pyrolysis conditions may be understood in terms of variations in active-site density, accessible surface area, and the catalytic effects of minerals. The active-site density is determined by the concentration of carbon edge sites and defects and by the concentration of hydrogen and oxygen (to some extent, also by sulfur and nitrogen) in the char. These chemical factors, combined with the mineral content and the pore structure, account for differences in char reactivity. Minerals have a significant positive effect on reactivity for low-rank coals. For most high-rank coals, minerals do not contribute greatly to the reactivity and may even have a negative impact because of pore blockage. Some minerals react with added catalysts and render them ineffective.[39]

The gasification or combustion reactions of char are generally described as falling into three rate-controlling regimes for which the reaction is limited by (i) intrinsic reactivity of the char itself, (ii) diffusion of reactants within the char pores, and (iii) diffusion of reactants between the char surface and the ambient atmosphere. These regimes are traversed successively as the temperature increases. At high

temperatures, the rate of chemical reaction may exceed the rate of transport of reactants to the surface, which is especially true for oxidation reactions. The mass-transport rate will be controlled by the char properties (porosity, pore-size distribution, and particle size), as well as the reaction conditions (pressure, temperature, and turbulence).

Research in this area should be directed at (i) defining appropriate characterization procedures for the char structure through reactivity measurements at temperature appropriate to gasifier conditions, (ii) developing a description of the varying reactivity during char gasification and (iii) developing a better understanding of the role of mineral matter and added catalysts.

12.3-3F. Secondary Reactions of Condensables

Secondary reactions of tars may be of the cracking type, which forms lighter tars, light oils ($<C_{10}$) and/or light gases ($<C_5$), or of the polymerization-condensation type, which leads to heavier tars, or, ultimately, coke and soot (although small amounts of light gases are eliminated). The nature and extent of the secondary tar reactions are influenced by coal type, temperature, ambient gas composition, mass transfer of the primary tars away from their source, and the characteristics of any surfaces that may be encountered. Depending on the process, operating conditions, and coal type, secondary tar reactions will have a minor or major impact in the following areas: (i) product distribution (between solid, liquid, and/or gas); (ii) product heating value; (iii) char reactivity (by obstruction of pores or active sites); (iv) disposition of sulfur, nitrogen, and oxygen among the products of coal pyrolysis; (v) formation of soot and polycyclic aromatic hydrocarbons (PAH); (vi) particle ignition and flame stability; (vii) coal plasticity and coke properties; and (viii) evolution of unreacted tars from the gasifier.

For mild gasification, secondary reactions are desirable to the extent that they improve the quality of the liquids produced, although they also reduce the overall yield of the liquids. Better knowledge of the fundamental nature of the secondary reactions is required in order to optimize the yields of these processes. Some information on homogeneous

tar-cracking reactions is available from previous work.[107-110] There is currently only qualitative information on heterogeneous reactions[107,108,111] and on the transformation of tar to soot.[112]

12.4. The Behavior of Coal Mineral Matter in Gasification

Inorganic constituents of coal consist of both discrete mineral particles (inclusions) and elements that are bonded to organic molecules. As the organic matter in the coal is gasified, the inorganic constituents form increasingly the bulk of the residual material of the gasification process. Depending on the type of process, this inorganic residue is removed as a dry, powdery fly ash, sintered ash, or molten slag. The physico-chemical transformations of the coal mineral matter depend on its chemical and mineralogical composition and its temperature-concentration history in the gasification process. Most of the information about coal mineral-matter transformation comes from coal-combustion studies, mainly because of the troublesome slagging and fouling of heat exchangers in coal-fired boilers. While heat-exchanger fouling is a lesser problem in coal gasification, removal of the ash from the gasifier and cleaning of the gas require knowledge of the state, chemical, and mineralogical composition of the ash and the particle size of the fly ash carried over from the gasifier with the product gas.

12.4-1. The Nature of Mineral Matter in Coal and Its Characteristics

Coal is a sedimentary deposit, which explains its widely variable overall composition. As mined, most coals contain shales, sandstones from adjoining strata, and also inorganic matter such as alkali- and alkaline-earth metals and sulfur, which were part of the coalified vegetation, are associated with the organic material, and are dispered on an atomic scale in the coal. These may be chemically combined with the carbonaceous material or as ions absorbed from groundwaters. Other minerals, such as sulfides and carbonates, form inclusions in voids in the coal seam between fracture surfaces of hard coals by deposition from percolating water. Table 12.4-1 lists some of the mineral compounds found in coals, along with their usual manner or mode of occurrence.[114]

Traditionally, ash chemistry was used for coal mineral-matter characterization. In recent years, new analytical methods have become available, which are capable of much more detailed and useful characterizations. Computer-controlled scanning electron microscopy (CCSEM), scanning transmission electron microscopy (STEM), and x-ray diffraction (XRD) have been used to determine the types, amounts, and size distributions of mineral matter in coal. Types of iron-bearing minerals can be distinguished quatitatively by Mossbauer spectroscopy. The electronic bonding structure and local atomic environment of inorganic species that are organically bonded within the coal macerals, such as sulfur, calcium and alkalies, may be identified by x-ray absorption fine-structure spectroscopy (EXAFS) and energy-loss spectroscopy (EELS). Other techniques, which have been used successfully, include Fourier-transform infrared (FTIR) spectroscopy, use of an electron microprobe, electron spectroscopy for chemical analysis (ESCA), proton-induced x-ray emmission (PIXE), etc. While in recent years significant progress has been made in the development of these new analytical techniques, their further development is essential for detailed characterization of the types, amounts, size distributions, and structures of inorganic matter in coal.

12.4-2. Behavior During Heating

In the initial stages of heating, the mineral matter undergoes a number of changes, some of which are shown in Fig. 12.4-1. First, at temperatures below 500 K, the water absorbed on the coal substance or combined with the mineral matter is dried off. At temperatures ranging from 500 to 1000 K, carbonates and sulfates decompose with significant associated weight loss in the ash as CO_2, SO_2, and SO_3 are evolved.

The organic material in the coal substance also undergoes thermal decomposition, yielding hydrocarbon vapors. Some elements, which are physically adsorbed or are organically combined in the coal such as chlorine and sulfur, evolve as volatiles; the organic sulfur may pyrolyze to give a elemental sulfur and its hydrites and the chlorine are probably released as HCl.[116]

Because of the weight loss associated with thermal decomposition of the ash, the weight of the ash determined by the ASTM test is usually lower than that of the original mineral content of the coal. The weight of

the original mineral matter is better approximated by the low-temperature ash determination[117] and is of the order of 20% greater than that of the ASTM ash.

A summary of minerals identified in coals is given in Table 12.4-1.

12.4-3. Mineralogical Transformations at High Temperatures

As the temperature exceeds 1300 K, alkalies in the form of salts (NaCl and KCl) are volatilized. Those bound in complex aluminum silicates are less likely to vaporize and, in these mineralogical forms, alkalies are less active in a slagging-fouling processes.

Sintering in the mineral matter begins to take place at temperatures as low as 1000 K. Because of interaction of the ash constituents and the formation of low melting-point eutectics, the melting point of the ash is usually lower than that of the pure mineral compounds. For example, at temperatures between 1150 and 1500K, illite ($2K_2O$ 3MgO Al_2O_3 $24SiO_2$ 12 H_2O) undergoes dehydration leading to the formation of spinel (crystalline magnesium-iron-aluminates) while the alkali, the silica, and the remainder of the alumina produce a glassy mass. The spinel then dissolves in this glassy mass. Parallel with these reactions and at about 1400 K, mullite ($3AL_2O_3$ $2SiO_2$) begins to form. Mullite also dissolves in the glassy melt and forms a liquid phase in the presence of alkalies. Because of the eutectics formed during the reactions in the slag, slag-melting temperatures may sometimes be reduced by high melting-point compounds, as for example CaO and MgO in acidic slags in SiO_2 in lime-containing basic slags.

Because of the complexities of the physico-chemical processes in slags, efforts to predict softening -melting behavior from the chemical composition of the ash have not met with much success. It is one of the challenging problems to determine the softening-sintering-melting behavior under the conditions found in the gasification process from the chemical and mineralogical composition of the mineral matter in the coal.

12.4-4. Ash Agglomeration

At elevated temperatures as in slagging gasifiers, the mineral inclusions in coal decompose, melt and form small spherical particles that

attach themselves to the receding carbonaceous particles.[118] Even though molten ash does not appreciably wet carbon surfaces,[119] only slight melting is needed to provide ash adherence since its surface tension is high (~ 320dyne/cm).[119] Because the ash is not separated from the carbon matrix during combustion, the ashed mineral particles will be drawn together and coalesce as the carbon surface recedes.[118,120,121]

The ash particle-size distribution depends on the processes of ash agglomeration, but it is also strongly influenced by the fragmentation of the char as it undergoes gasification. Recent research on heterogeneous reactions involving coal char indicate that the solid particle undergoes percolative fragmentation during its reaction. In the course of the reaction, the particle is penetrated by the gaseous reactant and becomes increasingly porous. At a critical porosity of about 0.7-0.8, the layer of the particle loses its structural integrity and breaks off as a fragment. In the regime controlled by chemical kinetics, the whole particle may be uniformly penetrated by the gaseous reactant and may disintegrate into fragments when the critical porosity is reached.

12.5. Mathematical Modeling

In order to understand and obtain quantitative predictions of how the individual chemical and physical steps described in Sec. 12.3 and 12.4 affect the overall gasification process, it is necessary to develop computational procedures which incorporate these steps in a comprehensive gasifier model. Models which are common to both gasification and combustion are being developed, and an extensive review of their status was presented by Smoot,[122,123] who noted that modeling of coal-reaction processes has not reached the point where significant use is made of it in process development for coal utilization.

12.5-1. Status of Model Development

We refer to Smoot[122,123] for review of this problem. Modeling of turbulent reaction processes is still in a state of development. At least 6 fixed-bed, 10 fluidized-bed and 14 pulverized-coal conversion models have been developed since 1970. In general, the approach used in advanced combustion models is sound. However, unresolved fundamental issues remain.

Table 12.4-1. Minerals identified in coals (after Gluskoter[113]).

Mineral	Chemical Formula	Association with Coal
Clay minerals		
Montmorillonite	$Al_2Si_4O_{10}(OH)_2 \ xH_2O$	This material is finely-dispersed in coal substance. It is the principal constituent of shales. Crystals are < 1 μm. Impregnation occurs in joints in brown coal.
Illite-sericite	$KAl_2(AlSi_3O_{10})(OH)_2$	
Kaclinite	$Al_2Si_4O_{10}(OH)_8$	
Halloysite	$Al_4Si_4O_{10}(OH)_8$	
Chlorite (prochlorite, penninite)	$Mg_5Al(AlSi_3O_{10})(OH)_8$	
Mixed-layer clay minerals		
Sulfide minerals		
Pyrite	FeS_2	The minerals occur in modules and crystals (10 cm to < 1 μm) in coal substance and in joints and cleats. Pyrite and marcasite are the principal sulphides. This is the principal form of iron in most hard coals.
Marcasite	FeS_2	
Sphalerite	ZnS	
Galena	PbS	
Chalcopyrite	$CuFeS_2$	
Pyrrhotite	$Fe_{1-x}S$	
Arsenopyrite	$FeAsS$	
Millerite	NiS	
Carbonate minerals		
Calcite	$CaCO_3$	The minerals occur in hard coals that are present mainly in joints and cleats. They constitute the principal form of calcium and magnesium and the secondary form of iron.
Dolomite	$(Ca, Mg)CO_3$	
Siderite	$FeCO_3$	
Ankerite (ferroan dolomite)	$(Ca, Fe, Mg)CO_3$	
Witherite	$BaCO_3$	
Sulfate minerals		
Barite	$BaSO_4$	Minerals are deposited from ground-waters.
Gypsum	$CaSO_4 \ 2H_2O$	
Anhydrite	$CaSO_4$	
Bassanite	$CaSO_4 \ \frac{1}{2}H_2O$	
Jarosite	$(Na, K)Fe_3(SO_4)_2(OH)_6$	These are principally formed as a result of weathering (aqueous oxidation of sulphides).
Szomolnokite	$FeSO_4 \ H_2O$	
Rozenite	$FeSO_4 \ 4H_2O$	
Melanterite	$FeSO_4 \ 7H_2O$	
Coquimbite	$Fe_2(SO)_3 \ 9H_2O$	
Roemerite	$FeSO_4 \ Fe_2(SO_4)_3 \ 12H_2O$	
Mirabilite	$Na_2SO_4 \ 10H_2O$	
Kieserite	$MgSO_4 \ H_2O$	
Sideronatrite	$2Na_2O \ Fe_2O_3 \ 4SO_3 \ 7H_2O$	
Chloride minerals		These are occasionally present as discrete crystals, often as ions adsorbed on coal substance (vitrinite). They can be recrystallized from solution after wetting.
Halite	$NaCl$	
Sylvite	KCl	
Bischofite	$MgCl_2 \ 6H_2O$	

Table 12.4-1. Continued

Mineral	Chemical Formula	Association with Coal
Silicate minerals		Major silicates occur with clay minerals. Biotite is the principal compound of potassium. Quartz is present as sediment in round to angular grains of ~1 mm to <1 μm. Impregnation of joints occurs in brown coal.
Quartz	SiO_2	
Biotite	$K(Mg, Fe)_3(AlSi_3O_{10})(OH)_2$	
Zircon	$ZrSiO_4$	These are accessory minerals and are usually present in minor and variable proportions.
Tourmaline	$Na(Mg, Fe)_3Al_6(BO_3)_3(Si_6O_{18})(OH)_4$	
Garnet	$(Fe, Ca, Mg)_3(Al, Fe)_2(SiO_4)_3$	
Kyanite	Al_2SiO_5	
Staurolite	$Al_4FeSi_2O_{10}(OH)_2$	
Epidote	$Ca_2(Al, Fe)_3Si_3O_{12}(OH)$	
Albite	$NaAlSi_3O_8$	
Sanidine	$KAlSi_3O_8$	
Orthoclase	$KAlSi_3O_8$	
Augite	$Ca(Mg, Fe, Al)(Al, Si)_2O_6$	
Hornblends	$NaCa_2(Mg, Fe, Al)_5(SiAl)_8O_{22}(OH)_2$	
Topaz	$Al_2SiO_4(OH, F)_2$	
Oxide and hydroxide minerals		
Hematite	Fe_2O_3	
Magnetite	Fe_3O_4	
Rutile	TiO_2	
Limonite	$FeO\ OH\ nH_2O$	These minerals are products of weathering.
Goethite	$FeO\ OH$	
Lepidocrocite	$FeO\ OH$	
Diaspore	$AlO\ OH$	
Phosphate mineral		
Apatite (fluorapatite)	$Ca_5(PO_4)_3(F, Cl, OH)$	
Combined with or adsorbed on organic matter		
Calcium	Ca	Some of these elements are particularly associated with specific coal minerals.
Magnesium	Mg	
Sodium	Na	
Sulphur	S	
Vanadium	V	
Nickel	Ni	
+ numerous other "trace" elements		

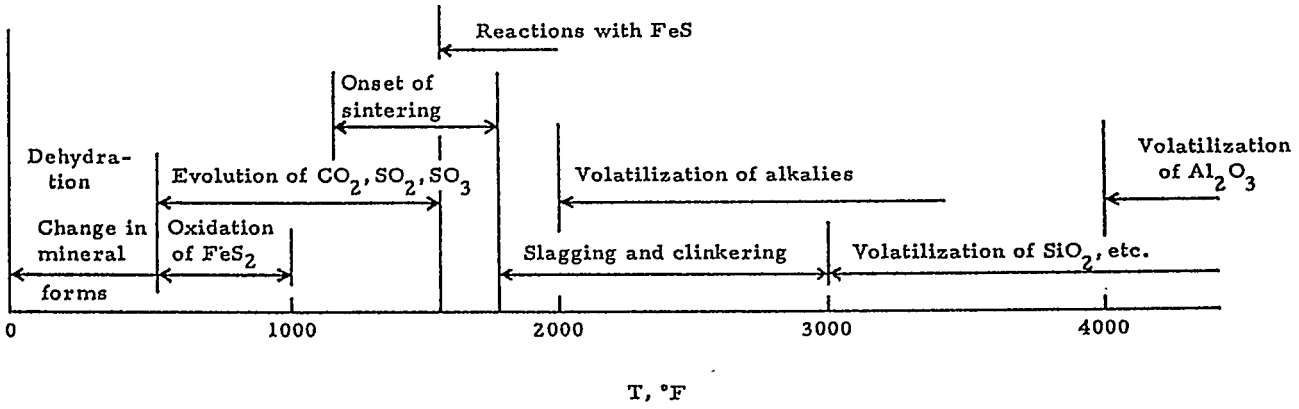

Fig. 12.4-1. Temperature ranges over which ash undergoes various chemical and physical transformations.[115]

Important among these are the progress of gasification reactions in porous char particles, fluid and particles dynamics, interactions of turbulence and chemical reactions, and the spatial dispersion of reacting particles in hot gas flows.

For the evaluation of computer codes, laboratory and pilot plant experiments are necessary, in which the effects of fluid dynamics, heat transfer and chemical kinetics on the progress of carbon conversion in the reactor may be studied independently. This approach requires special experimental facilities and measurements at levels of sophistication and detail that are not practicable in full-size plants. Such rigorous testing of models proved to be most useful for the introduction of computer codes of radiative heat-flux distribution into utility-boiler design-practice in the 1970s.[124]

12.6. Research Recommendations

We now present brief comments on the research recommendations for the gasification problem areas listed in Table 12.1-1 that have been discussed in this chapter.

12.6-1. Coal Characterization

While there are a number of standard characterization procedures for coal, they often do not provide information appropriate for advanced

processes. Methods are needed to provide organic structure, viscosity and reactivity parameters from which coal behavior in gasification can be accurately predicted.

Work is required to define mineral-characterization procedures and methodology to relate the test results to ash behavior under gasifier operating conditions.

12.6-2. Fundamental Processes in Gasification and Partial Gasification

The objective is to gasify coals of different rank reliably in the shortest time under the lowest severity conditions and with small amounts of tars or fines exiting from the reactor. For mild gasification, the objective is a high yield of quality products. These processes are controlled by heat transfer, pyrolysis rates, devolatilization, char gasification, and secondary reactions of condensables and gases.

12.6-2A. Heat Transfer

There is a lack of data on the fundamental parameters involved in heat transfer (heat capacity, emissivity, heats of reaction, effects of volatile evolution on convective heat transfer, coal thermal conductivity, etc.). While some data have been obtained and models have been developed for determination of heat capacity and emissivity, experiments should be performed to determine these properties for a variety of coals and conditions. Work relating to heats of reaction and parameters affecting convective heat transfer needs to be initiated. Heat-transfer calculations employing measured parameters should be validated under gasification conditions by employing well-instrumented laboratory-scale experiments which allow coal-particle temperature measurements.

12.6-2B. Pyrolysis Rates

Accurate determinations of the important chemical kinetic rate(s) in pyrolysis must be performed in experiments where coal-particle temperatures are directly measured or can be accurately determined. At heating rates above 10,000°C/sec, attention must be given to temperature gradients within the particle. Experiments should be compared by using an

agreed-upon standard model. This model may include one or more rate expressions, which are independent of heating rate or experimental geometry. The use of a small set of standard coal samples by several investigators should be encouraged.

12.6-2C. Devolatization, Formation of Gases, Condensables and Char

Work should proceed towards finding an acceptable standard model to describe the devolatilization process. Experimental and theoretical work is particularly needed on sulfur evolution, on tar formation and char viscosity (including depolymerization, mass transport, and crosslinking processes), and on the formation of char (swelling, pore structure and reactivity).

12.6-2D. Gasification of Char

There is a need to develop a better understanding of the chemical factors (i.e., functional group composition, minerals) which influence intrinsic reactivity and how the observed reactivity is affected by physical factors (pore structure). For catalytic gasification, the dispersion of catalyst in the char is an important issue, along with interactions of added catalysts with minerals already present in the char. The elutriation of highly unreactive carbon in the form of fines from gasifiers is a problem, the solution of which would benefit from a more fundamental understanding of gasification reactions.

Studies should include work on model chars made from pure compounds. Better measurements of surface area, active area, pore size, pore-size distribution, and density must be developed. The application of analytical techniques used in surface science and catalysis research would be beneficial, along with development of better mathematical representations of pore structures. Of importance is the extension of measurements of the fundamental phenomena to higher temperature ranges, which requires *in situ* measurements of particles by using probes for the purpose of surface characterization.

12.6-2E. Secondary Reaction of Condensables

There is a need for kinetic data and models for product evolution from the gas-phase cracking of tars for a wide range of coals. There is also need for information on the kinetics of soot formation from tar. Information is required on mechanisms and kinetics of secondary repolymerization reactions of tars, which occur on surfaces inside and outside of the parent coal particle. This work is important in understanding the yields and quality of co-products generated in mild gasification.

12.6-2F. Mineral-Matter Transformation

A quantitative understanding is needed of residual ash-particle formation. Theoretical developments, such as the recent application of percolation theory to the problem of char fragmentation, may be useful. Detailed characterizations of mineral distribution in coal and char at progressive stages of gasification are necessary for the development of a predictive model of mineral-matter transformation. Well-characterized coals and synthetic coal or char-like materials are essential in the critical evaluation of fundamental models of ash dynamics. Methods for the measurement of particle properties in the hot gasification environment require further work. The development of techniques to measure physical properties, such as viscosity and degree of sintering, at gasifier temperatures is important since the cooling which occurs on sampling may seriously alter these properties. Measurement methods for vapor-species concentrations are needed, as are also methods for correcting measurements of ash-chemical compositions during the condensation of vapor-phase compounds occurring in the sampling process. Particle temperature-time history measurements in practical gasifiers are needed as inputs to the ash-evolution model-development efforts.

12.6-3. Mathematical Modeling of Gasification Processes

We refer to Refs. 122 and 123 for elaboration of coal-combustion models relating to direct coal use. The requirements for gasification modeling are generally similar. We recommend studies on fixed-bed models

because of their importance in gasification and partial gasification. Support should also be provided for well-instrumented and flexible laboratory-scale experiments, which can be employed to validate selected aspects of the comprehensive codes.[59,124]

References

1. Annual Book of ASTM Standards, Sec. 5, Vol. 05.05, "Gaseous Fuels; Coal and Coke," ASTM,Philadephia, PA (1985).
2. A. Badzoich and P. G. W. Hawksley, Ind. Eng. Chem. Proc. Res. Dev. 9, 521 (1970).
3. J.M. Pohl, H. Kobayashi, and A.F. Sarofim, "The Effects of Temperature and Time on the Swelling of Pulverized Coal Particles," M.I.T. Industrial Liaison Program, Symp. Paper, Cambridge, MA (Oct. 2, 1979).
4. P.R. Solomon and D. G. Hamblen, in Chemistry of Coal Conversion, p. 121, R. H. Schlosberg ed., Plenum Press, NY (1985).
5. ASME Research Committee on Corrosion and Deposits from Combustion Gases, "Recommendation for Research Leading to New Bench-Scale Experiments for the Prediction of Slagging and Fouling Behavior" (1986).
6. R.C. Neavel, S.E. Smith, E.J. Hippo, and R.N. Miller, Fuel 65, 312 (1986).
7. Coal and Coal Products: Analytical Characterization Techniques, ACS Symp. Series No. 205, ACS, Washington, D.C. (1982).
8. Symposium on Physical Methods for Fossil Fuels Characterization, ACS Div. of Fuel Chem. Preprints 30 (1), 1-220 (1985).*
9. Symposium on New Applications of Analytical Techniques of Fossil Fuels, ACS Div. of Fuel Chem. Preprints 31, (1), 1-272 (1986).
10. G.R. Gavalas, Coal Science and Technology 4: Coal Pyrolysis, Elsevier Scientific Publ. Co., NY (1982).

---

* When multiple references appear to (symposium) volumes, these are not repeated. Instead, they are identified in this reference list by simply referring to the reference number that is used with the first-named entry referring to the (symposium) volume.

11. R.M. Davidson, "Nuclear Magnetic Resonance Studies of Coal," IEA Coal Research, Report No. ICTIS/TR32, London (Jan. 1986).
12. M. A. Wilson, R.J. Pugmire, J. Karas, L.B. Alemany, W.R. Woolfenden, D.M. Grant, and P.H. Given, Anal. Chem. 56, 993 (1984).
13. K.W. Zilm and G.G. Webb, p. 200 in Ref. 9.
14. P.C. Painter, R.W. Snyder, M. Starsinic, M.M. Coleman, D.W. Keuhn, and A. Davis, Appl. Spectros, 35, 475 (1981).
15. M. Sobkowiak, E. Riesser, R. Given, and P. Painter, Fuel 63, 1245 (1984).
16. B. Riesser, M. Starsinic, E. Squires, A. Davis, and P.C. Painter, Fuel 63, 1253 (1984).
17. D. W. Kueh, R.W. Snyder, A. Davis, and P.C. Painter, Fuel 61, 682 (1982).
18. P.C. Painter, M. Starsinic, E. Squires, and A.A. Davis, Fuel 62, 742 (1983).
19. P.R. Solomon, "Coal Structure," p. 95, ACS Advances in Chemistry Series, No. 192, ACS, Washington, D.C. (1981).
20. P.R. Solomon, D.B. Hamblen, and R.M. Carangelo, "Coal and Coal Products: Analytical Characterization Techniques," p. 77 in Ref. 7.
21. P.R. Solomon and R.M. Carangelo, Fuel 61, 663 (1982).
22. P.R. Solomon, D.G. Hamblen, R.M. Carangelo, J.R. Markham, and M.R. Chaffee, p. 1, in Ref.
23. P.R. Solomon and M.B. Colket, Fuel 57, 748 (1978).
24. P.R. Solomon, D.G. Hamblen, R.M. Carangelo, and J.L. Krause, 19th Symposium (Intl.) on Combustion, pp. 1139-1149 (1982).
25. E.M. Suuberg, W.A. Peters, and J.B. Howard, Thermal Hydrocarbon Chemistry, ACS Advances in Chemistry Series, No. 183, p. 239, ACS, NY (1979).
26. P.R. Solomon, R. H. Hobbs, D.G. Hamblen, W.Y. Chen, A. La Cava, and R.S. Graff, Fuel 60, 342 (1981).
27. R. Jain, Ph.D. Thesis, Calif. Inst. Tech., Pasadena, CA (1979).
28. G.R. Gavalas, P.H. Cheong, and R. Jain, Ind. Eng. Chem. Fund. 20, 113 (1981).
29. G.R. Gavalas, R. Jain, and P.H. Cheong, ibid 20 122 (1981).
30. W.S. Fong, Y.F. Khalil, W.A. Peters, and J.B. Howard, pp. 1-115 in Ref. 8.
31. W.S. Fong, Y.F. Khalil, W.A. Peters, and J.B. Howard, Fuel 65, 195 (1986).

32. C.J. Chu, R.H. Hauge, and J.L. Margrave, p. 87 in Ref. 9.
33. H.L.C. Meuzelaar, W. Windig, and G.A. Metcalf, p. 200 in Ref. 8.
34. R.M. Carangelo, P.R. Solomon, and D.J. Gerson, p. 152 in Ref. 9.
35. Om. P. Mahajan, R. Yarzab, and P.L. Walker, Jr., Fuel 57, 643 (1978).
36. I.W. Smith, pp. 1045-1065 in Ref. 24.
37. R.H. Essenhigh, Chemistry of Coal Utilization 2nd Supplementary Vol., M.A. Elliot ed., p. 1162, John Wiley & Sons, NY (1981).
38. N.M. Laurendeau, Progr. Energy Comb. Sci. 4, 221 (1978).
39. K.H. Van Heek and H.J. Muhlen, Fuel 64, 1405, (1985).
40. R.G. Jenkins, S.P. Nandi, and P.L. Walker, Jr., Fuel 52, 288 (1973).
41. L.R. Radovic and P.L. Walker, Jr., Fuel 62, 849 (1983).
42. B.W. Brown, L.D. Smoot, and P.O. Hedman, Fuel 65, 673 (1986).
43. W.F. Wells, S.K. Kramer, and L.D. Smoot, 20th Symposium (Intl.) on Combustion, p. 1539 THe Combustion Institute, Pittsburgh, PA (1984).
44. N.Y. Nsakala, R. Patel, and T.C. Lao, "Combustion and Gasification Characteristics of Chars from Four Commercially Significant Coals at Different Rank," Report No. 1654-6, ERPI, Palo Alto, CA (1982).
45. E.M. Suuberg, J.M. Calo, and M. Wojowicz, p. 186 in Ref. 9.
46. J.L. Johnson, ACS Div. of Fuel CHem. Preprints, 20 (4), 85 (1975).
47. P.R. Solomon, M.A. Serio, and S.G. Heninger, ACS Div. of Fuel Chemistry Preprints 31, (3), 200 (1986).
48. E. Raask, Mineral Impurities in Coal Combustion: Behavior, Problems, and Remedial Measures, Hemisphere Publ. Corp., Washington, DC (1985).
49. K.S. Vorres, Mineral Matter and Ash in Coal, ACS Symposium Series No. 301, ACS, Washington, DC (1986).
50. F.E. Huggins, G.P. Huffman, and R.J. Lee, pp. 239-258 in Ref. 7.
51. W.E. Straszheim and R. Markuszewski, p. 47 in Ref. 8.
52. D.G. Hamblen, P.R. Solomon, and P.E. Best, "Analysis of Mineral Constituents, Sulfur Forms, and Beneficiation Potential of Coal Using Electron Beam Microanalysis," presented at the Joint ASME/IEEE Power Generation Conference, Milwaukee, WI (Oct. 20-24, 1985).
53. A.L. Lee, ACS Div. Fuel Chem. Preprints 12 (3), 19 (1979).
54. D. Merrick, Fuel 62 540 (1983).
55. P.R. Solomon, R.M. Carangelo, P.E. Best, J.R. Markham, and D.G. Hamblen, "Analysis of Particle Combustion, Size, and Temperature by FT-IR Emission/Transmission Spectroscopy," p. 141 in Ref. 9.

56. P.R. Solomon, R.M. Carangelo, P.E. Best, J.R. Markham, and D.G. Hamblen, "The Spectral Emittance of Pulverized Coal and Char," presented at the 21st Symposium (Intl.) on Combustion, Munich, FRG (1986).
57. P.E. Best, R.M. Carangelo, J.R. Markham, and P.R. Solomon, Combustion and Flame 66, 47 (1986).
58. P.J. Foster and C.R. Howarth, Carbon 6, 719 (1968).
59. P.R. Solomon and M.A. Serio, "Evaluation of Coal Pyrolysis Kinetics," presented at NATO Workshop on Fundamentals of Physical-Chemistry of Pulverized Combustion, Les Arcs, France (July 28-Aug. 1, 1986).
60. P.R. Solomon, M.A. Serio, D.B. Hamblen, P.E. Best, K.R. Squire, R.M. Carangelo, and J.R. Markham, "Coal Gasification Reactions with on-Line FT-IR Analysis," Final Report DoE METC Contract No. DE-AC21-81FE05122, Advanced Fuel Research, East Hartford, CT (1986).
61. M.A. Serio, D.B. Hamblen, J.R. Markham, and P.R. Solomon, Energy and Fuels (in press 1987); see also M.A. Serio, P.R. Solomon, D.B. Hamblen, J.R. Markham, and R.M. Carangelo, "Coal Pyrolysis Kinetics and Heat Transfer in Three Reactros," Poster Session, 21st Symposium on Combustion, Munich, FRG (1986).
62. D.B. Anthony, J.B. Howard, H.C. Hottel, and H.P. Meissner, 15th Symposium (Intl.) on Combustion, p. 1303, The Combustion Institute, Pittsburgh, PA (1975); see also D.B. Anthony, Sc. D Thesis, M.I.T., Dept. of Chemical Engineering, Cambridge, MA (1974).
63. H. Kobayashi, J.B. Howard, and A.F. Sarofim, 16th Symposium (Intl). on Combustion, p. 1445, The Combustion Institute, Pittsburgh, PA (1984).
64. S. Niksa, L.E. Heyd, W.B. Russel, and D.A. Saville, 20th Symposium (Intl.) on Combustion, p. 1445, The Combustion Institute, Pittsburgh, PA (1984).
65. P.R. Solomon and M.B. Colket, 17th Sumposium (Intl.) on Combustion, p. 131, The Combustion Institute, Pittsburgh, PA (1978).
66. E.M. Suuberg, W.A. Peters,and J.B. Howard, p. 117 in Ref. 65.
67. P.R. Solomon and D.G. Hamblen, EPRI Final Report for Project RP 1654-8, EPRI, Palo Alto, CA (1983).
68. P.R. Solomon and D.G. Hamblen, Progr. Energy Comb. Sci. 9, 323 (1984).
69. P.R. Solomon, M.A. Serio, R.M. Carangelo, and J.R. Markham, Fuel 65, 182 (1986).

70. P.R. Solomon, M..A Serio, R.M. Carangelo, and J.R. Markham, pp. 1-266 in Ref. 8.
71. J.D. Freihaut, Ph.D. Thesis, Penn. State Univ., College Park, PA (1980).
72. D.J. Maloney and R.G. Jenkins, p. 1435 in Ref. 64.
73. F.C. Lockwood, S.M.A. Rizvi, G.K. Lee, and H. Whaley, p. 513 in Ref. 64.
74. J.S. Truelove, p. 523 in Ref. 64.
75. M. Jost, I. Leslie, and C. Kruger, p. 1531 in Ref. 64.
76. A.B. Witte and N. Gat, "Effect of Rapid Heating on Coal Nitrogen and Sulfur Release," presented at the DoE Direct Utilization AR & TD Contractors' Meeting, Pittsburgh, PA (1983).
77. P.R. Solomon and H.H. King, Fuel 63, 1302 (1984).
78. K.R. Squire, P.R. Solomon, R.M. Carangelo, and M.B. DiTaranto, Fuel 65, 833 (1986).
79. S.E. Stein, New Approaches in Coal Chemistry, pp. 97-129, B.D. Blaustein, B.C. Bockrath, and S. Friedman eds., ACS Symposium Series No. 169, ACS, Washington, DC (1981).
80. P.R. Solomon, p. 61, in Ref. 79.
81. D.B. Anthony and J.B. Howard AIChE J. 22, 625 (1976).
82. J.B. Howard, W.A. Peters, and M.A. Serio, "Coal Devolatilization Information for Reactor Modeling," Final Report AP-1803 for EPRI Project No. 986-5, EPRI, Palo Alto, CA (1981).
83. J.B. Howard, Chapter 12 in Ref. 37.
84. A.T. Talwaker, "Topical Report on Coal Pyrolysis," DoE Contract No. DOE/MC/19316-1408(DE83006592), (1983).
85. H. Juntgen and K.H. van Heek, Fuel Proc. Tech. 2, 261 (1979).
86. P.E. Unger and E.M. Suuberg, 18th Symposium (Intl.) on Combustion, p. 1203, The Combustion Institute, Pittsburgh, PA (1981).
87. P.E. Unger and E.M. Suuberg, Fuel 63, 606 (1984).
88. P.R. Solomon and H.H.King, Fuel 63, 1302 (1984).
89. P.R. Solomon and K.R. Squire, ACS Division of Fuel Chemistry Preprints 30 (4), 347 (1985).
90. S. Niksa, A.R. Kerstein, and T.H. Fletcher, p. 237 in Ref. 9.
91. S. Niksa and A.R. Kernstein, Combustion and Flame (in press, 1986).
92. W.S. Fong,W.A. Peters, and J.B. Howard, Fuel 65, 251 (1986).

93. E.M. Suuberg, W.A. Peters, and J.B. Howard, Ind. Eng. Chem. Proc. Design Dev. 17, 34 (1978); see also E.M. Suuberg Ph.D. Thesis, M.I.T., Cambridge, MA (1977).
94. P.R. Solomon and D.B. Hamblen, Progr. Energy Comb. Sci. 9, 323 (1983).
95. J.D. Freihaut and D.J. Seery, ACS Div. of Fuel Chem. Preprints 28 (4), 265 (1983).
96. A. Attar and G.G. Hendrickson,in Coal Structure, pp. 131-198, R.L. Meyers ed., Academic Press, NY (1982).
97. E.M. Suuberg, Chemistry of Coal Conversion, Chapter 4, p. 67, R.H. Schlosberg ed., Plenum Press, NY (1982).
98. E.M. Suuberg, J. Larsen, and A.L. Lee, Fuel 64, 1668 (1985).
99. G.A. Simons, Combustion and Flame 53, 83 (1983).
100. G.A. Simons, Combustion and Flame 55, 181 (1984).
101. G.A. Simons, "The Influence of Fluid Transport During Pyrolysis," Proceedings of the International Conference on Coal Science, p. 479, Pittsburgh, PA (1983).
102. G.A. Simons, Progr. Energy and Comb. Sci. 9, 269 (1983).
103. P.R. Melia and C.T. Bowman, paper presented at the Western States Section Conference Combustion Institute, Spring Meeting, University of Utah, Salt Lake City, UT (1982).
104. M. Oh, W.A. Peters, and J.B. Howard, "Modeling Mass Transport and Plasticity in Bituminous Coal Pyrolysis," p. 483 in Ref. 101.
105. J.R. Ashu, N.Y. Nsakala, O.P. Mahajan, and P.L. Walker, Jr., Fuel 57, 251 (1978).
106. R.H. Essenhigh and H. Farzan, p. 1105 in Ref. 24.
107. M.A. Serio, Ph.D. Thesis, M.I.T. Cambridge, MA (1984).
108. M.A. Serio, W.A. Peters, K. Sawada, and J.B. Howard, "Secondary Reactions of Nascent Coal Pyrolysis Tars," p. 533 in Ref. 101.
109. M.A. Serio, W.A. Peters, K. Sawada, and J.B. Howard, ACS Div. of Fuel Chem. Preprints 29 (2), 65 (1984).
110. K.R. Doolan, J.C. Mackie, and R.J. Tyler, Proceedings of the International Conference on Coal Science, p. 961, Sydney, N.S.W., Australia (1985).
111. M.R. Kahn, "Characterization of Mechanisms of Mild Gasification Processes and Catalytic Fuel Gas Conversion Low-Temperature Devolatization Studies," Fifth Annual Gasification Projects Contractors' Meeting, METC, Morgantown, WV (1985).

112. R.D. Nenninger, J.B. Howard, and A.F. Sarofim, p. 521 in Ref. 101.
113. H.J. Gluskoter, Ash Deposits and Corrosion due to Impurities in Combustion Gases, Hemisphere Publishing Co., Washington, DC (1977).
114. P.J. Jackson, Pulverized Coal Firing Workshop, L9 and L10, The University of Newcastle, NSW, Australia (1974).
115. W.T. Reid, External Corrosion and Deposits, J.M. Beer ed., Elsevier, NY (1971).
116. P.J. Jackson, "Combustion of Pulverized Coal. The Effect of Mineral Matter," Workshop, Dept. Chem. Eng., Univ. New Castle, NSW, Australia (1979).
117. H.J. Gluskoter, Fuel 44, 285 (1965).
118. A.R. Ramsden, Fuel 48, 121 (1969).
119. E. Raask, ASME Trans. Eng. Pwr. 88, 40 (1966).
120. E.L. Mitchell and G.K. Lee, Trans. Con. Inst. Min. Met. 65, 360 (1962).
121. P. Lightman and P.J. Street, Fuel 47, 7 (1968).
122. L.D. Smoot, Progr. Energy Comb. Sci. 10, 229 (1984).
123. S.S. Penner et al., Ref. 1 in Sec. 2.1.
124. T.R. Johnson, T.M. Lowes, and J.M. Beer, J.Inst. Fuel 47, 39 (1974).

APPENDIX: EFFECT OF CaO COMBINED FLUIDIZED-BED GASIFICATION AND PYROLYSIS*

If coal is pyrolyzed to produce gas and liquid products prior to combustion and gasification, higher thermal efficiency and decreased cost can be achieved as compared to gasification of the whole fresh coal. This observation applies when pyrolysis gas and liquids are of equal or higher value than heat or gas from whole coal. Figure 12A-1 illustrates a fluidized bed process with heat supplied by combustion. Medium heating value gas is produced by steam gasification of char and the coal is pyrolyzed in a third reactor, where heat is supplied by hot solids from the combusion reactor. In such a system, it is advantageous to use limestone to capture sulfur in all three reactors and to improve the heating value of gas produced by CO_2 capture and also the tar properties. The following are reactions involving CaO: CaO + multi-ring aromatics $\longrightarrow$ char + gas to reduce tar molecular weight, improve compatibility, reduce mutagenicity; CaO + phenols $\longrightarrow$ char + gas to reduce owygen content and toxicity; $CaO + H_2S \longrightarrow CaS + H_2O$ to produce low-sulfur gas; $CaO + CO_2 \longrightarrow CaCO_3$ to increase the gas-heating value and hydrogen content; $CaO + SO_2 + (\frac{1}{2})O_2 \longrightarrow CaSO_4$ to form non-polluting flue gas.

The sulfur compound and CO_2 reactions have been studied in a number of applications; however, selective reactions with multi-ring aromatics have been discovered relatively recently and their potential for improvement of tar properties and reduction of the amount of tar has received only limited laboratory study. Table 12A-1 shows results of studies on pyrolysis of pure HCs over CaO compared with pyrolysis over an inert material (quartz). For the aromatic compounds, the temperature for a given conversion to char and gas is reduced, while there is relatively little change in heptane conversion. This selectivity for multi-ring aromatic removal is also observed for pyrolysis of coal tar, as is shown by the data in Table 12A-2.

---

* Prepared by J.P. Longwell, Department of Chemical Engineering, Massachusetts Institute of Technology, Cambridge, MA 02139.

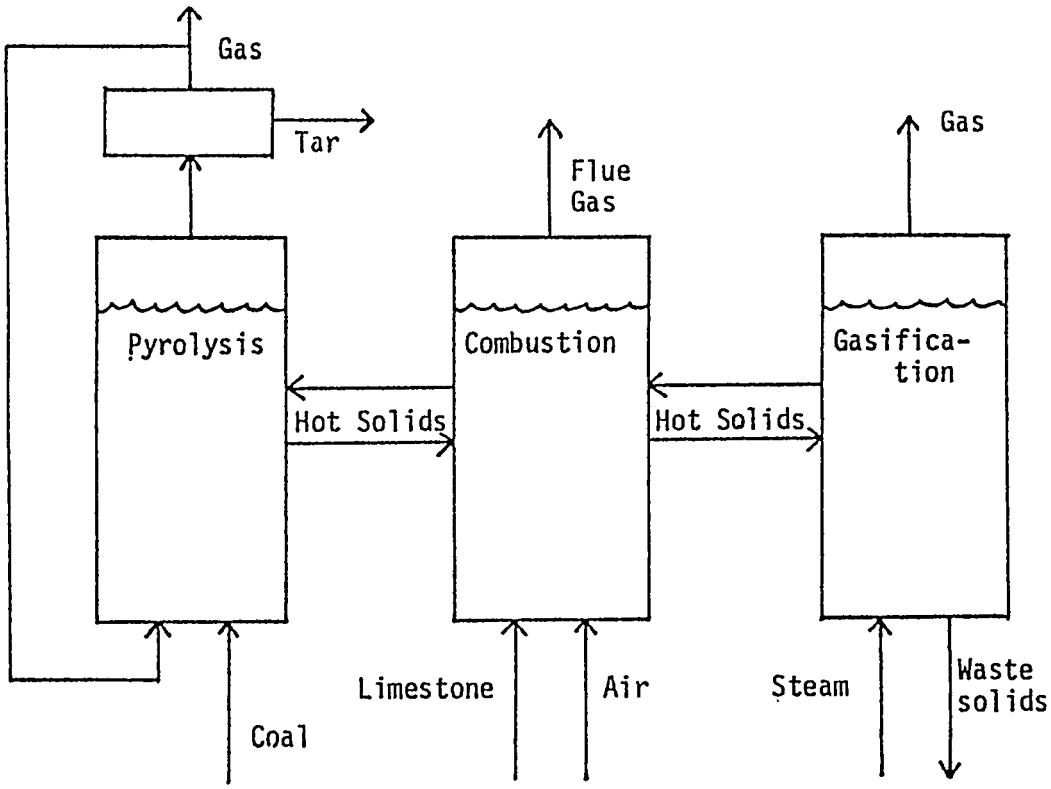

Fig. 12A-1. Schematic of a coal-gasification process following pyrolysis and combustion to obtain higher thermal efficiencies.

Table 12A-1. Results on pyrolysis of aromatic compounds over CaO and quartz.

Compound	40% conversion temperature, °C		Activation energy, kcal/mole	
	CaO	Quartz	CaO	Quartz
Toluene	710	850	46.2	79.5
1-Methylnaphthalene	600	775	25.4	43.4
1-Methylanthracene	490	730	12.0	46.0
n-Heptane	600	640	40.6	48.7

Table 12A-2. Effect of CaO on tar conversion.

Parameter	Tar Properties		
	Untreated tar	Thermal conversion	CaO conversion
Temperature, °C	---	800	550
Tar yield, %	100	60	60
Fraction of aromatic C	0.67	0.78	0.67
Weighted average molecular weight	600	540	530
Phenolic O, wt%	5	3.0	3.5
Relative mutagenicity	1	10	0.9

CHAPTER 13:
GAS SUPPLIES AND SEPARATION: ASH DISPOSAL; MATERIALS FOR GASIFIERS

13.1. Gas Supplies and Separation*

13.1-1. Introduction

Future efficient gasification systems are expected to utilize O_2-blown gasification rather than air-blown gasification. The advantages of having O_2 as the oxidation agent include a cleaner, higher-quality gasifier-product gas, smaller system sizes and less demanding gas clean-up requirements. However, these advantages must be constantly balanced against the cost associated with building and operating an air-separation plant to separate oxygen from air, which may become a significant part of the overall plant cost and usually requires large amounts of electricity. Thus, a careful evaluation of dominant parameters imposed on the air-separation plant and their relation to output-gas quality must be performed in order to optimize total system economics. Factors affecting the air-separation plant are O_2-purity, O_2-pressure, H_2O and CO_2 levels of the input air, turndown percentage, number of trains and, of course, plant size.[1] The impact of these variables on O_2-cost is shown in Table 13.1-1. There are several air-separation techniques that are applicable to coal gasifiers. A listing of these is given in Table 13.1-2, along with their present development and availability status. At present, cryogenic separation is the only commercially available technique for the large requirements of coal

---

* Unless otherwise indicated, information in this section has been abstracted by S.S. Penner and D.F. Wiesenhan from viewgraphs and references supplied to COGARN on July 11, 1986 by A. Smith of Air Products and Chemicals, Inc., P.O. Box 538, Allentown, PA 18105.

gasifiers. The MOLTOX* system will probably see application of large-scale coal-gasification systems by the mid-1990s. A brief overview of these technologies follows.

13.1-2. Cryogenic Air Separation

Cryogenic air separation is the most widely used procedure for large-scale (>100 tons of O_2 per day) applications. This procedure has relatively low specific energy consumption and may be readily used to achieve high gas purity while N_2 and Ar by-products are easily recovered. Cryogenic air separation is a mature technology but improvements leading to lower costs may be possible. For O_2-plants producing more than ~200 TPD of O_2, power requirements account for more than 50% of the oxygen cost.[1] As the size of the plant is increased, the fraction of oxygen cost attributable to energy consumption also increases (see Fig. 13.1-1). The energy requirements for cryogenic air-separation plants may become a significant fraction of the total energy output of a coal-gasification plant, up to 15% in some cases.[1]

A schematic diagram of a dual-distillation column, low-pressure cryogenic air-separation cycle, as commonly used to provide purities better than 99.5%, is shown in Fig. 13.1-2. Water and CO_2 enter with the air and are removed by using either a reversing heat exchanger (which combines impurity removal with primary heat exchange) or a molecular sieve adsorption system.

A problem endemic to O_2-plants located near coal gasifiers is higher than normal ambient CO_2 concentrations (~2000 ppm vs ~350 ppm). This excess CO_2 prevents the use of adsorption clean-up and results in higher equipment and energy costs.

The specific power requirements remain constant for purities $\leq$95%. Typical energy-use rates for delivering O_2 at 615 psia are 500 kWh/ton of O_2 for existing plants and ~360 kWh/ton of O_2 for newer cryogenic plants.[2]

---

* MOLTOX is a trademark of Air Products and Chemicals, Inc.

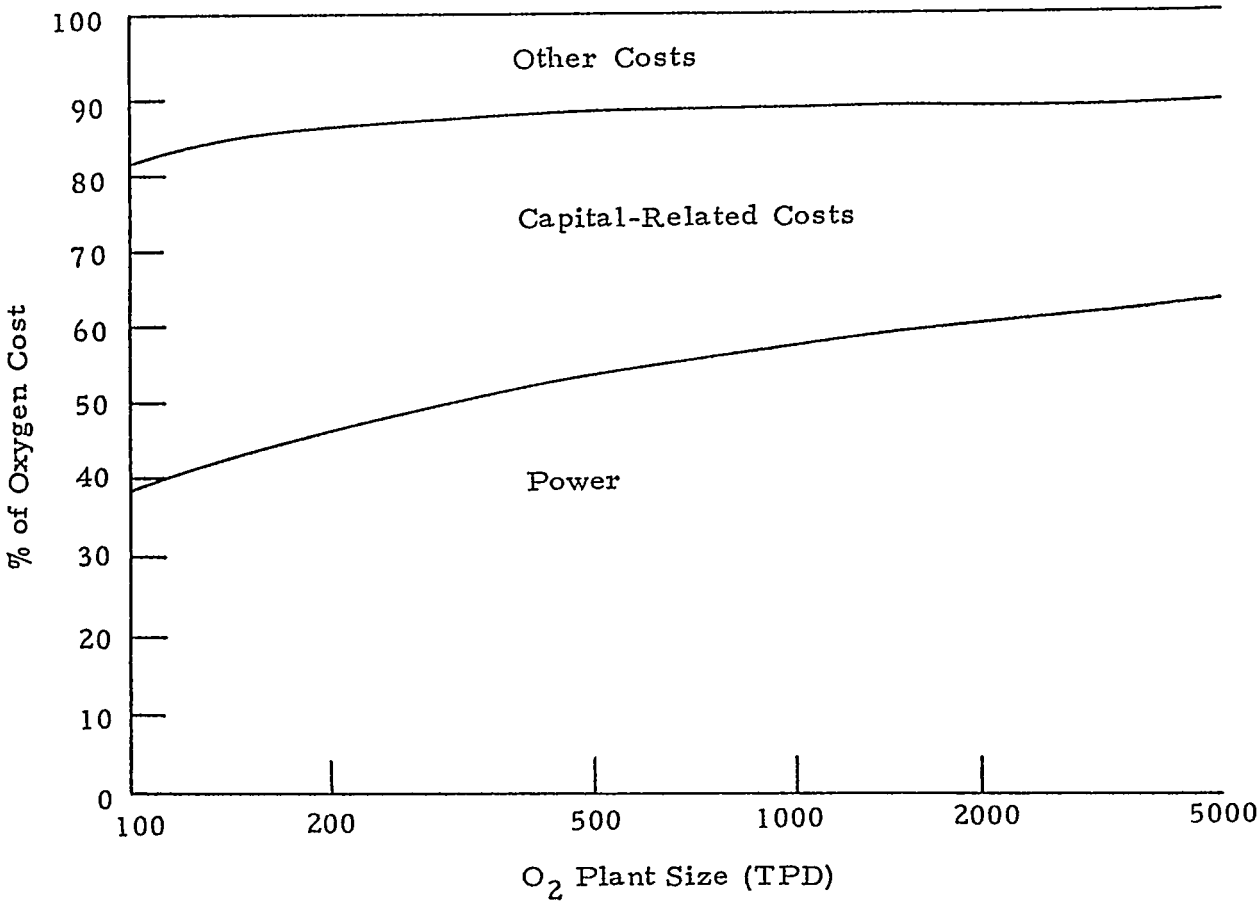

Fig. 13.1-1. Components of the oxygen cost for cryogenic air-separation; reproduced from Ref. 1.

Table 13.1-1. Effects of oxygen plant/gasifier interface variables on oxygen cost; reproduced from data presented by Air Products and Chemicals, Inc.

Variable	Change in variable	O_2-cost impact
Purity	99.5 vs 90%	5 - 15%
Pressure	1200 vs 100 psig	15 - 20%
Plant size	1000 TPD vs 6000 TPD	18%
Turndown	65% vs 85%	3 - 5%
No. of trains	Single vs 2 to 6	3 - 8%

13.1-3. The MOLTOX System

A promising new air-separation method being developed is the MOLTOX system. A MOLTOX plant will use electricity at about half the rate of existing cryogenic plants.[2] This improvement is accomplished with a molten mixture of alkali nitrates and nitrites which react chemically with O_2 in the compressed air. About 99.8% purity is reached after a reversible reaction in the required heating and/or depressurization step. Heat removal from the waste N_2-exhaust recovers a major portion of the energy used to compress or heat the input air. Recent funding by DoE has culminated in the construction of a 0.25 TPD-O_2 plant, which has been operating since March 1986.

Two operating modes are possible: pressure-swing absorption (PSA) or thermal-swing absorption (TSA). The former is best suited to integration with pressurized gases of gas-turbine power plants. The TSA mode is applied by using the heat recovery and steam generation section of industrial and utility steam boilers. A combination of these two modes is

Table 13.1-2. Air separation technologies and their development status; reproduced from data presented by Air Products and Chemicals, Inc.

Technology	Status
Cryogenics	Mature
Absorption	Mature
Membranes	Developing (small units are available)
Chemical (MOLTOX™)	Developing (pilot-plant stage)
Others: solid membrane electrochemical bench scale studies	Developing (R&D stage)

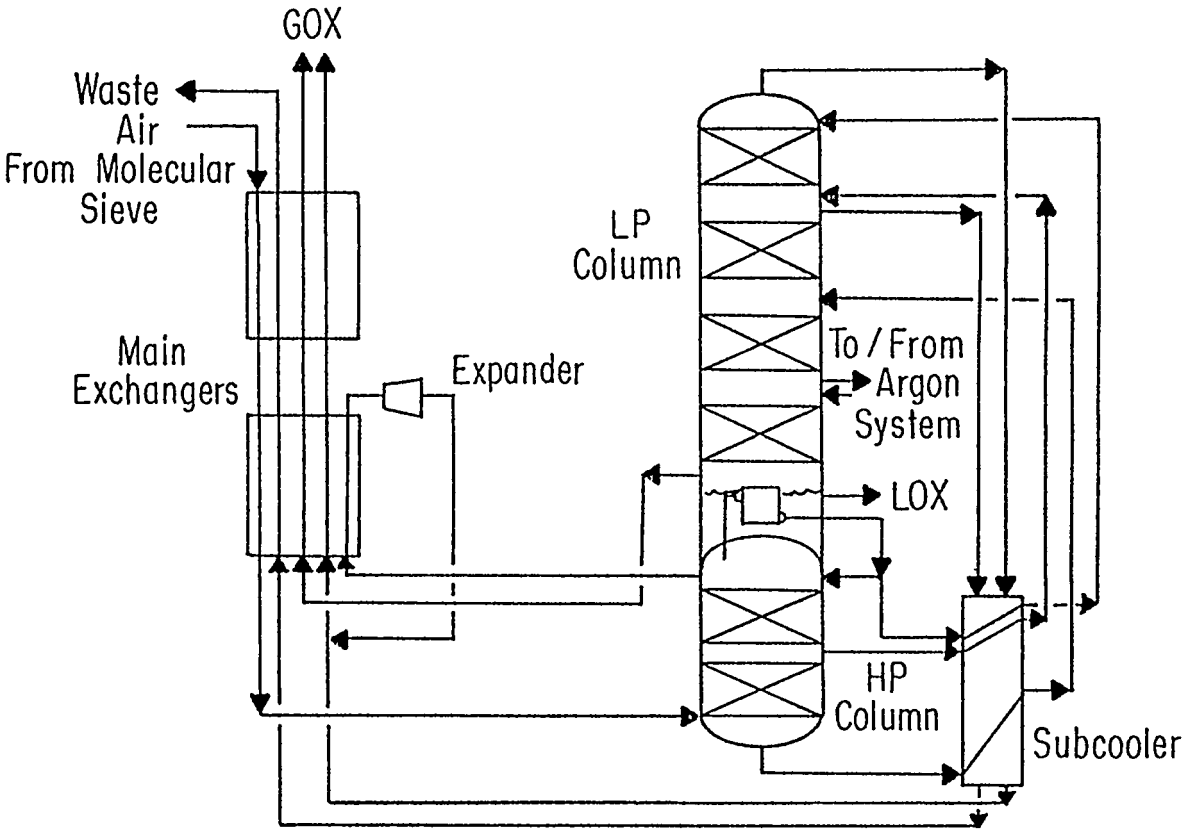

Fig. 13.1-2. Schematic diagram of a dual-distillation column, low-pressure cryogenic air-separation system; reproduced from Ref. 1.

practical when both heat and pressure head are available for recovery. Schematic diagrams showing PSA and TSA are found in Fig. 13.1-3.

Prior to entering the MOLTOX unit, the air is dried and the CO_2 is removed. The inlet temperatures and pressures are either 510 or 650°C and 0.41 or 1.2MPa, respectively, depending on the operating mode. In the absorber, the air contacts the molten salt (a mixture based on Na and K) and reacts according to the process $MNO_2^- + (1/2)O_2 \rightarrow MNO_3^-$. The oxygen is thus removed with the salt from the bottom of the absorber. The molten salt then flows to the desorber where the reverse reaction $MNO_3^- \rightarrow MNO_2^- + (1/2)O_2$ occurs, thus liberating gaseous oxygen. This last step requires either a pressure reduction (PSA) or a temperature increase (TSA). Nitrogen, inert gases, and unreacted oxygen leave the absorber at essentially the same temperature and pressure at which they entered.

Depending on the amount of heat input available to the MOLTOX unit, energy requirements will be less than for a new cryogenic plant. At

zero available heat input, energy requirements are ~300kWh/ton of O_2.[2] With $8X10^6$ Btu/ton of O_2 available, this value is reduced to slightly more than 200 kWh/ton of O_2.[2] These savings are important, especially since the MOLTOX system has higher capital costs and higher operation and maintenance costs (see Table 13.1-3) than a cryogenic plant.

Compared with cryogenic systems, a 1000 TPD-O_2 MOLTOX Plant producing 600 psig of O_2 at 99.5% purity and operating at 100% capacity for 340 days per year over 15 years is economically advantageous for electricity costs greater than 4¢/kWh.[2] For the projected mid 1990s electricity price of 7.5¢/kWh, present MOLTOX units offer a 12% cost reduction over new cryogenic systems. These savings are expected to increase to 23% for future MOLTOX units.[2] At 7.5¢/kWh, the MOLTOX Process will yield a lower-bound estimate of $33/ton of O_2.

Approval for construction of a small (0.25 TPD-O_2) plant was given in January 1985. This plant was built to assess and rectify problems in the following areas: TSA/PSA and TSA-only operational modes; salt losses through vapor or corrosion; salt stability; absorption/desorption kinetics; salt-loop equipment designs and adequacy of construction materials; long-term operability; and gas purities, impurities, and by-products. A simplified experimental system capable of addressing these issues was implemented.

A particular difficulty is the high corrosiveness of the salt. Extensive monitoring equipment was installed and different alloys and ceramic materials have been or will be tested to find optimal materials for salt exposure.

The plant began operation in March 1986. At a production rate of 0.12 TPD-O_2, 99.9% pure O_2 was obtained, which was within 92% of theoretical equilibrium recovery for the operating conditions employed. After four days of good operation, a centrifugal pump constructed out of 316 SS failed. This failure was attributed to corrosion, cavitation, or a combination of these two effects. A redesigned pump was constructed out of new materials and has been incorporated.

Future plans call for a 50 TPD-O_2 plant, partly financed by oxygen users or by other oxygen suppliers. Especially sought after is metallurgical expertise to solve the corrosion problems. Other factors to

be studied in this plant are the heat-integration systems and plant scale-up. Another aspect to be examined that may lead to lower costs is the reduction of required input H_2O and CO_2 from the present levels of 1 ppm.[3] Plants capable of producing 500 TPD of O_2 are expected to be available in the early 1990s.

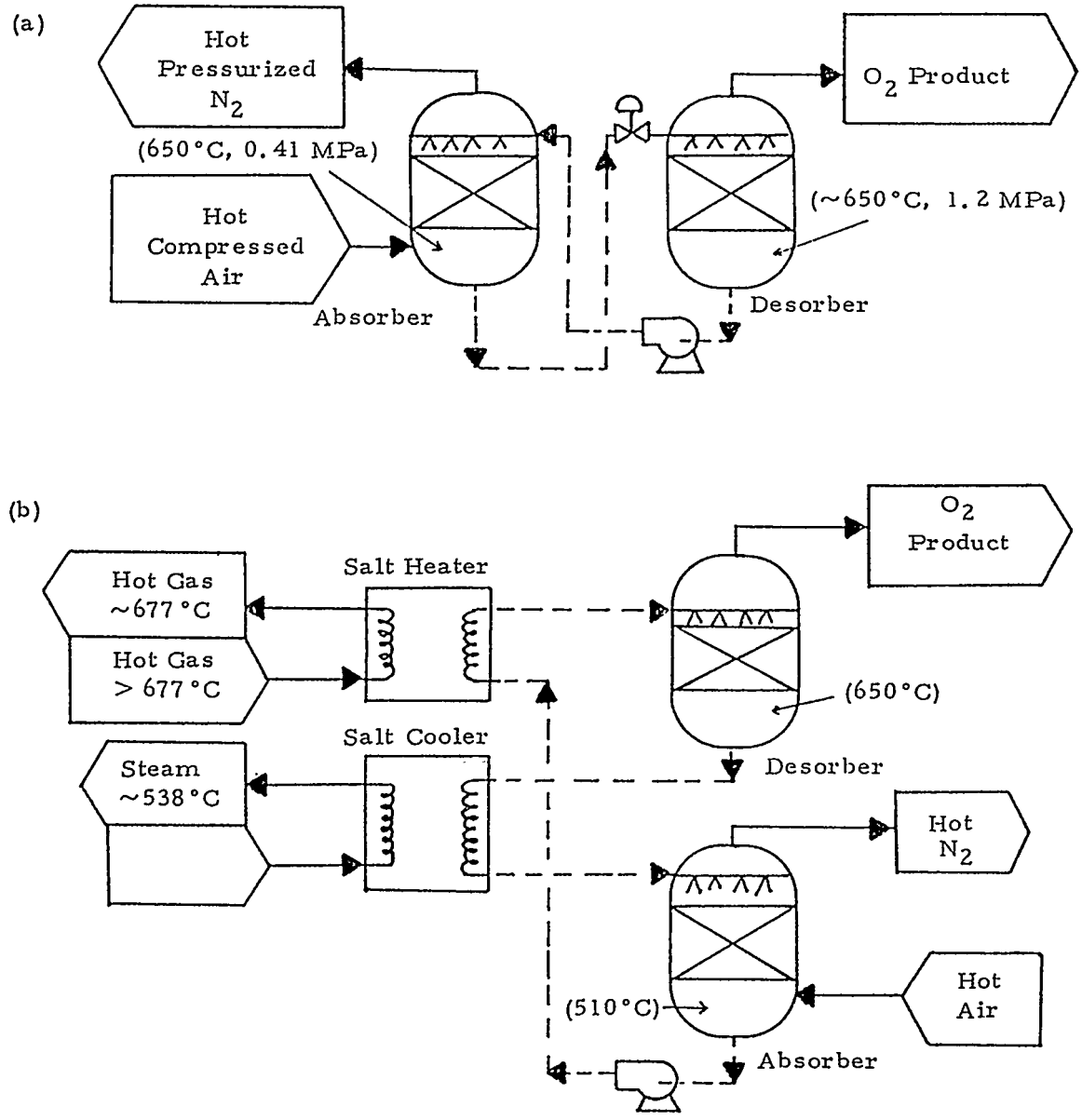

Fig. 13.1-3. The two operating modes of the MOLTOX air-separation system are shown: (a) pressure-swing absorption (PSA), (b) temperature-swing absorption (TSA); reproduced from Ref. 2. indicates integration with an external process.

Table 13.1-3. Cost comparison between a new cryogenic plant and a MOLTOX plant, both producing 99.5%-pure O_2 at 600 psig, 1000 TPD, and operating for 340 days per year; the cryogenic data refer to the reference task 1 report, May 1985, DoE/CE/40544-TI.

	Cryogenic plant	MOLTOX plant
Capital investment	$18.6MM	+ 10% to 35%
Cost component	Oxygen cost ($/T)	Cost differential from cryogenic plant ($/T)
Capital related	$12.03	+ $1.00 to 4.50
O & M	4.74	+ 1.00 to 2.50
Electricity at 7.5/10.0¢/kWh	27.58/36.77	-12.00 to -16.00
% savings for total O_2 cost	44.35/53.54	-5.00 to -14.00

13.1-4. Other Air-Separation Systems

Systems using membranes, adsorption, or other techniques exist and may be useful as oxygen generators for coal gasifiers. However, many factors prevent their application. Because of their low state of maturity, these techniques are not yet suitable for large-scale applications. They will probably also require more electrical energy per unit product than the two techniques previously discussed.

13.1-5. Research Needs

Cryogenic air-separation units are the only O_2-supply systems presently available for coal gasifiers. Associated costs for these systems may be reduced by using improved compressor design, improved air pretreatment techniques, or reduction of the sensitivity of the cost to

O_2-quality. Since this is a mature technology, large gains are not likely to be achieved.

Since the primary cost associated with air-separation systems is energy consumption, efficient processes using less electricity are desirable. Gains can be made by optimizing mechanical systems, but significant gains are realized if the waste heat from another process is used as an energy source, as is done in the MOLTOX process. The MOLTOX system will soon become applicable in coal-gasification plants, where sufficient amounts of waste heat are available.

The following problems need to be assessed in the MOLTOX system: (i) Material selection leading to corrosion reduction. (ii) Efficient integration of the heat-transfer systems of the MOLTOX plant with the heat-export systems of the host plant. (iii) Increasing the level of input CO_2 that can be effectively handled, especially when the MOLTOX plant is located near a coal gasifier. (iv) General problems involved in scaling up to the large requirements of a coal-gasification plant must be identified and assessed. (v) Research leading to increased understanding of the molten salt is necessary, e.g., salt losses, kinetics, and salt-loop equipment design.

When an oxygen plant is integrated with a coal gasifier, it is frequently difficult to optimize the plant and meet changing requirements such as purity, amount, turndown time, etc. Different gasification systems (SNG, IGCC, etc.) will have different demands. Proper optimization routes are not clear at this time and should be pursued.

The study of alternative air-separation techniques should be continued. The most promising new procedure for coal-gasification applications will probably be a process based on membrane technology.

References for Section 13.1

1. J. Klosek, A. R. Smith and J. Solomon, :The Role of Oxygen in Coal Gasification, unpublished, Air Products and Chemicals, Inc., Allentown, PA (1986).
2. D. C. Erickson, W. R. Brown, B. R. Dunbobbin, and R. G. Massey, "MOLTOX™ Chemical Air Separation System - A Progress Report," unpublished, see Ref. 1 (1986).

3. Air Products and Chemicals, Inc., "MOLTOX™ Oxygen System Status Report, April 1986," unpublished, see Ref. 1 (1986).

13.2. Utilization and Disposal of Ash From Gasifiers*

A considerable amount of testing has been performed on ash products from coal-gasification processes at pilot- and commercial-size plants. Regulations regarding permissible leachates into water are set by Federal and state standards and allow for the quantities of ions in the water that may be leached from the ash. In all instances, EPA standards have been easily achieved for ash samples from the Texaco, Shell, KRW, Lurgi, and British Gas/Lurgi gasification processes. It should be noted that more severe standards for metal ions in water may be set by state than by Federal regulations. The ash product from the Cool Water, Texaco-based plant was declared to be non-hazardous by the California State Department of Health when it was tested according to the severe standards of California. During coal gasification, the ash in the coal is melted in the gasifiers (Shell, Texaco, Lurgi, Dow, etc.) The resultant ash product is a glassy, hard solid. This material has been heated to relatively high surface temperatures and is relatively impervious to leaching by ground water percolating through deposits in landfills.

In the US, coal ash from pulverized fuel combustion has established local markets for a number of special applications. Table 13.2-1 shows the amount of ash from pulverized coal plants that is produced. Coal ash from pulverized fuel plants is produced in the form of (i) light, fluffy fly ash that is carried out of the furnace by the combustion gases and (ii) bottom ash that represents ash that has been melted in the furnace. In the US, markets for low-density fly ash absorbs only about 15% of the available ash, whereas a larger portion of the denser bottom ash is used commercially for a wide number of applications (Table 13.2-2). Markets for ash from coal are site-specific since the selling price is relatively low ($2-8/ton). For all uses, shipping costs affect the distance that the ash

* This section has been written by S.B. Alpert.

can be transported before its use becomes eonomically unattractive. Table 13.2-2 also shows representative markets for US coal ash.

In the US, coal-gasification plants have only recently been operated on a scale at which representative ash is being produced. A major incentive in developing markets for this by-product is to avoid the expense of land-fill disposal at costs of $5-20/ton, depending on location and other site-specific factors.

Table 13.2-1. Coal ash from conventional US combustion plants in 10^6 mt/yr).

Ash \ Year	1979	1983	1995 (estimated)
Fly ash	52.2	52.4	82
Bottom ash and boiler slag	16.1	17.9	28
Total	68.3	70.3	110

Table 13.2-2. Ash utilization in the US during 1983, in 10^6 mt/yr.

Application	Fly Ash	Bottom Ash	Slag
Cement	3.5	0.4	0.3
Structural fill	1.4	1.1	0.2
Road base	0.5	0.3	0.1
Asphalt mix	0.1	0.1	0.1
Snow and ice control	0.1	0.4	0.2
Grit, roofing, gravels	--	--	1.5
Grouting	0.2	0	0
Coal mining	0.2	0.1	--
Miscellaneous	1.5	0.4	0.1
Total utilized	7.5	2.8	2.5
Total disposal	44.8	11.2	1.4
Total produced	52.4	14.0	3.9

Table 13.2-3. Representative applications for coal-gasification ash.

Market	Applications
Agricultural use	Soil stabilization, soil conditioner, soil neutralization, acid water treatment
Industrial use	Sandblasting, roofing granules, industrial fillers, mineral wool, sludge stabilization
Cement, concrete	Concrete aggregate and concrete extender
Road construction	Road ballast, base, asphalt, construction material
Soil stabilization	Landfill
Resource recovery	Concentrate and recover minerals (this is a long-term potential)

New generic applications may be developed by comparing the properties of ash products from coal gasification with required specifications for mineral products. Considerable screening work is generally required. Representative markets are summarized in Table 13.2-3.

A DoE program to evaluate ash utilization from a number of representative gasifiers and using a variety of US coals is recommended. Test work on applications should be performed cooperatively with producers, using ash products from operating plants.

13.2-1. Environmental-Impact Studies

Technology exists for acceptable disposal of coal-ash wastes. Environmental issues in handling and disposal of ash are: (i) air-related issues involving fugitive dust emissions from ash piles and handling; (ii) groundwater contamination and contamination resulting from run-off and percolation; (iii) land-use related considerations, including ash stability, pile erosion, and structural stability; and (iv) ecological and biological impacts. All of these issues are site-specific. Acceptable environmental controls should be achievable because of the relatively benign character of the ash produced from coal-gasification plants.

Long-term testing and evaluation of sites where ash is stored are being performed. DoE should review these programs but a generic environmental program may not be appropriate because of the site-specific nature of environmental controls.

13.3. Construction Materials for Coal Gasification*

13.3-1. Introduction

The materials used for construction in coal-gasification plants are subjected to highly aggressive environments at elevated temperatures under conditions of severe erosion, corrosion, and mechanical and thermal stresses. During the past decade, progress has been made in studies of the candidate materials, in both laboratory experiments and under operating conditions in coal-gasification plants. The following are the major materials problems that must be addressed: (i) gaseous corrosion of metals and refractories; (ii) slag corrosion of refractories; (iii) erosive wear; (iv) the materials/design interface and economic considerations including life-cycle costs; and (v) nondestructive examination. Several excellent reviews have been published in recent years. The following summary is based on information presented in Refs. 1-7.

13.3-2. High-Temperature Corrosion

Degradation of materials at elevated temperatures results from both corrosion wastage and loss of structural integrity. Chemical reactions with the ambient environment may cause rapid wastage or intense localized attack, which limits component life. This process leads to serious losses in plant performance and availability, as well as to increased costs.

Gaseous corrosion of metallic materials leads to oxidation, sulfidation, carburization, and nitridation. These reactions are complex because of interactions between the multiple reactive species present in the

---

* This section has been written by M.T. Simnad, Center for Energy and Combustion Research and Dept. of Applied Mechanics and Engineering Science, University of California, San Diego, La Jolla, CA 92038.

environment and the alloying elements in alloy components. Predictions of alloy performance are based on thermochemistry and kinetic factors, which include time-dependent considerations of the nature of the reaction products.

The composition of the gas phase depends on coal feedstock, gasification agent (air, oxygen, or steam), type of reactor, and operating temperature and pressure (Table 13.3-1). Natesan[1,2] has presented a generalized approach for the evaluation of reaction potentials in complex gas mixtures and concluded that, in coal-gasification atmospheres involving reactive species such as oxygen, sulfur, and carbon, sulfidation of the alloy is the major mode of material degradation. Alloys that develop protective oxide scales are needed to limit corrosion rates to acceptable levels. High chromium and aluminum contents in the iron-, nickel-, and cobalt-base alloys lead to the formation of relatively stable oxide films. High-nickel alloys form low-melting Ni-sulfide eutectics in the scale or interior of the base alloy even in gas environments with low to moderate sulfur partial pressures. For this reason, alloys with high chromium and fairly low nickel contents are selected for use in coal-gasification systems (Table 13.3-2). The inter-relationships among oxygen and sulfur partial pressures in the gas phase, the alloy composition, and the test temperature and pressure have been determined.[2]. These data have provided information needed to establish the critical oxygen pressures that allow the formation of stable protective oxide scales on alloy surfaces (see Figs. 13.3-1 and 13.3-2, Table 13.3-3).

There is a need for more detailed studies of nucleation and lateral growth of chromium-rich oxides for high-chromium alloys on exposure to environments with low partial pressures of oxygen and in the presence of sulfidation. The oxidation-sulfidation behavior of candidate alloys has been examined in different mechanistic regimes defined by the temperature and oxidant (oxygen and sulfur) potentials.[2] A number of reaction sequences have been postulated as a result of these studies and are depicted in Fig. 13.3-3. The higher growth rate of the sulfide gives rise to sulfide overgrowth above the oxide and sulfide nuclei. Outward cation diffusion through the scale leads to the formation of voids in the subscale. The presence of high Al and Ti in the alloy stabilizes the oxide nuclei relative to the sulfide by preferential oxide formation.

The refractory materials used for linings and components of coal-gasification plants are also subject to corrosion at elevated temperatures (Table 13.3-4). The refractories are aggregates of ceramic grains bonded with sintered cement or fused matrices (Tables 13.3-5 and 13.3-6). For conditions of severe erosion, high alumina-type refractories are used. When high thermal conductivity is required, silicon carbide refractory shapes are employed. Gaseous SiO will form in the presence of hydrogen or water vapor in the gas phase. The process causes loss of silica from the refractory bricks containing silicates (such as firebrick) and deterioration of the bricks by erosion and mechanical weakening. Low-silica refractories are used in the working linings of non-slagging regions in order to mitigate losses of silica by reactions with hydrogen and/or steam. The preferred refractories are dense castables of high-fired, dense fireclay aggregates, bonded with high-purity alumina cements or dense high-alumina fireclay brick.

Table 13.3-1. Comparison of operating conditions in coal gasifiers and other industrial processes; reproduced from Ref. 1. Unless indicated otherwise, compositions are given in vol%.

Compound or Parameter	Low-Btu Lurgi	Low-Btu Winkler	High-Btu Synthane	High-Btu Hygas (steam-iron)	Fluid-catalyst cracking-unit regenerator	Ammonia-plant secondary-reformer	Slagging Texaco	Slagging Bi-Gas
CO	13.3	19.0	10.5	7.4	7	6.4	35.6	12.0
CO_2	13.3	6.2	18.5	7.1	9	3.9	12.8	13.0
H_2	19.6	11.7	17.5	22.5	-	28.0	24.8	15.0
H_2O	10.1	11.5	37.1	32.9	17	50.8	26.2	52.0
CH_4	5.5	0.5	15.4	26.2	-	0.1	0.07	7.0
C_2H_6	-	-	0.5	1.0	Trace	-	-	-
H_2S (ppm)	0.6	1300	0.3	1.5	-	-	0.11	0.5
Other	37.5 N_2	51.1 N_2	-	-	61 N_2	10.8 N_2	0.28 N_2	-
Process T, °C	621-760	815-1010	982	Above 500	Above 700	787	1550	1650
Process p, MPa	2.41-3.10	0.101	6.89	6.89	0.28	1.38-2.07	3	7

Table 13.3-2. Candidate metallic materials for application in coal-gasification plants; from the National Materials Board (1977). The data are from A. M. Hall, Battelle Columbus Laboratories, Columbus, Ohio, and are reproduced from Ref. 1.

Designation	Classification	Nominal composition, %							Application
		C	Mn	Si	Cr	Ni	Mo	Others	
15Cr-3Mo	Alloy white iron	4.00	0.85	0.50	15.00		2.75		Wear parts for pumps, valves, feeders
Stellite 12 (trademark of the Stellite Division of Cabot Corp.)	Hard facing alloy	1.80	-	-	29.00		-	59.0 Co 9.0 W	
A-387 (Grade D)	Cr-Mo plate steel	0.15	0.40	0.40	2.25		1.00		Shells, heads, ducts
A-516	C-Si plate steel	0.27	0.70	0.25	-	-	-		
A-533	Mn-Mo-Ni plate steel	0.25	1.25	0.25	-	0.85	0.50		
310	25/20 stainless steel	0.20	1.00	1.00	25.00	20.00	-		Exposed internals, and penetrations, high-temperature cyclones
50Ni-50Cr	Wrought heat-resistant alloy	-	-	-	50	Bal	-		
Alloy 400	Formerly monel	0.12	0.90	0.15	-	Bal	-	31.5 Cu	Shell liner

From the National Materials Advisory Board (1977). The data are from A. M. Hall, Battelle Columbus Laboratories, Columbus, Ohio, and are reproduced from Ref. 1.

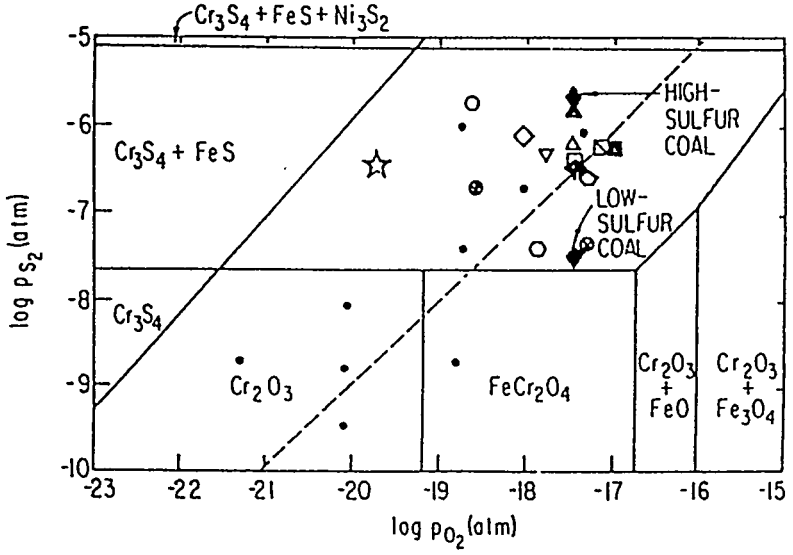

Fig. 13.3-1. Thermochemical diagram for Type 310 stainless steel at 871 °C, showing an experimentally-determined kinetic boundary (dashed line). Open and solid symbols represent low- and medium-Btu gasifier conditions, respectively; black dots are experimental gas potentials (reproduced from Ref. 2).

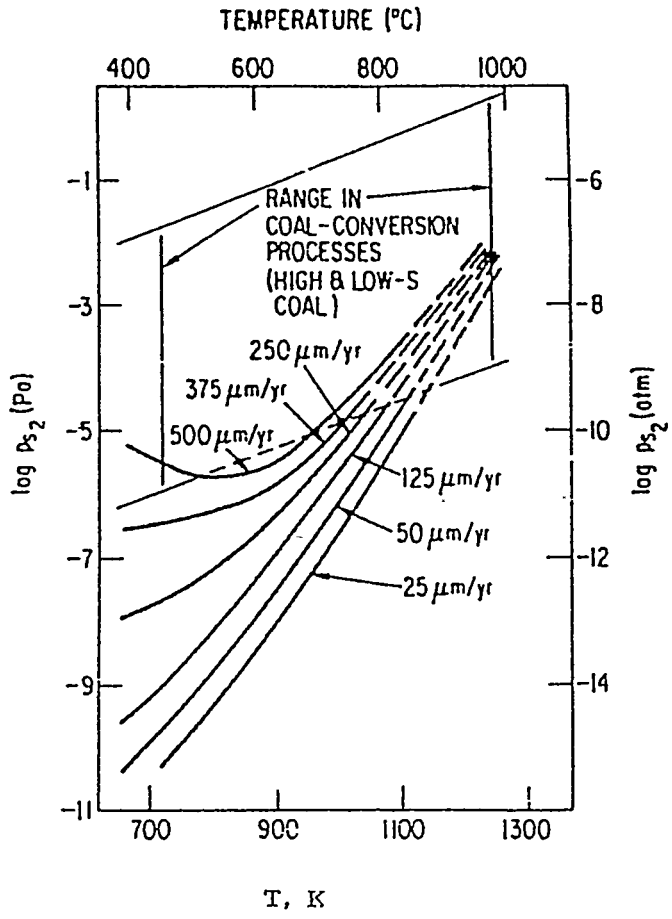

Fig. 13.3-2. Isocorrosion rate curves for types 304 and 316 stainless steel as a function of sulfur potential; reproduced from Ref. 1.

Table 13.3-3. Stability of alloy elements in medium (27% H_2, 28% H_2O, 31% CO, 13% CO_2, 1% H_2S) and low (12% H_2, 8% H_2O, 20% CO, 8% CO_2, 4% CH_4, 47% N_2, 1% H_2S) BTU coal-gasification atmospheres; reproduced from Ref. 5.

	Phase stability (phase can be formed in the gas between 300 and 1200°C				
	Element	Oxide (MO)	Sulphide (MS)	Carbide (MC)	Equilibrium phase in stable equilibrium with gas
Alloy bases	Fe	X	X		MS
	Ni		X		MS
	Co		X		MS
Desulphurizer	Mn	X	X		MS
Deoxidizer	Si	X	X		MO
Reactive additions	Cr	X	X	X	MO
	Al	X	X		MO
	Ti	X	X	X	MO
Solute strengtheners	Mo		X		MS

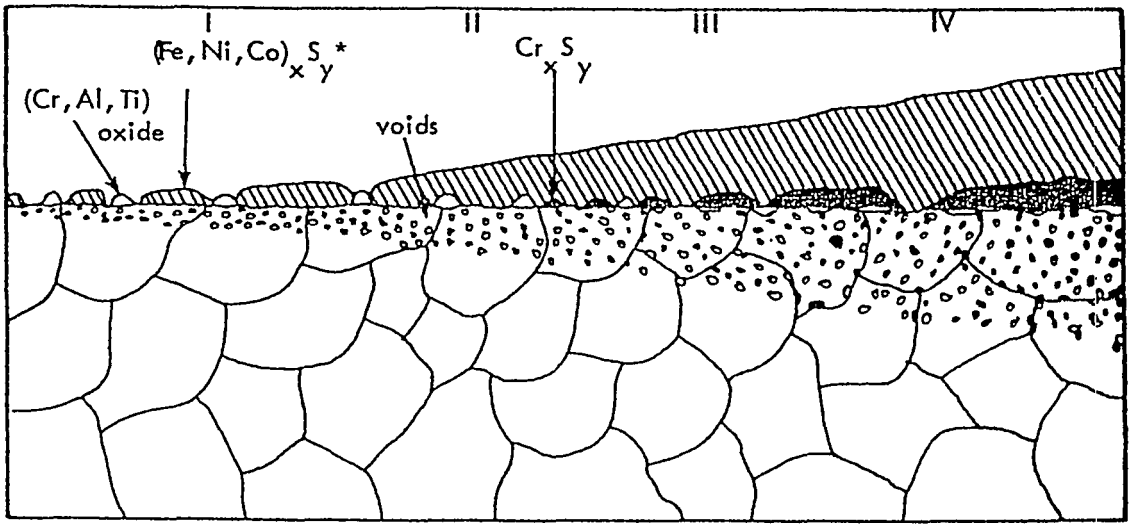

I Competition; II Overgrowth: III Cr_xS_y Formation;
IV Dissociation & Internal Sulfidation

Fig. 13.3-3. Reaction model for oxidation-sulfidation in mixed oxidant environments; reproduced from Ref. 1. An asterisk (*) indicates that, if the base metal sulfide is molten at the test temperature, islands of Cr_xS_y oxides and Cr-depleted alloy exist in the outer scale after cooling due to grain boundary attack by the liquid.

Table 13.3-4. Forms of gaseous corrosion of ceramic materials; reproduced from Ref. 1.

Reaction	Result
Reaction with steam	Leaching of SiO_2, $AlPO_4$, Ca
Reaction with hydrogen	Reduction of solid SiO_2, and Fe_2O_3 to gaseous SiO and Fe/FeO
Reaction with carbon	Disintegration by CO attack through deposite of C near Fe in refractory causing highly local stresses
Reaction with alkali vapor (Na, K)	Change in refractory/ceramic composition through direct reaction with Na, K

Table 13.3-5. Candidate structural ceramic materials and their properties; reproduced from Ref. 1 and based on data of M. G. Coombs and D. M. Kotchick (1979).

Candidate materials	Strength	Linear thermal expansion × 10^6		Thermal conductivity at 982°C (1800°F)		Maximum use temperature, °C(°F)	Fabricability
		cm/cm-°K	(10^6 in/in-°F)	Watts/°K-m	(Btu/hr-°F-ft)		
LAS, MAS and AS	Moderate	0.4 to 5.4	Low to moderate (0.2 to 3.0)	Low 3.46	Low (2.0)	982 (1800) 16	Good
Al_2O_3	Moderate to good	8.1	High (4.5)	10.38	Low (6.0)	1648 (3000+)	Good
Mullite	Moderate	4.5	Moderate (2.5)	4.3	Low (2.5)	1648 (3000+)	Good
Si_3N_4 hot-pressed	High	3.2	Moderate ((1.8)	15.6	Moderate (9)	1537 (2800)	Poor
Si_3N_4 reaction-bonded	Moderate	3.2	Moderate (1.8)	8.7	Low (5)	1537 (2800)	Good
Si_3N_4 sintered	High	3.6	Moderate (2.0)	17.3	Moderate (10)	1371 (2500)	Good
SiC hot-pressed	High	4.3	Moderate (2.4)	39.8	Good (23)	1537 (2800)	Poor
SiC sintered	Moderate to high	4.5	Moderate (2.5)	19.0	Moderate (11)	1537 (2800)	Good
SiC siliconized	Moderate	5.0	Moderate (2.8)	19.0-34.6	Good (11-20)	1343 (2540)	Good

Table 13.3-6. Chemical composition (in wt%) of several refractories; reproduced from Ref. 1 and based on data of R. E. Dial (1975). Castables are items 1 to 5 and shapes are 6 to 13.

Refractory	Bubble Al_2O_3		Dense Al_2O_3		SiC	Al_2O_3		Fused cast Al_2O_3				SiC	
	1	2	3	4	5	6	7	8	9	10	11	12	13
Al_2O_3	94.6	94.1	96.0	96.7	6.6	99.2	99.4	99.3	98.7	94.5	94.5	0.7	0.3
SiO_2	0.5	0.5	0.1	0.1	2.2	0.5	0.3	0.1	0.5	1.1	0.1	8.5	1.3
Fe_2O_3	0.2	0.2	0.1	0.1	1.8	0.1	0.1	0.1	0.1	0.1	0.1	0.7	0.3
CaO	4.2	4.7	3.6	2.7	5.5	0.1	0.1	0.1	0.1	0.3	0.1	0.2	0.2
Alkalis	0.4	0.4	0.2	0.3		0.1	0.1	0.4	0.04	3.9	5.2		
Other					82.7 (SiC)				0.5 (B_2O_3)			89.6 (SiC) 18.5 (Si_3N_4) 79.1 (SiC)	

Refractories containing free iron or iron-oxide-bearing compounds are subject to disintegration by carbon deposition (via decomposition of CO to C and CO_2), which leads to high local stresses that spall the refractory. This phenomenon occurs in the temperature range 400-650°C. Another cause of destruction of alumina-silica refractories is reaction with alkalies, which results in a 30% volume expansion that causes the refractory to spall. Western lignite coals contain sodium and have been reported to cause alkali-attack failure in a slagging-type gasifier, where a mullite refractory failed after 125 hours of exposure at about 1000°C.

In slagging coal-gasification systems, corrosion of refractories by molten slag occurs by a complex physiochemical process. The rate of corrosion is governed by mass transport of material across the boundary layer, which thus involves fluid flow and diffusion. Both thermodynamic and kinetic processes must be considered, as well as the pore structure and grain boundaries of the refractory and the nature of the reaction products. The physical, chemical and thermal properties of the liquid slag, refractory, and reaction products determine the corrosion of the refractories by liquid slags. The solubility of the refractory in the molten slag is an important parameter, especially the solubility of the grain boundary or bonding phases. It has been reported that alumina-silica and lime-silica refractories are suitable for use only up to about 1500°C and that, with high silica slags, the zirconia and chromium oxide refractories are more suitable.[1] For the more fluid low-silica slags, the chrome-magnesite and pure magnesia refractories are preferred.

The falling temperature gradients in the liner affect the composition gradients. The solubility of the refractory in the slag decreases with decreasing temperature, while the slag viscosity increases and diffusion decreases. These changes cause the corrosion, material transport, and penetration rates to decrease and eventually stop.[1] As a result, an equilibrium thickness of water-cooled refractory lining is established, which depends on the thermal conductivity of the refractory and the minimum temperature of the chemical reactions. High thermal conductivity and high minimum reaction temperatures are desirable under slagging conditions. Also, good resistance to abrasion, cracking, and spalling are important criteria in the selection of refractories for slagging gasifiers. Cooling plates penetrating into the refractory lining

are effective in forming a chilled slag layer or reducing solubility, material transport, and slag penetration, thereby greatly increasing operating life. Thin refractory linings on water-cooled walls are used in commercial slagging gasifiers, with the linings applied over studded metal tubes forming part of the metal wall. Candidate linings include fireclay, chrome ore, silicon carbide, alumina, and zircon sand (Zr silicate). The bonding agents that are used in applying the liners include calcium aluminum cement, phosphate compounds, sodium silicates, clay, boric acid, sulfur cement, and organic compounds. The water-cooled thin linings last 1-2 years; the longest lifetimes have been achieved with silicon-carbide containing vanadium additions, because of the high thermal conductivities and abrasion resistance.

The presence of particulate matter in the gas stream will enhance the degradation of alloy components by erosion-corrosion and sulfidation. Char-particle deposits act primarily by lowering the oxygen pressure in their vicinity and thereby promote sulfidation reactions.

13.3-3. Low-Temperature Corrosion

The aqueous solutions in coal-gasification systems are highly corrosive to the structural materials in components such as heat exchangers, fractionation columns, condensers, slurry pipelines, scrubbers and quench systems. These solutions contain dissolved aggressive gases, alkalis, salts, and organic acids, which may give rise to intense localized corrosion such as pitting, crevice corrosion, and stress-corrosion cracking. The selection of alloys under these service conditions depends on the specific impurities that are present in the aqueous media. In extensive, statistically designed, environmental tests, the concentrations of the different chemical species were varied systematically over a temperature range of 121 to 239°C.[1] The results indicate that the corrosion rates ranged from a low of less than 0.025 mm/yr for high-nickel alloys, austenitic stainless steels, and titanium, to rates exceeding 2.5 mm/yr for carbon steel, 410 SS and 430 SS, and above 5mm/yr for copper- and aluminum-base alloys. Stress-corrosion cracking is particulary severe in (i) austenitic stainless steels that have been heat-treated in the sensitizing temperature range of 450 to 700°C and (ii) in weld areas.

The presence of hydrogen in coal-gasification product streams may lead to degradation of the pressure-vessel materials (generally low Cr-Mo steels such as Fe-2.25Cr-1Mo). Hydrogen attack of the steel results in loss of ductility and fracture toughness. The conventional approach in determining the operating limits for these vessels is to use Nelson curves. These curves are based on an empirical compilation of failure data from the petrochemical industries. However, recent studies of hydrogen attack in pressure-vessel steel have addresssed the influence of environmental and metallurgical parameters. The goal of these studies is to provide models that can be used to correlated engineering and laboratory data and also to predict eventually the behavior under operating conditions. However, reliable fracture analysis can only be carried out when additional data are generated on the effects of hydrogen on residual stresses, plasticity, fatigue crack-growth rate, creep, and creep-fatigue interactions.

13.3-4 Erosive Wear

Erosive wear by solid particles entrained in gas streams is usually explained in terms of two models. One model is applicable to ductile materials and involves the mechanism of plastic flow. The second model explains wear for brittle materials in terms of micro-fracture. Both models include a number of parameters related to both the impacting particles and the impacted materials.

The properties of the impacting particles include size, shape, hardness, velocity, angle of particle impingement, and the loading density of the particles in the flowing stream. The properties of the impacted materials that influence wear include microstructure and mechanical properties and hardness. For example, for stainless steels, the resistance to wear decreases with increasing temperature because the ductility decreases correspondingly. Alloys having a well-dispersed carbide in a high-yield strength matrix show the least wear[3]. In ductile materials, erosion resistance is inversely proportional to the flow resistance of the material.

In brittle materials, erosion is influenced by porosity, as well as by hardness and toughness. Hence, high-density material has superior

wear resistance (Figs. 13.3-4 and -5). The wear model for brittle materials is based on the suggestion that surface cracks formed by particle impingement nucleate larger cracks, which results in material being removed by localized fracture. There is a need for information on the variation of hardness, ductility, and toughness of the refractory materials as a function of temperature. The best correlation appears to be between erosion rate and compressive strength of refractories (Table 13.3-7). Erosion rates may also be improved by enhancing the properties of the bonding material.

The mechanism of erosion is also influenced by the size of the impinging particles. Large particles tend to bridge the distance between the aggregate grains in refractories, whereas fine particles undercut the aggregate and cause much higher erosion rates. At elevated temperatures where the refractories have some ductility, their erosion behavior is similar to that of a metal rather than a brittle ceramic. Erosion rates are also influenced by flow conditions, fluid mechanics of the gas stream, temperatures, and corrosiveness of the ambient environment.

13.3-5. Mechanical Properties

The complex gas environment affects the mechanical properties of the materials, both by intergranular penetration of sulfur and by breakaway corrosion. These corrosion rates are difficult to predict for long-term service. Experimental studies on the mechanical properties of the materials in gas environments include measurements of uniaxial tensile strength, uniaxial and biaxial creep rupture, low-cycle fatigue, impact, and stress-corrosion cracking.

Tensile tests of candidate alloys after exposures of 1000 hr at 649°C to air and gas mixtures with 0.5% H_2S at 68 atm have been reported.[1] The results indicate that, with gas compositions which allow the formation of oxide films, there is a negligible effect on the tensile properties and impact strength of all of the selected alloys except for IN-657 (48Cr-50Ni-1.5Nb), which had an elongation value of zero after exposure to the gas environment. On the other hand, the similar alloy IN-671 (48Cr-51.5Ni-0.4Ti) showed no significant loss of ductility after exposure to the mixed-gas environments. These results illustrate the striking

difference caused by Ti and Nb additions. Other high-Cr alloys (Incoloy-800 and type 310 SS), when exposed for 1000 hr to gas mixtures with a wide range of oxygen and sulfur partial pressures between 750 and 982°C, show a decrease in strength with a decrease in oxygen partial pressure in the preexposure environment.

The results of creep-rupture tests indicate that, if the oxygen partial pressure is below a threshold value, the creep-rupture life and rupture strain are significantly lowered. Susceptibility to stress-corrosion cracking of several alloys was tested in oxidizing-sulfidizing and oxidizing-sulfidizing-carburizing atmospheres. The results are summarized in Fig. 13.3-6.

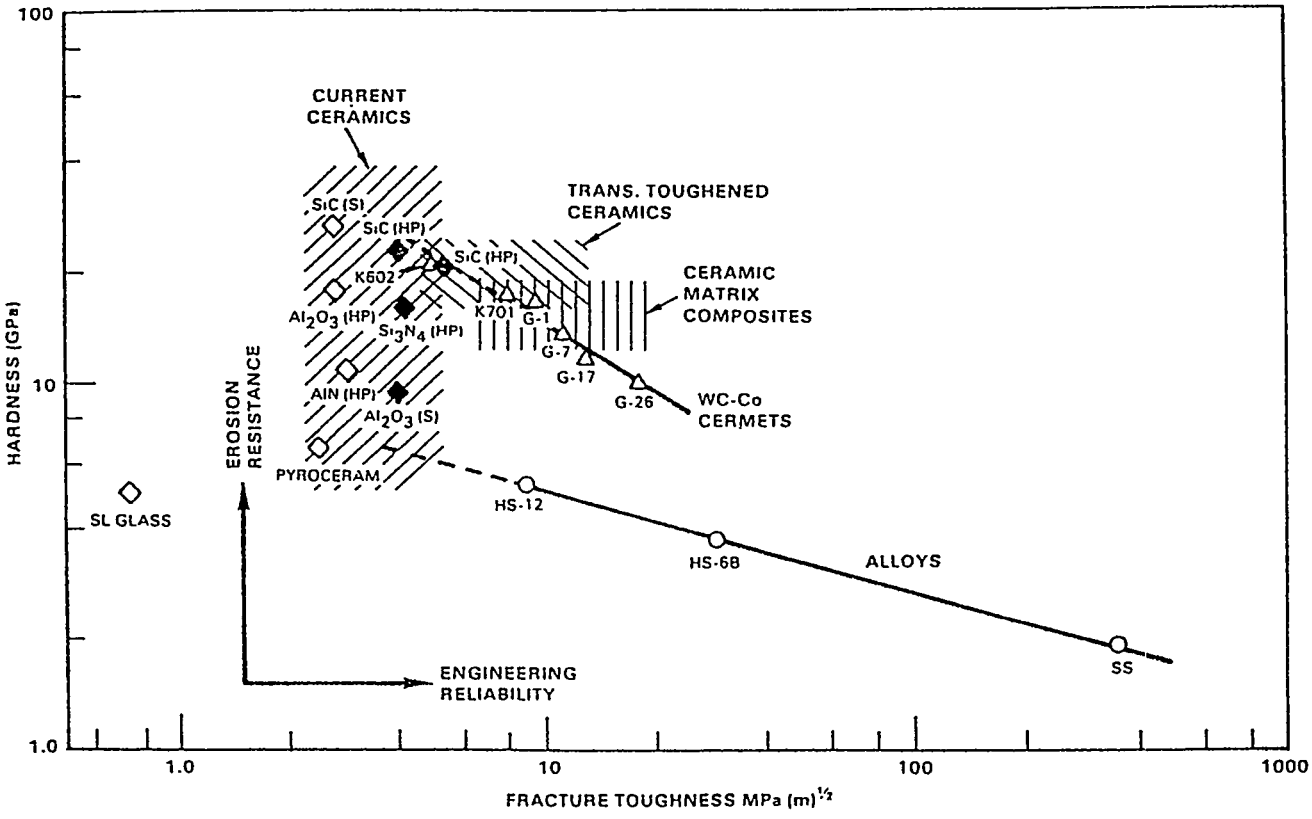

Fig. 13.3-4. Summary of ranges of properties pertinent to erosion resistance for different classes of materials; reproduced from Ref. 3.

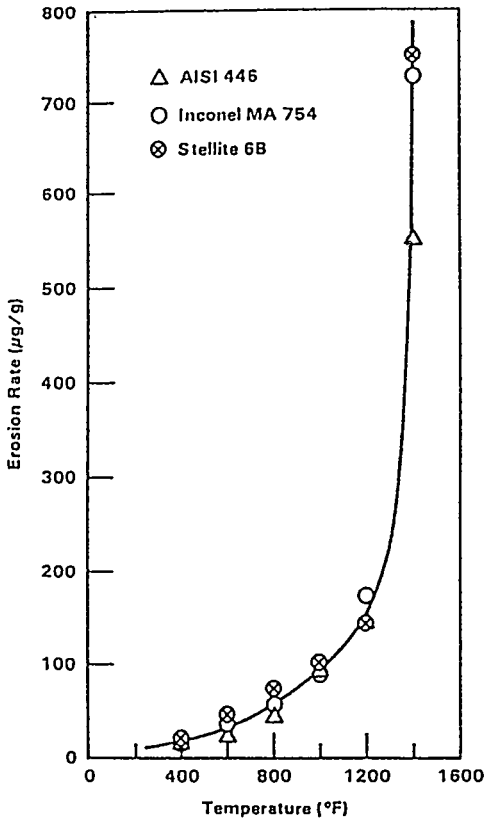

Fig. 13.3-5. Temperature dependence of erosion of high-temperature alloys (flue gas, 12 μm alumina particles at nominally 30°); reproduced from Ref. 3 and based on EPRI data.

Table 13.3-7. Properties and erosion characteristics of selected ceramics; reproduced from Ref. 3.

Ceramic	Grade	Hardness (GPa)	Fracture toughness ($MPam^{1/2}$)	Erosion characteristics	Erosion rate† $(\Delta V/V) \times 10^{10}$
Soda-lime glass	Float glass	5.2	0.75	Microcutting/ lateral cracking	2200
Glass-ceramic		6.6	2.4	Microcutting/ microflaking (transgranular)	210
AlN	Hot-pressed	10.9	2.9	Microflaking (transgranular)	1.6
Al_2O_3	Hot-pressed	17.7	2.7		1.4
SiC	Sintered	26.1	2.7		0.7
B_4C	Hot-pressed	31.0	--		0.3
SiC	Hot-pressed	22.7	4.0	Intergranular wear	19
SiC	Hot-pressed	20.7	5.3		10
Si_3N_4	Hot-pressed	15.9	4.2		5
Al_2O_3	Sintered	9.4	4.0		6.5

†Test conditions: velocity = 135 m/sec, θ = 90°, 8% silica oil slurry.

Pressure vessels in second-generation coal-gasification plants being developed in the US require higher temperatures and/or pressures than the early systems. Fabrication technology imposes limitations on pressure-vessel size and wall thickness. An example of the relation between design pressure and wall thickness for a pressure-vessel steel is shown in Fig. 13.3-7. Table 13.3-8 and Figs. 13.3-8 and 13.3-9 show allowable stress values for low alloy steels based on the ASME Boiler and Pressure Code, Section VIII, Division 1 and 2. In thick-section fabrication, quenching and tempering are required to meet code requirements. The problem of hydrogen attack on pressure-vessel steels must be addressed in operations at higher temperatures and pressures. Refractory linings have to be used in the vessels in order to limit the wall temperatures to less than about 325°C. Monolithic linings are preferred and are also said to be relatively cost-effective.

Heat exchangers are used for the recovery of sensible heat from hot gases produced by gasifiers prior to such operations as scrubbing, in preheating gasification air or raw materials, or to generate steam. The heat-exchanger materials function with oxidizing gases on one side and complex reducing gases on the other. Boiler-tubing-alloy recommendations are listed in Table 13.3-9. The use of structural ceramics for high-temperature heat-exchangers has been limited by the need for a statistical approach to the design and the lack of ASME codes for structural ceramics. Recent advances in the development of structural ceramics for heat exchangers may be of importance to future coal-gasification technology.

13.3-6. Materials for Syngas Coolers of Slagging Gasifiers

The development of entrained-flow, slagging coal-gasifiers is of interest for the production of electric power with gas turbines and steam-generating systems in integrated, combined-cycle power plants. The results of recent studies on materials for syngas coolers in slagging gasifiers have been described.[5] At temperatures above 650°C, few materials resist rapid corrosion by the gases with higher sulphur and lower oxygen activities found in the medium- or low-BTU atmospheres (Table 13.3-10) because the Fe-Ni sulphides melt above this temperature. Thermodynamic and

kinetic factors favor the formation of sulfide-reaction products on many of the candidate metals and alloys. Guidance in the selection of materials is provided by thermodynamic and kinetic data, as well as by analyses of gas equilibria.

In the combined-cycle coal gasification plant, the tubular heat exchanger metal walls are maintained at 250-500°C, with gas inlet temperatures of 1100-1200°C. A minimum of 23-25% Cr is required in ferritic chromium steels for good resistance to corrosion at 400-500°C (Fig. 13.3-10). A clad or overlay of an alloy such as Fe-19Cr-6Al-0.8Hf provides excellent protection on low alloy steels. Even better corrosion resistance to sulfidation at 400-500°C is exhibited by high-Cr austenitic stainless steels such as types 309 and 310 and also by the cast alloy HK40. Titanium and Ti-6Al-4V alloys are reported to have the best resistance to corrosion among all of the materials tested at 300-500°C. They should be more cost-effective in use on a life-cycle basis than coated low alloy steels for long-term service at temperatures below 400°C in syngas coolers (Table 13.3-11).[5]

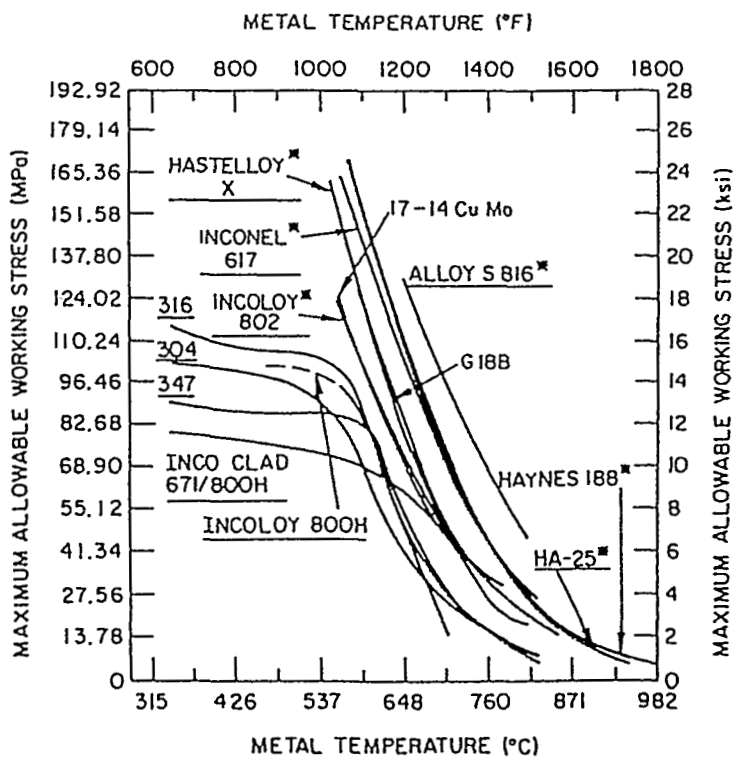

Fig. 13.3-6. Maximum allowable working stress for several candidate tubing materials for fossil gas applications; reproduced from Ref. 1 and based on data of D. E. Thomas et al (1976).

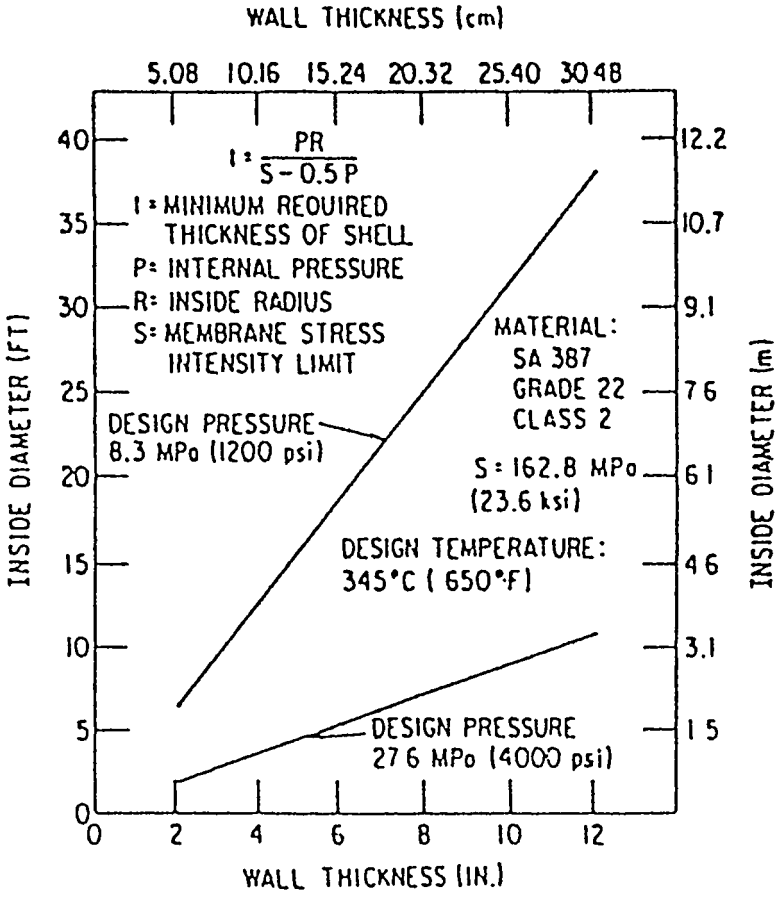

Fig. 13.3-7. Relationship of design pressure to inside diameter and wall thickness of pressure vessels, based on limits of current technology; reproduced from Ref. 1 and based on data of D. A. Canonico et al (1978).

13.3-7. Nuclear Heat Steam-Gasification of Coal

There has been much interest in several countries in coupling the steam-gasification process with a high-temperature nuclear reactor (HTGR).[6,7] The fluidized bed is now contained in a pressure vessel made of boiler steel with inside insulation. The intermediate heat exchanger between the primary reactor-coolant helium and the coal gasifier is subjected to high temperatures and is also in direct contact with the coal/steam fluidized bed. Special high-temperature alloys have been developed for this type of application, with the heat exchanger subjected to aggressive conditions. The heat exchanger is immersed in the fluidized-gas

generator at temperatures ranging from 750 to 950°C and at a pressure of about 40 bars. The fluidized bed consists of finely ground coal which is fluidized by steam. The commercial alloy Incoloy-800 was selected in Germany as base composition for 70 experimental alloys, with and without the addition of minor alloying elements to improve its corrosion resistance to an acceptable level under these conditions. The wet crude gas contains about 50 vol% of steam and the dry gas contains H_2, CO_2, CO, CH_4, and traces of H_2S. The alloy, which was found to be acceptable after 10,000 hr of exposure, has a composition (in wt%) of 25-27 Cr, 30-32 Ni, 0.06-0.12 Ce, with the balance made up of Fe. The Ce serves to mitigate spalling of the oxide film during thermal cycling by improving the adherence of the scales. It also improves the resistance to corrosion and internal oxidation.

Table 13.3-8. Design stress values for typical gasifier plate steels; reproduced from Ref. 1 and based on data of D. A. Canonico et al (1978).

Material		Minimum tensile strength, MPa (ksi)	Minimum yield strength, MPa (ski)	Maximum allowable stress (Sect. VIII Div. 1), -29 to 343°C MPa (ksi)	T °C(°F)	Design stress intensity (Sect. VIII Div. 2), MPa (ksi)
A-516-70	CS	482 (70)	262 (38)	121 (17.5)	260 (500) 343 (650) 371 (700)	141 (20.5) 127 (18.4) 126 (18.3)
A-204-B	C-$\frac{1}{2}$Mo	482 (70)	276 (40)	121 (17.5)	260 (500) 343 (650) 371 (700)	155 (22.5) 148 (21.4) 145 (21.0)
A-204-C	C-$\frac{1}{2}$Mo	517 (75)	296 (43)	129 (18.7)	260 (500) 343 (650) 371 (700)	167 (24.2) 158 (22.9) 156 (22.6)
A-302-B	Mn-$\frac{1}{2}$Mo	552 (80)	345 (50)	138 (20.0)	260 (500) 343 (650) 371 (700)	184 (26.7) 184 (26.7) 184 (26.7)
A-533-A,B,C	Mn-Mo-Ni	552 (80)	345 (50)	138 (20.0)	260 (500) 343 (650) 371 (700)	184 (26.7) 184 (26.7) 184 (26.7)
A-387-22C12	$2\frac{1}{4}$Cr-1Mo	517 (75)	310 (45)	119 (17.2)	260 (500) 343 (650) 371 (900)	159 (23.0) 158 (22.9) 117 (17.0)

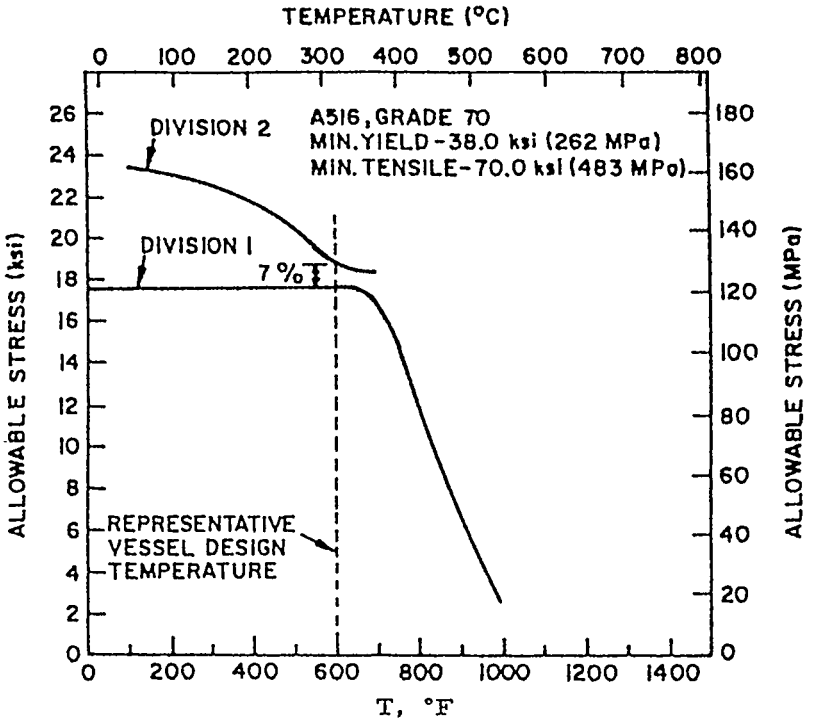

Fig. 13.3-8. Comparison of the allowable stresses os Section VIII, Division 1 and the allowable stress intensities of Section VIII, Division 2 for SA 516 grade 70 steel; reproduced from Ref. 1 and based on data of D. A. Canonico et al (1978).

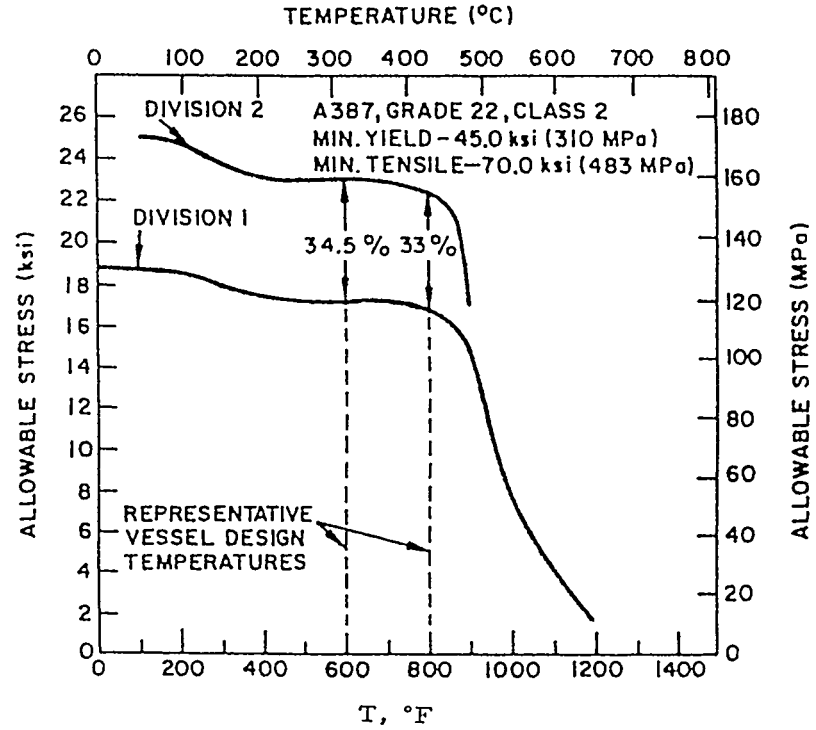

Fig. 13.3-9. Comparison of the allowable stresses of Section VIII, Division 1 and the allowable stress intensities of Section VIII, Division 2, for SA 387 grade 22 class 2 steel; reproduced from Ref. 1 and based on data of D. A. Canonico et al (1978).

Table 13.3-9. Boiler tubing alloy recommendations (based on stress and fireside/steam side corrosion); reproduced from Ref. 1 D. E. Thomas et al (1976).

Pressure, MPa (psi)	Temperatures		
	538°C (1000°F)	649°C (1200°F)	760°C (1400°F)
2.41 (350)	$2\frac{1}{4}$Cr-1Mo		347 SS Inco Clad 671/800H Incoloy 802
3.10 (450)	-		Incoloy 82
4.10 (600)	$2\frac{1}{4}$Cr-1Mo	304 SS Incoloy 800H Incoloy 802	Incoloy 802
4.31 (625)	$2\frac{1}{4}$Cr-1Mo		-
7.58 (1100)	$2\frac{1}{4}$Cr-1Mo	304 SS Incoloy 800H Incoloy 802	Inco Clad 671/800H Incoloy 802 Inconel 617
8.96 (1300)	-	Incoloy 802	-
12.40 (1800)	-	Incoloy 802	-
13.78 (2000)	-	316 SS 347 SS Incoloy 802	- - -
15.16 (2200)	-	Incoloy 802	Incoloy 802 Inconel 617
16.54 (2400)	304 SS/Incoloy 800H	304 SS Incoloy 800H Incoloy 802	Incoloy 802 Inconel 617 HA 188
24.12 (3500)	304 SS/Incoloy 800H	304 SS Incoloy 800H Incoloy 802	Inconel 617 HA 188 S 816
31.00 (4500)	304 SS/Incoloy 800H	Incoloy 802 Incoloy 617	S 816
34.45 (5000)	304 SS/Incoloy 800H	Incoloy 617	S 816

Table 13.3-10. Representative coal-gasification atmospheres; reproduced from Ref. 5. The product gas compositions are given in vol%.

Compounds	MPC[a]	Medium BTU[b]	Low BTU[c]
H_2	24	30	12
H_2O	39	14	8
CO	18	44	20
CO_2	12	10	8
CH_4	5	-	4
N_2	(NH_3-1)	2	47
H_2S	1	0.6	1
H_2O:H_2	1.62	0.47	0.67
CO_2:CO	0.66	0.23	0.40
H_2O+CO_2	51	24	16

[a]MPC laboratory test atmosphere modelled after the Hygas pilot-plant product gas.

[b]Oxygen-blown slagging gasifier.

[c]Air-blown gasifier.

Table 13.3-11. Based on the results of 1500-3000 hr tests. The listed materials and coatings are considered to have good potential for further testing, evaluation, or development as syngas-cooler components; reproduced from Ref. 5.

Alloy coating	Maximum temperature, °C			
	< 300	300	400	500
T-11, 22 steels	X			
16-18Cr steels		X		
23-25Cr steels				X
Types 304, 347SS			X	
Types 309 and 310SS, HK40				X
Titanium				X
T-11 alonized				X
T-11 chromized				X
T-11 sprayed aluminum		X		

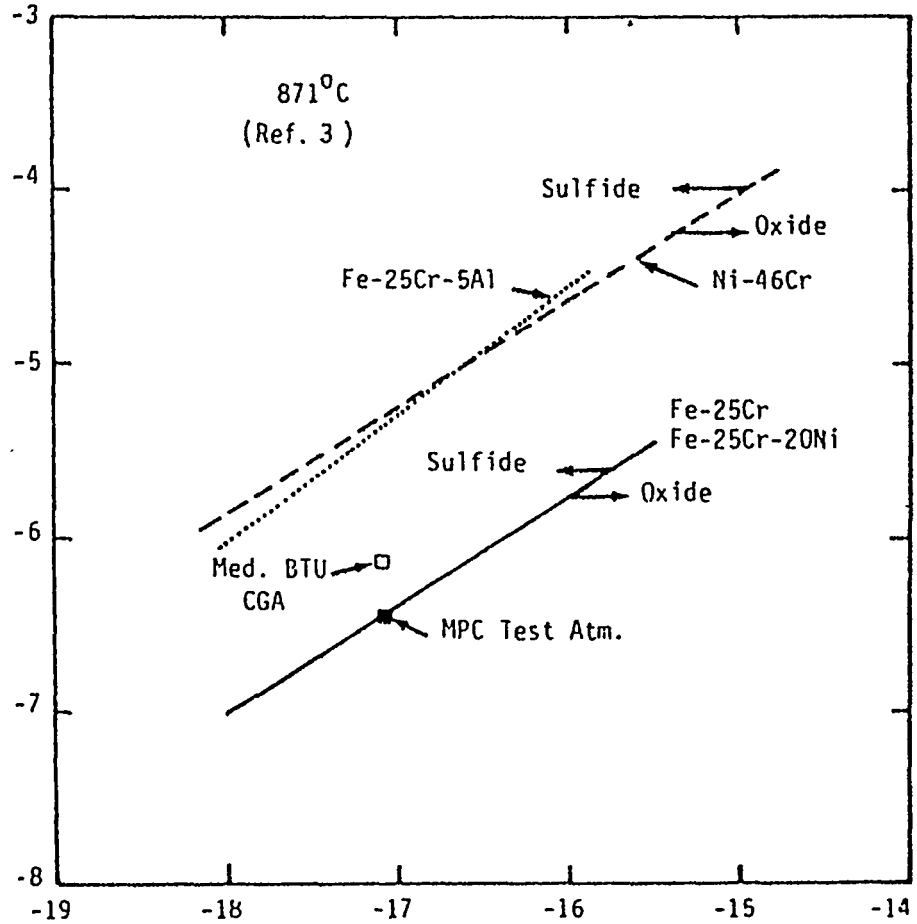

Fig. 13.3-10. Oxide-sulphide transition boundaries (ordinate = log p_{S_2}, abscissa = log p_{O_2}), pressures in atmospheres. Reproduced from Ref. 5 and based on data of R.A. Perkins and S.J. Vonk (1979).

References for Section 13.3

1. W.A. Ellingson, K. Natesan, and T. Vojnovich, "Materials of Construction," pp. 488-610 in The Science and Technology of Coal and Coal Utilization, B.R. Cooper and W.A. Ellingson eds., Plenum Press, NY and London (1984).
2. K. Natesan and W.T. Bakker, "Corrosion in Coal Gasification Systems," pp. 185-194 in Proc. Conf. on "Materials for Future Energy Systems," 1-3 May, 1984, Washington, DC, American Society for Metals, Metals Park, Ohio (1985).

3. I.G. Wright, A.R. Olsen, and S. Ibarra, "Erosion-Resistant Materials for Critical Areas of Coal Liquefaction and Coal Gasification Systems," ibid. pp. 205-216.
4. A.G. Imgram and R.A. Swift, "Pressure Vessel, Piping, and Welding Needs for Coal Conversion Systems," ibid. pp. 217-233.
5. R. A. Perkins, "Materials for Syngas Coolers of Entrained Slagging Gasifiers," pp. 219-258 in Corrosion Resistant Materials for Coal Conversion Systems, D.B. Meadowcroft and M.I. Manning eds., Applied Science Publishers, London and NY (1983).
6. H.J. Schroter and K.H. Van Heek, "Status of Coal Gasification in Europe and Related Requirements on Materials," ibid. pp. 181-218.
7. W. Schendler, "High Temperature Corrosion of Materials for Steam-Coal Gasification Utilizing Nuclear Process Heat," ibid. pp. 201-218.

CHAPTER 14:
INTRODUCTION TO COSTING*

Capacity-factored estimating and equipment-factored estimating represent the two primary techniques used in the conceptual-estimation of synfuels projects. These two techniques and their limitations will be discussed. We conclude with an overview of the assessment of risk associated with an estimate. Before describing these approaches to conceptual estimating, cost definition must be established. Our objective in estimating is to establish the selling price or installed cost of a new facility. The selling price is composed of the following four major cost elements: (i) Direct field costs are those of the permanent physical plant facilities and include field material, subcontracts, and labor. (ii) Indirect field costs include all of the construction support of the permanent facility. (iii) Home-office costs include all labor and expenses associated with engineering of the facility. (iv) Other costs include sales taxes, escalation, and contingency.

Figure 14-1 shows a typical distribution of project costs between the four major cost elements. The largest cost element is the direct field cost. This is the primary element we focus on in defining the data base used for conceptual estimation. The variable nature of the remaining costs elements causes us to treat these items only at the total project level, after the direct field costs have been established for all processes, utilities, and offsites.

Capacity-factored estimates for new process units are derived from the battery-limit costs of similar units of the same or different capacities (i.e., coal gasification, gas cooling and scrubbing, steam generation, etc.). Through the use of normalized historical data, the capacity-factored estimating technique can be used to scale the costs of similar

---

* This chapter has been written by D. Pescarolo, Fluor Technology, Inc., 3333 Michelson Drive, Irvine, CA 92780.

process plants to arrive at the direct field costs within the battery limits of the new process facility. Direct field costs within the data base contain normalized man-hours and material dollars. After scaling to the new plant capacity, labor efficiencies, wage rates, and material escalation can be applied to adjust for new plant location and timing.

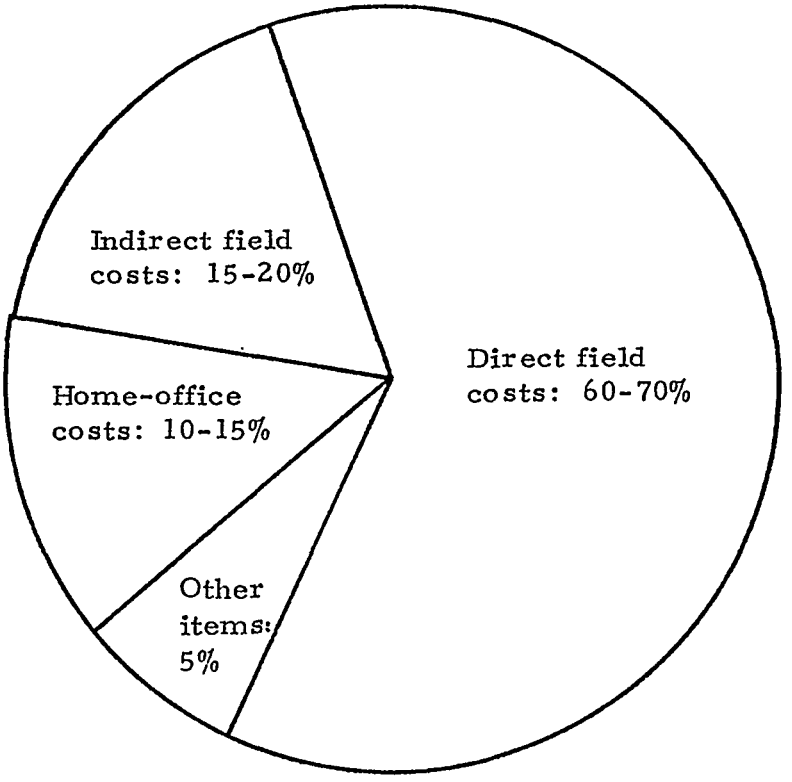

Fig. 14-1. Relative costs of the four major cost elements in the total project cost.

The accuracy associated with the capacity-factored estimate depends on several key factors. Most critical is the similarity of the base or reference plant to the new plant. Significant differences in configuration, operating conditions, or feedstock will greatly reduce the accuracy of the estimate. Coal composition and legislated environmental constraints are some of the major items driving the design configuration and the costs associated with early synfuels studies. The accuracy of the estimate is related to our confidence in the design basis.

In the absence of a closely-matched process plant that may be used in capacity-factored estimating, an equipment-factored estimating approach is used. Here, each piece of equipment represents a module. The equipment modules become building blocks of a process unit. Each equipment module includes all costs required to install that piece of equipment at the direct field-cost level. Each equipment item must be defined in terms of capacity, metallurgy, and design pressure and temperature. These are the mandatory data elements needed to establish the direct field costs associated with equipment items. The accuracy associated with the cost of a process unit estimated through this approach is related to our ability to recognize all equipment items required to operate the process unit at the required stream factor. Table 14.1 summarizes data required to support EXPONE, an equipment-factoring estimating tool.

The firmer the design, the greater the confidence in the estimate. Soft areas in process or design definition must be clearly segregated and analyzed for cost-growth potential. The quality of an estimate then depends on the information known at the time of the estimate. Contingency is normally applied to mitigate the cost-growth potential associated with the unknown. Items that must be considered in establishing contingency are project definition, labor efficiency, materials pricing, subcontractor performance, estimated tolerances, minor scope changes, minor schedule delays, process uncertainties, wage rates, and environmental impositions.

One of the most important factors causing estimate uncertainty for conceptual facilities is the level of process and project definition when the estimate is made. Uncertainty and risk in an estimate can be defined and measured through the use of probability models. If properly performed, this analysis results in a valuable tool for management. Management thus has a vehicle to go from qualitative to quantitative statements about uncertainty in terms of probability of underrunning the estimated cost. The proper use of a risk model enables us to identify weak links, thereby quantifying cost-growth potential. Management may then concentrate on design issues causing greatest uncertainty.

For a $300 million plant, Fig. 14-2 shows the probability of underrun curve for a capacity-factored estimate. The factored or conceptual estimate confidence of underrun is less than 30%. To increase this value to 50%, 13% contingency would have to be added; 31% additional contingency

would yield a 75% confidence of underrun. Bringing conceptual studies to 50% probability of underrun is the norm.

Figure 14-3 shows the probability of an underrun curve for a detailed estimate. For this case, the engineering of the $300 million plant is 40% complete; orders have been placed for 90% of the machinery and equipment. The resulting curve shows a greater probability of underrun, and the 50% probability is achieved with 3% contingency.

Figure 14-4 shows both the capacity-factored-estimate and the detailed-estimate probability of underrun curves. The greater confidence in underrun shown on the detailed estimate is a function of the maturity of design. Figure 14-4 clearly shows the influence of design development on confidence in the estimate. The absolute cost difference between the conceptual and detailed estimates is not great in this example. This type of result is obviously not always obtained, but if it is accepted that one of the major uses of conceptual estimates is to determine process configuration alternatives; then, the absolute cost is not critical. Instead, cost differences are important. Thus, the ability to use consistent data and estimating tools for each design case is of paramount importance in conceptual estimating. If properly done, costs are then driven by design configuration alone and not by differences in estimating techniques.

Table 14-1. Mandatory and desired input data for the EXPONE equipment-factored estimate.

Mandatory Data:	equipment definition, capacity, metallurgy, design pressure, design temperature.
Desired Data:	mechanical flow diagrams, project specifications, piping transpositions, equipment-data sheets, equipment-price quotations, major electrical equipment pricing, electrical one-line diagrams, plot plans, building and structure sketches.

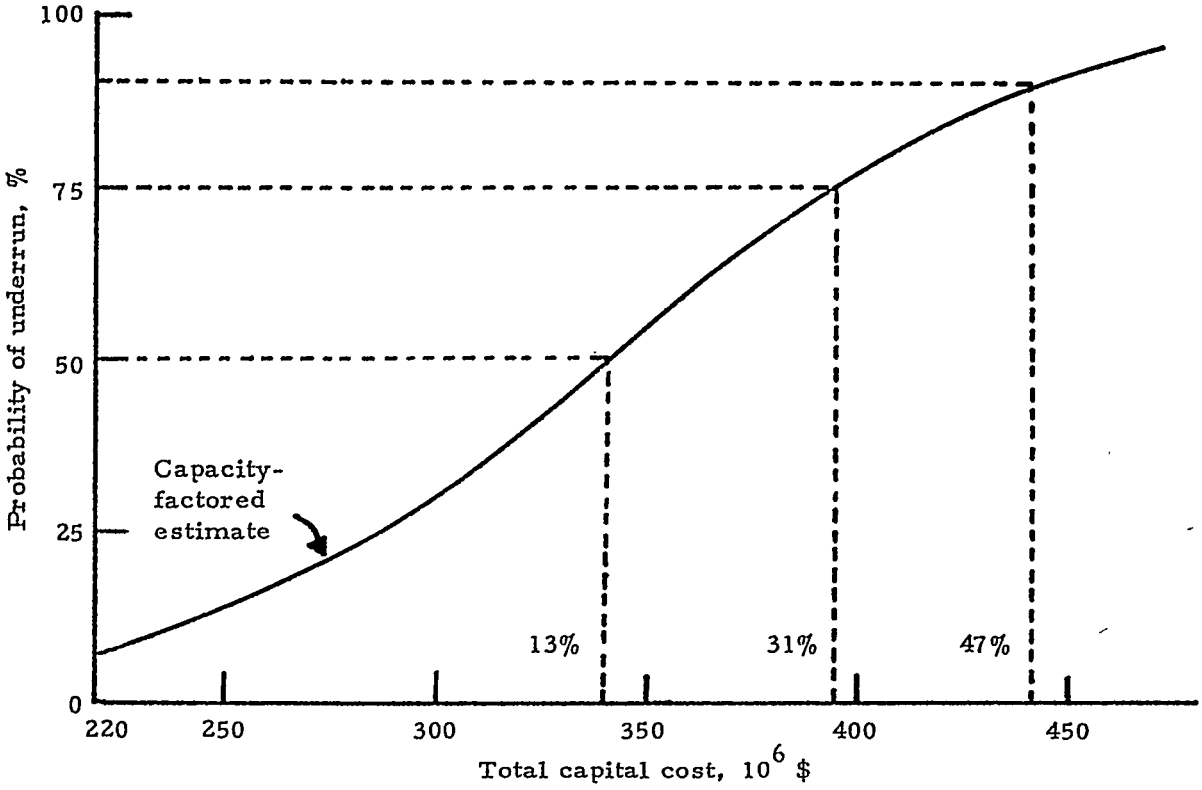

Fig. 14-2. Cumulative probability for a capacity-factored estimate of a $300 million plant.

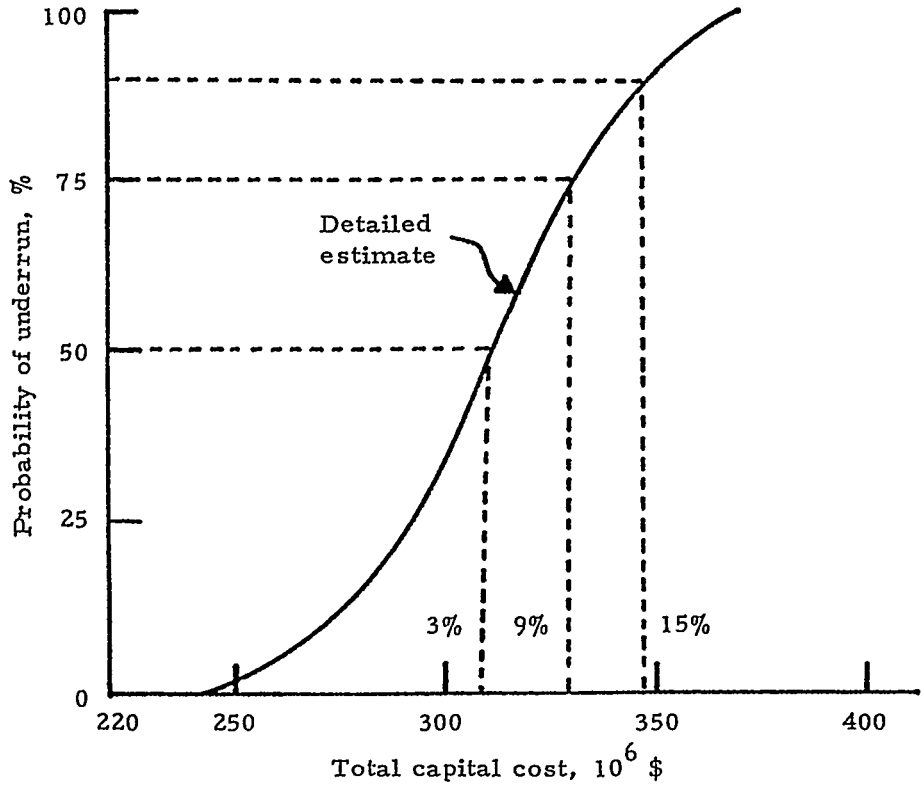

Fig. 14-3. Cumulative probability for a detailed estimate of a $300 million plant.

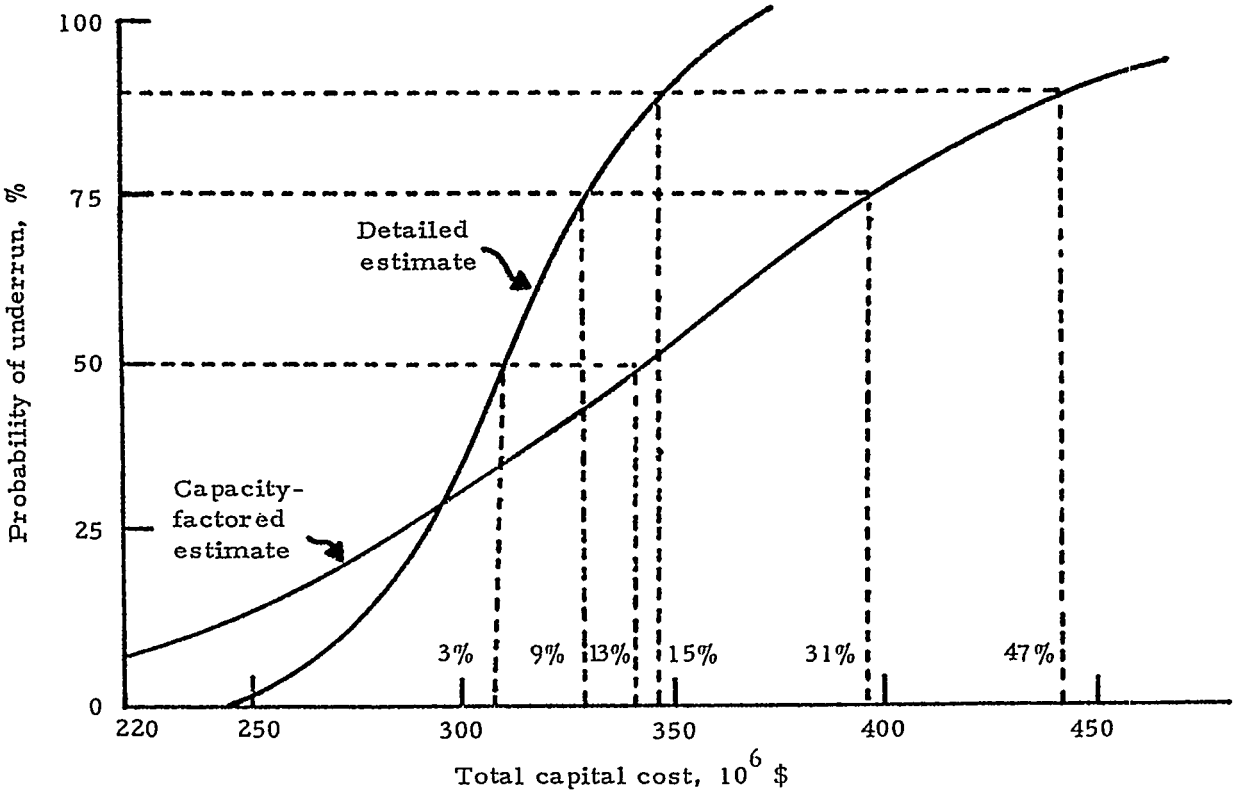

Fig. 14-4. Cumulative probabilities for a $300 million plant based on a detailed estimate and a capacity-factored estimate.

In summary, conceptual estimating data and tools, when properly used with probability simulations, are major contributors to the decision-making process between design alternatives and in determining plant economics.

APPENDIX: GENERAL REMARKS ON COAL-GASIFICATION SYSTEMS*

A convenient manner of viewing gasifiers is illustrated in Fig. A-1.[1] In the gasification zone, product gas and ash are formed by reactions involving oxygen, steam and coal (a). The gasification zone is intimately coupled with the devolatilization region (b) and (c). Devolatilization is accomplished either by mixing the feed coal with hot gas in a countercurrent flow (b) or by creating a completely stirred mixing region (c). In both cases, heating is accomplished by hot gases from the gasification zone, char is returned to the gasification zone, and hot exit gases are removed from the devolatilization zone.

R.V. Shinnar[1] defines an ideal gasifier as a unit in which the heats of combustion and gasification are exactly balanced, whereas practical gasifiers are non-adiabatic and operate with heat removal. In practice, excess steam, gas and fines recycle are used at high gasifier outlet temperatures, with or without a waste-heat boiler (as in the Winkler).

An extensive overview of gasifier performance based on stoichiometric, kinetic, and thermodynamic considerations is given by Denn and Shinnar in Ref. 2. Deviations from optimum conditions imposed by process constraints are detailed, and further insight into the operation of the three basic gasifier types (moving-bed, entrained-flow, and fluidized-bed) is obtained by computer modeling.[2] Comparisons between actually operating gasifiers are made and ideal operating conditions are identified.[2]

A-1. Stoichiometry of Coal Conversion[1]

The conversion of coal with elemental composition CH_aO_b ($a \approx 0.8$, $b \approx 0.1$ to 0.2) by oxygen (in the ratio R moles of O_2 per mole of C) and water (Su+Sp moles of H_2O per mole of O_2) is described by the following stoichiometric equation if m moles of CH_4 are formed per mole of C and RSp moles of H_2O remain per mole of C:

---

* Based on a presentation by R. Shinnar (Department of Chemical Engineering, CUNY, NY 10031) at the Fourth Technical Meeting of COGARN.[1] This Appendix has been prepared by S.S. Penner and D.F. Wiesenhahn.

$$CH_aO_b + RO_2 + R(Su + Sp)H_2O \rightarrow (2 - 2R - SuR - b - 2m)CO + [SuR + (a/2) - 2m]H_2 + (2R + SuR + b + m - 1)CO_2 + m \times CH_4 + RSp \times H_2O \ , \qquad (A\text{-}1)$$

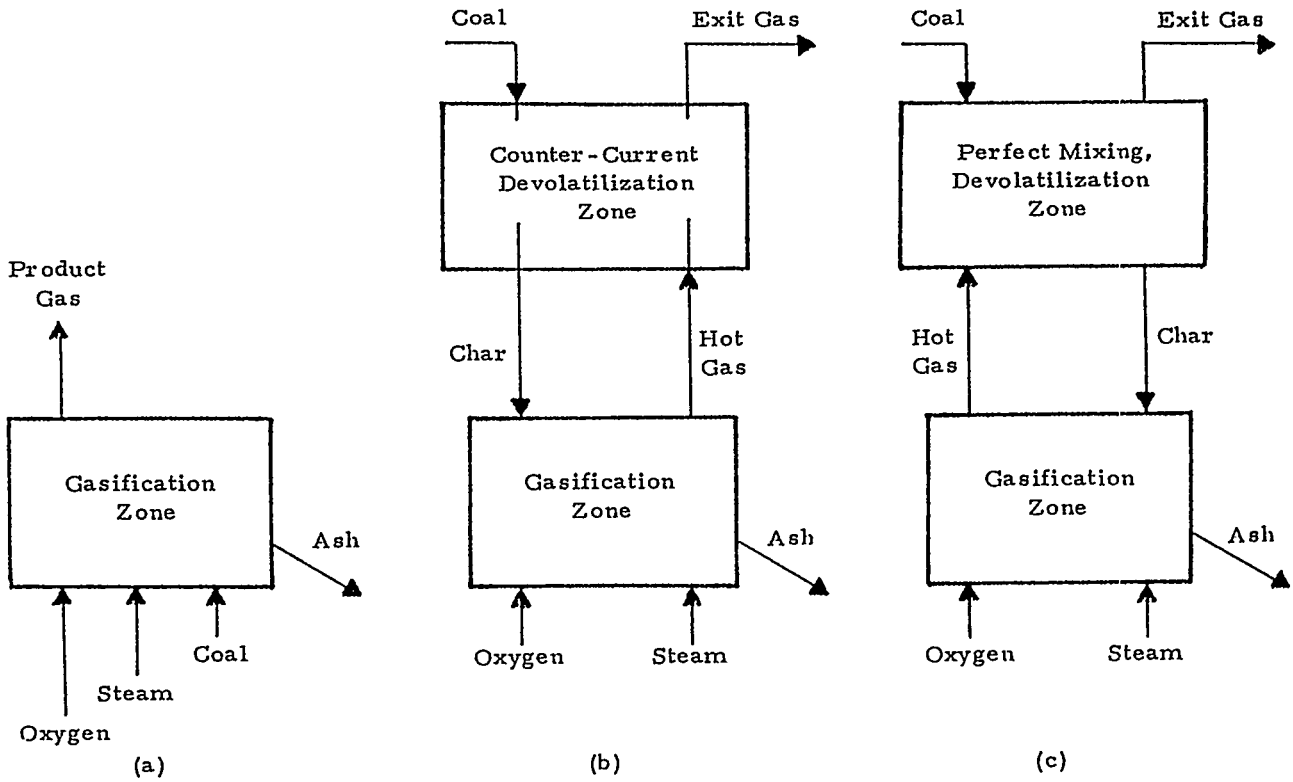

Fig. A-1. Schematic representation of gasifiers; from Ref. 1.

where the coefficients multiplying CO, CO_2 and H_2 follow immediately from mass conservation in view of the stoichiometric inputs of reactants. A parameter that does not depend on either the water-feed or methane-production rates may be formed by adding the overall stoichiometric coefficients of CO and H_2 per mole of CH_aO_b to 4m. The result has been termed a stoichiometric invariant and is given by

$$I = (2 - 2R - SuR - b - 2m) + [SuR + (a/2) - 2m] + 4m = 2 - b + (a/2) - 2R \ . \qquad (A\text{-}2)$$

The parameter I is seen to depend only on the oxygen-feed ratio R and on the coal composition (a and b). In the absence of methane formation (m = 0) and without feed CO_2 or the addition of H_2O to effect gas conversion (Su = 0 or Su+Sp = Sp = 0), all of the carbon is converted to CO when the coefficient of CO_2 in Eq. (A-1) vanishes, i.e.,

$$R = R_c = (1/2)(1-b) \text{ or } 2 - 2R_c - b = 1 \ . \qquad \text{(A-3)}$$

This limiting value of $R = R_c$ represents the minimal oxygen-to-carbon ratio for complete conversion of C to CO; with b = 0.1 to 0.2, $0.40 \leq R_c \leq 0.45$. For $R > R_c$, some of the carbon must be converted to CO_2. In terms of I [compare Eq. (A-2)], the difference between R and R_c becomes

$$R - R_c = (1/2)\{[1 + (a/2)] - I\} \ . \qquad \text{(A-4)}$$

The molar heat of combustion of CO to form CO_2, the HHV for the molar heat of combustion of H_2, and one third of the molar heat of combustion of CH_4 when using the HHV for the water formed are all nearly equal (≈68 kcal). Thus, the total heat of combustion of the product gases, measured in units of 68 kcal, is approximately

$$h = 2 - 2R - SuR - b - 2m + SuR + (a/2) - 2m + 3m = I - m \ , \qquad \text{(A-5)}$$

where we have used Eq. (A-2). It is apparent from Eq. (A-5) that methane formation reduces the reaction heat unless it affects I. That methane formation increases I follows immediately from the fact that carbon conversion to methane reduces oxygen requrements (i.e., it reduces R) and hence increases I according to Eq. (A-2).

Shinnar has emphasized the importance of minimizing the costs of feed steam and oxygen. This cost is roughly proportional to R(4.1 + Su + Sp) since oxygen feed costs roughly 4.1 times as much as steam feed. Cost minimization requires minimizing the unused steam in the product gases (RSp) per mole of CH_aO_b. In the absence of methane production (m = 0), the steam feed rate for gasification and shift is bounded by the requirements that it must less than or equal to the value that makes the coefficient of CO in Eq. (A-1) greater than or equal to zero and it must be greater than

or equal to the value required to make the coefficient of CO_2 in Eq. (A-1) greater than or equal to zero, i.e.,

$$SuR \leq 2 - 2R - b \ , \quad SuR \geq 1 - b - 2R \ ;$$

combining these two inequalities and replacing b according to Eq. (A-3), we find that

$$(2/R)(R_c - R) \leq Su \leq (2/R)[R_c - R + (1/2)] \ . \qquad (A\text{-}6)$$

Easily measurable gasifier parameters are the cold-gas composition and the flow rates of oxygen, coal and product gas. The extent of carbon and steam conversion and the fines flow rate are difficult to measure.

A-2. Gasifier Efficiency

Shinnar and Kuo[3] measure the gasifier efficiency by the ratio of non-recoverable energy in the feed to the LHV of the product gases. This ratio, per mole of CH_aO_b, is proportional to

$$E_L = [R(Su + Sp) + 4.1R]/$$
$$[(2 - 2R - SuR - b - 2m) + 0.85[SuR + (a/2) - 2m] + 2.85m]$$

since the relative LHVs of CO, H_2 and CH_4 are proportional to 1, 0.85 and 2.85, respectively. In terms of moles of reactants and products per mole of CH_aO_b, the quantity E_L may be written as

$$E_L = [(H_2O) + 4.1(O_2)]/[(CO) + 0.85(H_2) + 2.85(CH_4)] \ , \qquad (A\text{-}7)$$

where quantities in parentheses denote moles per mole of CH_aO_b. For an SNG plant, the applicable heating values are the HHVs, which are in the ratio 1, #1 and 3 for CO, H_2 and CH_4, respectively, and the denominator in Eq. (A-7) therefore becomes $(CO)+(H_2)+3(CH_4)$; the resulting value of E for this system is designated as E_{CH_4}. The lower E_L or E_{CH_4}, the higher the net gasifier efficiency.

For practical systems, Shinnar[1] defines a revised oxygen-consumption ratio as

$$R = (O_2)/(C)x \ ,$$

where x = fractional carbon conversion and R (in mole/mole) represents the moles of O_2 required in practice per mole of carbon converted. Furthermore, with CO_2 feed, Shinnar [1] replaces the stoichiometric invariant I of Eq. (A-2) by the following invariant:

$$\frac{(X_{CO} + X_{H_2} + 3X_{CH_4})/[X_{CO} + X_{CO_2} + X_{CH_4} - (\dot{CO}_2)/\dot{M}]}{2 + (a/2x) - (b/x) - 2R,} = \qquad \text{(A-8)}$$

where X_i = mole fraction of species i in the net dry product gas, $(\dot{CO}_2)$ = CO_2 feed rate (lb-mole/hr), and $\dot{M}$ = net dry product-gas flow rate (lb-mole/hr). Here, the numerator on the left side of Eq. (A-8) is proportional to the product-gas heating value, while the denominator represents carbon-species conservation.

Practical gasifiers operate with R_c-R close to zero, with both positive and negative values occurring (see Tables A-1 and A-2). Thus, the Lurgi dry ash and slagger gasifiers should be viewed as the only true gasifiers; future design calculations for the KRW show that it may also become a true gasifier. In terms of feed costs for oxygen and steam, the Lurgi slagger and KRW design are cheaper than the Texaco and Shell gasifiers which, in turn, are superior to the Lurgi dry ash and KRW PDU for Illinois No. 6 coal (Table A-1). Similar data for German Braunkohle are also given in Table A-2.

The parameter E_L defined in Eq. (A-7) represents the steam and oxygen feed cost per unit of syngas produced. It generally decreases rapidly as the temperature is raised above about 1200°F and then levels off at higher temperatures. Because of the large effect of E_L on gasification cost, gasifier operating temperatures tend to be determined by the minimum temperature above which E_L no longer decreases with rising T. This statement is consistent with the fact that costs related to steam and oxygen may be as high as 50% of total syngas-production costs, whereas

gasification costs alone fall in the range of 10 to 20%. Critical gasifier parameters are coal conversion, thermal efficiency, tar formation, and gas requirements.

Because of its large steam requirement (which is needed for the gasifier to remain below the ash-fusion temperature), the Lurgi dry ash gasifier has a relatively large value of E_L (2.6 for Illinois No. 6 coal). The Lurgi slagging gasifier requires less steam and has a resultant lower value of E_L.[2] Steam requirements for the Lurgi dry ash gasifier are lower for higher-reactivity coals (compare Tables A-1 and A-2), resulting in a relatively lower value of E_L for reactive coals.

Table A-1. Performance characteristics of selected gasifiers on Illinois No. 6, Pittsburgh No. 8, and West Kent coals.†

Parameters	Lurgi dry ash	Lurgi slagger	Texaco	Shell	KRW (PDU, TP-034-2)	KRW design estimate	U-Gas
	Illinois No. 6 coal				Pittsburgh No. 8 coal		West Kent coal
T, °F	1600	2700	2700	3000	1793	1850	1831
p, psia	315	300	600	365	230	600	15
H_2O/coal, mole/mole	2.42	0.298	-	0.027	0.43	0.29	1.34
O_2/coal, mole/mole	0.286	0.259	0.463	0.435	0.44	0.30	0.45
C conversion, %	99.3	99.5	99	99.3	76.0	89.6	93.8
Gas composition (dry)							
CO	15.36	58.05	51.69	61.46	43.38	51.5	26.1
CO_2	31.4	1.94	10.6	1.65	35.30	9.3	33.4
H_2	42.9	30.41	35.1	30.6	18.04	25.9	37.4
CH_4	8.78	7.76	0.09	0.04	1.83	10.4	2.8
Gasifier efficiency E_L= steam and oxygen feed cost per mole of steam divided by the syngas value produced per mole of CO‡	2.6	0.86	1.45	1.31	3.30	0.98	2.70
E_{CH_4}	2.14	0.77	1.36	1.24	3.07	0.84	2.38
L_C	1.39	1.56	1.31	1.38	0.77		1.18
Oxygen consumption $R = (O_2)/(C)\gamma$, mole/mole, with γ=fractional carbon conversion	0.286	0.259	0.463	0.435	0.68	0.34	0.48
R_c-R	0.182	0.161	-0.015	-0.031	-0.21	0.12	-0.01

†From R. V. Shinnar, presentation at the Fourth Technical Meeting of COGARN.

‡$E_L = [(H_2O)_F + 4.1(O_2)_F]/[(CO)_P + 0.85(H_2)_P + 2.85((CH_4)_P]$, F=feed, P=product.

Table A-2. Performance characteristics of selected gasifiers for US Western and German Braunkohle.†

Parameters		Lurgi dry ash	Shell	KRW	U-Gas	Winkler	HTW
Coal Type		Wyoming	Texas lignite	N.D. lignite	Wyoming	German Braun-kohle	German Braun-kohle
T, °F		900	2530	1566	1570	1300	
p, psia		460	160	230	30	30	150
H_2O/coal, mole/mole		1.74	-	0.31	0.65	0.69	
O_2/coal, mole/mole		0.23	0.45	0.37	0.29	0.33	0.34
C conversion, %		96	98.4	88.1	89.9	89.2	96
Gas composition (dry)	CO	18.8	52.4	39.0	33.6	34.7	
	CO_2	29.6	6.2	31.6	15.6	19.4	
	H_2	38.8	28.8	24.2	36.6	41.7	
	CH_4	11.9	0.1	4.2	3.8	3.1	
E_L		1.64	1.43	1.73	1.44	2.1	
E_{CH_4}		1.34	1.36	1.54	1.27	1.9	
L_C		1.63			1.28		
$R = (O_2)/(C)\chi$		0.23	0.46	0.42	0.33	0.37	0.36
R_c-R		+0.17	-0.06	-0.06	+0.07 (-0.05)	+0.03	-0.02

†From R. V. Shinnar, presentation at the Fourth Technical Meeting of COGARN.

Results for equilibrium calculations of E_L as a function of temperature are shown in Fig. A-2 under four sets of assumptions for an Eastern US coal. Similar results are shown in Fig. A-3 for a Western US coal. The values of E_L for actually operating gasifiers are also indicated on these figures. All gasifiers, except for the Lurgi slagger and the Lurgi dry ash gasifier (with Western US coal), operate well above the theoretical equilibrium value of E_L. The calculations show a broad minimum for E_L and little gain in efficiency if temperatures are raised above ~1300K. Also predicted is sensitivity of the value of E_L at low temperature when methane production is ignored (curves A and B). Thus, operation at $T \lesssim$ 1300K requires methane formation for efficient operation.[2]

A-3. Fluidized-Bed Gasifiers[1]

Fluidized-bed gasifiers are distinguished by their utility in handling a wide variety of coals, including subbituminous coals, lignites, and coal fines. They are relatively safe and adaptable to two-stage countercurrent operation. However, they yield low conversion, require dilute oxygen for operation, fines recirculation is difficult to achieve, and the returned fines have short residence times and low reactivity. Clinkering and agglomeration of caking coals are problems, especially in the vicinity of the feed systems.

In the absence of tar and with pure carbon as char, a gasifier has 7 major components (CO, CO_2, H_2O, O_2, H_2, C, CH_4) and 3 major elements that undergo chemical changes (C, H, O), which leaves 4 degrees of freedom. Of these, one is represented by the constraint that there should be no oxygen in the product and another by the existence of shift equilibrium (H_2O + CO $\rightleftarrows CO_2 + H_2$). Hence, there remain two free operating parameters.

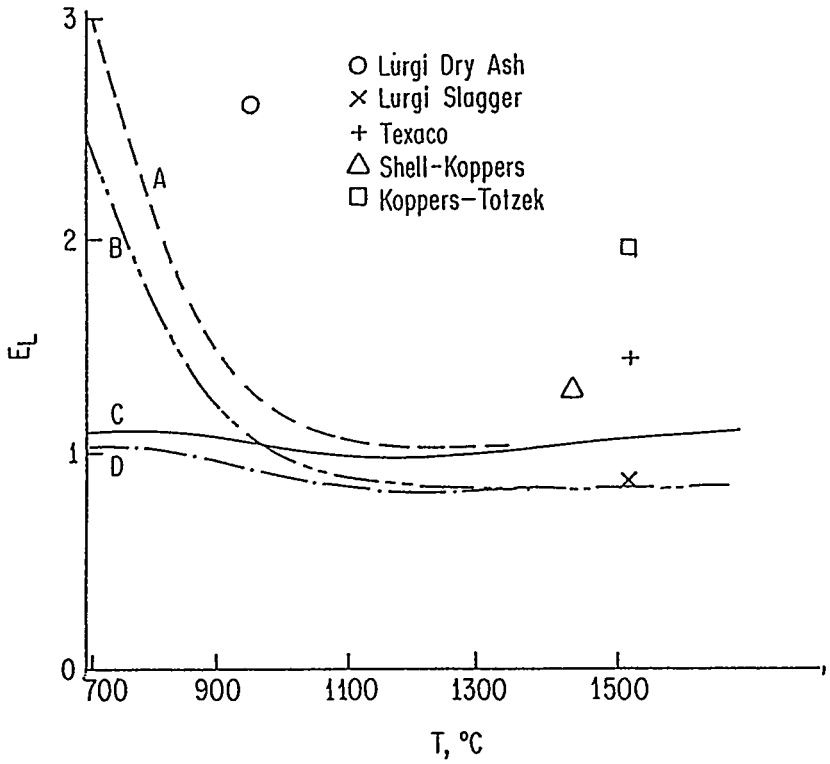

Fig. A-2. Calculated equilibrium and actual values of E_L for an Eastern US coal; reproduced from Ref. 2. The following assumptions apply to the calculated curves; A, well-mixed reactor, no methane formation; B, countercurrent reactor, no methane formation; C, well-mixed reactor, methane at equilibrium; D, countercurrent reactor, methane at equilibrium; from Ref. 2.

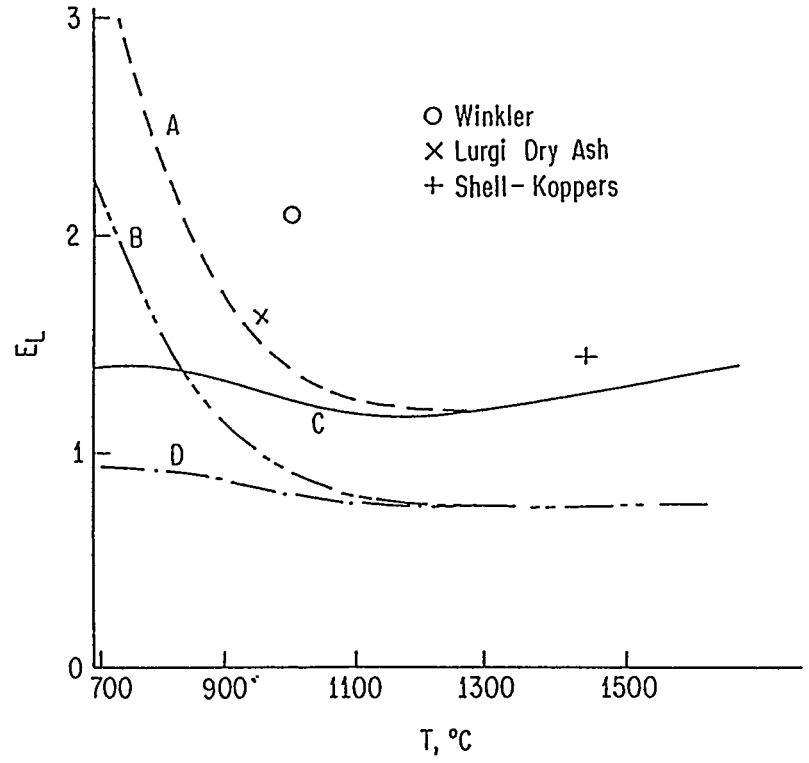

Fig. A-3. As in Fig. A-2 but using a Western US coal; from Ref. 2.

References

1. R.V. Shinnar, presentation at the Fourth Technical Meeting of COGARN, May 1986.
2. M.M. Denn and R.V. Shinnar, "Coal Gasification Reactors" in Chemical Reactor & Reaction Engineering, pp. 499-543, Carberry and Varma eds., Marcel Dekker, New York, NY (1986).
3. R.V. Shinnar and J.C. Kuo, "Gasifer Study for Mobil Coal to Gasoline Processes," Final Report, FE-2766-13/UC-90D, US DoE, Germantown, MD (1978).

GLOSSARY OF SYMBOLS AND ABBREVIATIONS

A	= ampere
Å	= Angstrom = 10^{-10} meter
AAQS	= Ambient Air Quality Standards
AC	= alternating current
AFC(s)	= alkaline fuel cell(s)
AI	= artificial intelligence
ANL	= Argonne National Laboratory
ASTM	= American Society for Testing Materials
atm	= atmosphere
BGC	= British Gas Corporation
BOD	= biological oxygen demand
BPD	= barrel(s) per day
BPY	= barrel(s) per year
BTU	= British thermal unit(s)
BTX	= benzene(s), toluene(s), and xylene(s)
°C	= degree(s) Celsius
cal	= calorie
CARS	= coherent anti-Stokes Raman scattering
cc	= cubic centimeter
CCG	= catalytic coal gasification
CF	= cubic foot (feet)
Ci	= Curie
cm	= centimeter = 10^{2} meter
CNG	= Consolidated Natural Gas
COD	= chemical oxygen demand
COGARN	= (Working Group for) Coal Gasification Research Needs
C_s	= sulfide capacity defined in Eq. (8A-4)
CWCGP	= Cool Water Coal Gasification Program
d	= day or particle diameter
D	= diesel fuel(s)

DC = direct current
DoE = US Department of Energy
d.q. = direct quench
E = theoretical electrochemical potential
EG = ethelyne glycol
EPA = US Environmental Protection Agency
EPRI = Electric Power Research Institute
ERC = Energy Research Center
ETU = engineering test unit
F = Faraday unit
^{o}F = degree(s) Fahrenheit
FBSD = fluidized-bed slurry dryer
FCC = fluidized-bed catalytic cracking
FC(s) = fuel cell(s)
FGD = flue-gas desulfurization
ft = foot (feet)
FT = Fischer-Tropsch
FTIR = Fourier-transform infrared spectroscopy
g = gram
G = gasoline(s)
ΔG, ΔG_R^o = Gibbs free energy of reaction
GPCGP = Great Plains Coal Gasification Program
GRI = Gas Research Institute
h, hr = hour
ΔH, ΔH_R^o = enthalpy of reaction
HC(s) = hydrocarbon(s)
HGT = heavy gasoline treating
HHV = higher heating value
HRSG = heat-recovery steam generator
HTGR = high-temperature gas-cooled (nuclear) reactor
HTS = high-temperature shift
Hz = Hertz (s^{-1})
i = current
id = inside diameter
IGCC = integrated coal-gasification combined cycle

IGT = Institute of Gas Technology

in = inch

IRMCFC = internal-reforming molten-carbonate fuel cell

K = degree(s) Kelvin or equilibrium constant

KRW = Kellogg-Rust-Westinghouse (gasifier)

ℓ = liter(s)

LASS = laser spark spectroscopy

lb = pound(s)

LCD = levelized constant dollars

LDV = laser-doppler velocimetry

LHV = lower heating value

LIF = laser-induced fluorescence

LTS = low-temperature shift

m = meter

MCFC(s) = molten-carbonate fuel cell(s)

Me = methanol

METC = Morgantown Energy Technology Center

mill = 10^{-3} dollar

MOGD = Mobil's process for the conversion of olefins to gasolines and diesel fuels

mol% = mole percent

mt = metric ton

MTBE = methyl tert-butyl ether

MTG = methanol-to-gasoline (conversion)

MTO = methanol-to-olefin(s) (conversion)

n = number of equivalents per mole

NESHAP = National Emissons Standards for Hazardous Pollutants

NG = natural gas

NMR = nuclear magnetic resonance

NSPS = New Source Performance Standards

ORNL = Oak Ridge National Laboratory

p = pressure

p_i = partial pressure of component i

PAFC(s) = phosphoric-acid fuel cell(s)

PAH(s) = Polycyclic aromatic hydrocarbon(s)
PC = pulverized coal
PDF = probability density function
PDU = process development unit
PETC = Pittsburgh Energy Technology Center
PM = photomultiplier
PNA(s) = polynuclear aromatic(s)
ppm (ppmv) = parts per million (by volume)
PSA = pressure-swing absorption
psia (psig) = pounds per square inch absolute (gauge)
R = molar gas constant
RCRA = Resource Conservation Recovery Act
RGS = raw gas shift
ROM = run-of-mine
RON = research octane number
s = seconds
ΔS = entropy of reaction
SASOL = city in South Africa where the South African Coal, Oil and Gas Corporation built its initial plant for syncrude production from coal
SCE = Southern California Edison Company
SCF = standard cubic foot (feet)
SCGP = Shell Coal Gasification Process
SEM = scanning electron microscope
SG = synthesis gas
SI = swelling index
SMDS = Shell middle-distillate synthesis
S/N = signal-to-noise ratio
SNG = substitute (or synthetic) natural gas
SPC = single-particle counter
SPEFC(s) = solid polymer electrolyte fuel cell(s)
SRS = stimulated Raman scattering
SS = stainless steel
T = temperature

TARGET = Team to Advance Research on Gas Energy Transformation
TBE = tert-butyl ether
TCGP = Texaco Coal Gasification Process
TDS = total dissolved solids
TSA = temperature-swing absorption
TSCA = Toxic Substances Control Act
TOC = total organic carbon
TPD = ton(s) per day
TPY = ton(s) per year
TSP = total suspended particulates
TSS = total suspended solids
TVA = Tennessee Valley Authority
UPA = United Power Association
UTC = United Technologies Corporation
V = volt(s)
VA = vinyl acetate
vol% = percent by volume
w/w = weight divided by weight
WH = watt-hour
WGS = water-gas-shift reaction
wt% = weight percent

Greek Symbols

ε = emissivity, Carnot efficiency
η = overpotential
θ_i = angle defined in Fig. 11.5-2
λ = wavelength
ϕ = phenyl radical
ω_p = pump-laser frequency
ω_s = Stokes-laser frequency
σ = width of distribution

Prefixes

k	= kilo = 10^{3}
m	= milli = 10^{-3}
M, MM	= Mega = 10^{6}
μ	= micro = 10^{-6}
N	= normal
n	= nano = 10^{-9} or normal
p	= pico = 10^{-12}

FORMAL REVIEWS OF THE COGARN REPORT

At the request of the DoE Project Officer for this study, the COGARN report was submitted for independent review and comments to the following experts on coal science and gasification: H. Heinemann (Lawrence Berkeley Laboratory, University of California, Berkeley), J.P. Henley (Dow Chemical, Plaquemine, LA), G.R. Hill (University of Utah, Salt Lake City), J.D. Holmgren (KRW Energy Systems Inc., Madison, PA), W.E. Schlinger (Texaco Inc., Universal City, CA), and R. Shinnar (City University of New York, NYC). Insofar as the reviewers' comments dealt with corrections or specific changes, these have been incorporated in the final text. Policy recommendations are reproduced here because they may be of general interest and complementary to the views of COGARN members. The writers addressed their reviews to the COGARN chairman.

H. Heinemann, Senior Scientist, Lawrence Berkeley Laboratory, 1 Cyclotron Road, Berkeley, CA 94720

I have had an opportunity to review the draft of the COGARN report, which you sent me with your letter of December 25, 1986. This is an excellent and very helpful report.

I believe that the recommendations are clear and acceptable. As stated in the report, the priorities will vary from individual to individual, depending on his outlook and interests. Perhaps one should distinguish in the recommendations between developmental needs and research needs. Items 2 and 11 are obviously urgent for further development and should receive highest priority in that category. Items 5 and 6 would fall into the same group. By listing priorities for research separately, the impression of greater urgency might be created by giving them ratings on the 1 to 10 scale which would compete with ratings in the developmental area.

I have not read all the tutorials, but am particularly impressed with Chapter 5, which presents a survey which can serve as guidelines for the future and will even be helpful in teaching. As a minor criticism of this chapter, I miss references to our work on the slurry reactor,

particularly the papers by Stern et al. in Chemical Engineering Science [40, No. 10, 1917 (1985)] and I and EC Process Design and Development [24, 12-13 (1985)].

I had previously seen a draft of Chapter 7, which includes our own work on gasification. Since I had previously approved of it, I can only repeat that it states matters fairly.

I believe that this report will be very useful in our own work on coal gasification, as well as in the obvious need to persuade funding organizations to support work in the area if at all possible on an expanded scale. I am deeply concerned about the continuing efforts to disregard and deemphasize this very important area at a time when research should be emphasized, perhaps over development, because we may have a period during which novel ideas and concepts can be brought forward toward commercialization without working under the pressure of immediate needs.

John P. Henley, Research Associate, Louisiana Applied Science and Technology Laboratories, Dow Chemical USA, P.O. Box 150, Plaquemine, LA 70765-0150

I certainly appreciate the opportunity to review the document produced by the COGARN group on research need for coal gasification. This type of project is most valuable in light of our shifting emphasis in synthetic fuel research.

The tutorial sections of the report were excellent in describing each area of technology. Each section was both thoroughly researched and well written. The respective authors should be commended for their work.

After reading the executive summary containing the prioritized list, I went through the exercise of ranking these in the order as I saw them. As one might expect, my background being private development, the order was rather different. From this I concluded that I would agree completely with your statement on page 8, "priority assignments reflect the background and problem areas faced by individual investigators . . .". To get a better idea of what experts in each area believe is important, I think it would have been most informative to have at least four separate priority lists, one each representing academia, industry, not-for-profits

(EPRI, GRI, etc.), and government-financed institutions. While no particular one could ever be considered "best," this would allow the researcher to evaluate each group's consensus with regard to his own specific are of interest.

In general, I would like to say that the report should be quite useful as a reference source to evaluate research needs. The COGARN group should be commended for their fine work.

G.R. Hill, Dept. of Fuel Chemistry, University of Utah, Salt Lake City, UT 84108

The volume "Coal Gasification" is a very thorough review of research and development of coal-gasification processes and might well constitute a major section of a new supplement of Lowry's "The Chemistry of Coal Utilization," the coal R&D "Bible." The Assessment of Research needs, per se, is stated briefly, almost perfunctorily, in the executive summary. It would be very useful to have the volume (even minus the executive summary) published and made available to those involved in coal gasification research and development.

If this use of the volume is possible, there should be added an important section on co-production of gas and oil, i.e.,of primary coal liquid distillates. Because of the historical classification of coal conversion into gasification and liquefaction, process paths for the production of gas and oil or of char and oil have been orphans. Research and development done under special designations (e.g., mild gasification or partial liquefaction), have largely fallen through the cracks between the total conversion processes, in reviews such as this. Since these processes appear to require much milder conditions, they are less costly. It is essential that they not be overlooked.

Chapter 2 in the present volume is a very detailed summation of the possible and necessary research programs needed in each of the areas described in detail in Chapters 3 through 14. The great simplification in the Table ES-1 list of priority research and development areas is readily apparent as one studies detailed recommendations in all 12 areas in Chapter 2. Chapters 3 through 14 will be invaluable references for those planning for or engaged in coal gasification and its applications.

The authors of the treatise are to be commended for the thoroughness of their comprehensive work.

J.D. Holmgren, Vice President - Technology Development, KRW Energy Systems, Inc., P.O. Box 334, Madison, PA 15663-0334

Overall, I think the document is an excellent summary on coal-processing technologies, applications, and research and development needs. In my opinion, the first two chapters are really the heart and muscle of the report. The Executive Summary is brief and to the point and the use of Table ES-1 provides a simplified way of identifying R&D priorities. One suggestion that might provide a little more data would be to use a matrix table in which the priorities could be listed in row form and the scale at which activities would be conducted, such as bench, laboratory, pilot, demonstration, etc., would be listed in columnar form.

Chapter 2, "Overview of Coal-Gasification R&D Needs" is a good companion to the Executive Summary and, in general, one obtains a good synopsis of each of the subsequent chapters to follow. Some sections are more detailed than others and Sec. 2.5 on "Gasification for Synthesis of Fuels and Chemicals" could be abbreviated.

Chapter 3, "Gasification for Electricity Generation," provides a good summary for power-generation applications and the Cool Water details are very appropriate. The description of gasification systems that could be used is good for the Shell and Texaco gasifiers; however, the information for U-GAS is much too detailed and relates largely to R&D results.

Chapter 4, "Coal Gasification for SNG Production," is an excellent chapter. It has good organization and good balance of fundamentals, technologies, specific processes, and economics.

Chapter 5, "Gasification for the Synthesis of Fuels and Chemicals," is a good chapter but is much more detailed than most of the other chapters in the publication. The information could be summarized to provide a more concise and effective text. In addition, the outline could make better use of numerical paragraph indexing to help the reader understand where he is within the text.

Chapter 6, "Coal Gasification in Fuel-Cell Applications," is a good, short and hard-hitting chapter.

Chapter 7, "Use of Catalysts During Gasification," is another short, good, and effective chapter with good use of visual and tabular summaries and good references.

Chapter 8, "Gas-Cleaning Processes for Coal Gasification," is much too brief in view of the importance of gas cleaning for coal gasification. There is some duplication on acid-gas removal with Chapter 4, Sec. 4.4, but this is not distracting.

Chapter 9, "Environmental Issues," is a good chapter, which identifies requirements and presents information regarding environmental characteristics for various gasification systems. For the amount of information presented, the list of references is rather brief.

Chapter 10, "Coal Beneficiation," is another area that I believe to be extremely important for the utilization of coal and this particular chapter is much too brief. The information presented relates primarily to old technologies and the discussion is extremely brief on the development that are currently underway. I believe that it would be helpful to have more information presented on advanced clean-coal technologies that are currently under development and demonstration.

Chapter 11, "Optical Diagnostics for In Situ Measurements in Pulverized-Coal Combustion Environments," is an excellent chapter, particularly for people who are involved in R&D studies. In the future, some of these technologies will be used on commercial systems to provide better control and system diagnostics.

Chapter 12, "Fundamentals of Coal Conversion and Relation to Coal Properties," is an excellent chapter that summarizes a great deal of information with tables and charts and correlates this information with a significant reference list.

Chapter 13 deals with "Gas Supplies and Separation; Ash Disposal; Materials for Gasifiers." The section on oxygen systems should include some specific information of pressure-swing absorption systems that have been developed and are applicable for smaller gasification applications or for systems with lower oxygen-purity requirements. The other sections on ash and materials of construction are adequate.

Chapter 14, "Introduction to Costing," was a disappointment to me in that the material did not relate to economics of coal gasification and utilization. There have been many economic studies completed for EPRI and GRI that could have been used to provide detailed information for this particular chapter. The important problem is not so much the probability of over- and under-runs on cost estimation, but rather what are some of the real projected costs for coal-gasification applications. I would hope that this chapter could be redone and information provided in at least the following three areas: (i) summary of techniques (models) used to generate economic cost data; (ii) a general summary showing capital and product costs for various coal-gasification applications; (iii) a general summary showing the distribution of capital and operating costs by components/ systems for specific coal-gasification applications.

The Appendix includes information prepared by Shinnar. We have worked closely with Shinnar over the past few years, and I am quite familiar with his approach for evaluating different gasification technologies. I certainly think this information should be included; however, I feel there should be a more detailed preamble on how his technique fits with other gasification-evaluation schemes.

Again, I thought the efforts were outstanding and the report will be extremely useful to many people. I realize that many of my comments are quite general, but I do hope that they will provide some feeling regarding the balance of material within this document.

W.G. Schlinger, Associate Director, Gasification, Alternate Energy and Resource Department, Texaco Inc., 10 Universal City Plaza, Universal City, CA 91608-1097

I have made an attempt to review the rather impressive document you put together for DOE on the assessment of research needs for coal gasification. I must confess, I concentrated primarily on the first three sections. A few specific comments are detailed below.

As far as the overall report is concerned, the consensus appears to be that work in all areas that you have identified is needed. You do not identify any areas where effort should be discontinued or significantly reduced. DOE, with their limited funding, probably should concentrate the

funds they have in areas which are most likely to solve some of the energy shortfall problems of the future.

One of the most important items in your report is Table ES-1, in which you assign priorities based upon the consensus of COGARN members. In general, the areas of highest priority (those rated above 6.0) are in agreement with our thinking. Some of the items, however, are much more costly than others to pursue on a high-priority basis. Some indication of cost effectiveness needs to be identified.

Chapter 2 ("Overview of Coal Gasification R&D Needs") is a well-written summary. The need to decrease the cost of an IGCC plant is certainly important and well recognized by the Committee. As I told your Committee in Morgantown, hot gas cleanup and more efficient and less costly air-separation plants are two areas which could accomplish such a cost reduction.

You have done a very creditable job of assembling a mass of information. All of your Committee members should be congratulated.

R. Shinnar, School of Engineering, Department of Chemical Engineering, The City College, The City University of New York, New York, NY 10031

Table ES-1 (p. 2) I find it hard to understand why item 9 got such low priority. Why is it not tied to item 13? Also, how can we summarize present results without a reasonable model for comparison? (i) I find no comment on the fluidized-bed gasification program. It was the heart of my DoE paper and received most of the support in the past. Should this effort be completed and summarized or should it be abandoned? I am strongly for the first option. This aspect should have been more thoroughly discussed.

Fig. 4.5-1 (p. 62) The report gives some economic estimates comparing KRW to Lurgi. As I pointed out in my inputs, there is absolutely no experimental or theoretical basis for the mass balances on which these estimates are prepared. The same holds for similar estimates made for U-GAS. Furthermore, a dry bottom in Lurgi is a totally nonrealistic base case for Eastern coal. A more realistic base case would be a BGC slagger,

which is practically the only presently available viable option for SNG from Eastern coal.

pp. 29-37 No mention is made of the fact that the U-GAS pilot plant operated at 50 psi, which is totally unsuitable for a combined-cycle power plant. There is no way to predict the operation of such a gasifier at higher pressures. The only way is to operate a pilot plant at the desired pressure, which is about 300 psi for a combined-cycle power plant. On the other hand, KRW has operated the gasifier at 300 psi in an airblown mode. This operation with added limestone at 2000°F was their most successful overall run in any mode and could be useful for a combined-cycle power plant.

Appendix (p. 267) The comment on fluid-bed gasifiers is much more negative than I intended. It is correct as applied to present-day pilot plants. I would suggest to add the following paragraph:

> The advantages of fluid-bed gasifiers are: (a) ability to handle low-grade coals (for some coals, it is the only suitable gasifier); (b) higher safety than entrained-bed gasifiers.

There is a substantial hope that the disadvantages of present fluid-bed gasifiers for Eastern coal will be overcome by proper use of cheap catalysts such as limestone. The results of KRW with lime in an airblown operation are very promising. Limestone reduces agglomeration and allows operation at higher temperature, which could substantially reduce the need for dilution of the oxygen. Catalysis could also lead to high carbon conversion. Since a substantial effort has been devoted to fluid-bed gasifiers, it is highly desirable to investigate the effect of catalysts on oxygen-blown fluid-bed gasifiers.